2015

The role of myocardin related transcription factor A in controlling the commitment of progenitors to adipose lineage versus osteoblastic lineage

BOSTON UNIVERSITY

SCHOOL OF MEDICINE

Dissertation

THE ROLE OF MYOCARDIN RELATED TRANSCRIPTION FACTOR A IN CONTROLLING THE COMMITMENT OF PROGENITORS TO ADIPOSE LINEAGE *VERSUS* OSTEOBLASTIC LINEAGE

by

HEJIAO BIAN

B.Sc., Sichuan University, 2009

Submitted in partial fulfillment of the

requirements for the degree of

Doctor of Philosophy

2015

Approved by

First Reader _____

Stephen R. Farmer, Ph.D.

Professor of Biochemistry

Second Reader _____

Paul F. Pilch, Ph.D.

Professor of Biochemistry

ACKNOWLEDGEMENTS

I would like to express my appreciation and thanks to all the people who have contributed to this thesis. First of all, I would love to thank my thesis advisor Dr. Stephen Farmer for all the support, mentorship and encouragement throughout my thesis research. His enthusiasm for scientific research, endless novel insights and optimistic attitudes towards setbacks would always inspire me in my future career and life. It was also my great pleasure to work with a group of brilliant researchers in our laboratory. I would like to give special thanks to my best friend Chendi Li for all her help, advice, support and companionship as a great friend and colleague throughout my graduate school. Dr. Hong Wang, Dr. Heng (Mike) Guo, Dr. Meghan McDonald and Lynes Torres have provided me with much-appreciated suggestions and guidance for my thesis research as well.

I would also like to thank my thesis committee members: Dr. Barbara Schreiber, Dr. Paul Pilch, Dr. Orian Shirihai, Dr. Bob Varelas and Dr. Matthew Nugent, for serving on my thesis committee and contributing in so many ways to this work. I'm very fortunate to have Dr. Barbara Schreiber as my thesis committee chair. She organized all the pre-thesis meetings and also helped me to adjust smoothly to the graduate school life as an international student when I first joined the department. I would like to acknowledge Dr. Paul Pilch with deep appreciation for been my second reader and providing constructive suggestions for the work presented in this thesis. Thank Dr. Bob Varelas, Dr. Orian Shirihai and Dr. Matthew Nugent for their novel and thoughtful suggestions and criticisms for my work. I would also love to express special thanks to Dr.

Matthew Layne for advice, help and generous donation of transgenic animals and reagents throughout my graduate work. I would like to thank Dr. Barbara Smith for initiating the collaboration with our laboratory, which made this thesis research possible.

I would like to extend my gratitude to Zackery Webster, Gabriel Macdonald and Dr. Elise Morgan for their guidance and help with the experiments performed at the Orthopaedic and Developmental Biomechanics Laboratory. I'm grateful to Dr. Shannon Carroll and Dr. Larry Luchsinger for their help with transgenic animal work techniques and their constructive suggestions. Thank you to my kind and helpful colleagues from Pilch, Varelas, Peressi and Layne laboratories for generously sharing all the equipment and reagents with us. I'm also extremely grateful to all the staff at GMS office and Department of Biochemistry for their help every step of the way.

We are grateful to Dr. Eric Olson from UT Southwestern Medical Center (Texas) for the $MRTFA^{+/-}$ mice and also for the support for our research by NIH grants DK51586, DK098830 (SRF) and HL078869 (MDL).

A special thanks go to my family. Words cannot express how grateful I am to my parents Liping Li and Jianhua Bian for all their sacrifices on my behalf and their unconditional love and support. I'm also grateful to my new family: the English family, my in-laws, my brother and all my friends for their support, encouragement and love. At the end I would like to express my deepest appreciation to my beloved husband and soulmate Taylor English for all the editing and for always being there for me in the moments of need.

THE ROLE OF MYOCARDIN RELATED TRANSCRIPTION FACTOR A IN CONTROLLING THE COMMITMENT OF PROGENITORS TO ADIPOSE LINEAGE *VERSUS* OSTEOBLASTIC LINEAGE

HEJIAO BIAN

Boston University School of Medicine, 2015

Major Professor: Stephen R. Farmer, Ph.D., Professor of Biochemistry

ABSTRACT

The differentiation of osteoblasts and bone marrow adipocytes are closely associated yet mutually exclusive processes that are essential for maintaining bone homeostasis. Various diseases have been shown to develop once the delicate balance between adipogenesis and osteoblastogenesis is disrupted. Investigating the underlying molecular mechanisms of the osteoblasto-adipogenic switch under osteoporotic conditions will facilitate our understanding of the pathogenesis of osteoporosis and may eventually lead to the development of clinical therapeutic approaches for this life-threatening disease. While changes in cell morphology and cytoskeletal integrity can alter pre-committed mesenchymal stem cell (MSC) differentiation of certain lineages, previous studies have shown that cellular morphological changes can affect the early commitment of pluripotent MSCs via modulation of Ras homolog gene family, member A (RhoA) activity. The RhoA pathway regulates actin polymerization to promote the incorporation of globular-actin (G-actin) into filamentous-actin (F-actin). Actin

polymerization releases G-actin bound myocardin-related transcription factors (MRTFs), which translocate to the nucleus and co-activate serum response factor (SRF) target gene expression. Exactly how the RhoA-actin-MRTF-SRF circuit is involved in the regulation of early commitment of MSCs remains poorly understood. Here we show that global MRTFA knockout mice (MRTFA KO) exhibited lower body weight, shorter femur and tibia lengths, and decreased trabecular bone volume. Furthermore, bone marrow MSCs isolated from MRTFA KO mice showed increased adipogenesis and brown fat gene expression as well as compromised osteoblastogenic differentiation as compared to WT controls. Treatment of WT bone marrow MSCs with the SRF inhibitor, CCG1423, mimicked these effects in that the compound inhibited osteoblastogenesis and promoted adipogenesis. Over-expression of MRTFA or SRF inhibited adipogenesis and enhanced osteoblastogenesis in C3H/10T1/2 cell lines, whereas over-expression of dominant-negative MRTFA or SRF variants had the opposite effects. In conclusion, our study identified MRTFA as a crucial regulator of skeletal homeostasis *via* regulating the balance between adipogenic and osteoblastogenic differentiation of the MSCs. Furthering our understanding of how the RhoA-actin-MRTFA-SRF circuit is involved in regulating the fate commitment of MSCs may ultimately lead to novel therapeutic strategies for treating osteoporosis and obesity.

TABLE OF CONTENTS

LIST OF TABLES

LIST OF FIGURES

LIST OF ABBREVIATIONS

AA	ascorbic acid
ABP	actin binding protein
Adipoq	adiponectin
Adrb3	beta-3 adrenergic receptor
AGEs	advanced glycation end products
Alpl	alkaline phosphatase
Arp	actin-related protein
BAT	brown adipose tissue
Bglap	bone gamma-carboxyglutamate protein (osteocalcin)
βGP	β-glycerophosphate
BMI	body mass index
BMP	bone morphogenic protein
BV	bone volume
Cdc42	cell division control protein 42 homolog
C/EBP	CCAAT enhancer binding protein
Cidea	cell death activator CIDE-A

Col1a1	collagen type 1α 1
Col3a1	collagen type 3 α 1
Conn. D.	connectivity density
Cox7a	cytochrome c oxidase polypepetide 7A1, mitochondrial
CTX-1	cross linked C-telopeptide
DN-MRTFA	dominant negative MRTFA
DN-SRF	dominant negative SRF
ELISA	enzyme-linked immunosorbent assay
Elovl3	ELOVL fatty acid elongase 3
ER	estrogen receptor
FABP	fatty acid binding protein
F-actin	filamentous-actin
G-actin	globular-actin
GEFs	Rho guanine nucleotide exchange factors
HFD	high fat diet
IBMX	isobutylmethylxanthine

Igf	insulin like growth factor
IGFBP	insulin like growth factor binding protein
INDO	indomethacin
LFD	low fat diet
LRP5	lipoprotein related receptor 5
MAPK	mitogen activated protein kinase
Micro-CT	micro-computed tomography
MKL1	megakaryoblastic leukemia 1 (also known as MRTFA)
MRTF	myocardin-related transcription factor
MSC	mesenchymal stem cell
MSCV	murine stem cell virus
mTOR	mammalian target of rapamycin
PGC	peroxisome proliferator-activated receptor gamma co-activator
PINP	procollagen I N-terminal propeptide
Ppar	peroxisome proliferator-activated receptor
PTH	parathyroid hormone

Rac	Ras-related C3 botulinum toxin substrate
RANKL	nuclear factor κ B ligand
RhoA	Ras homolog gene family, member A
ROCK	Rho-associated protein kinase
Runx2	Runt-related transcription factor 2
RXR	retinoid X receptor
SAP	SAF-A/B, Acinus, and PIAS
SMA	smooth muscle actin
SMAD	small mothers against decapentaplegic
SMC	smooth muscle cell
SMI	structure model index
Spock	testican (osteonectin)
Spp1	secreated phosphoprotein 1 (osteopontin)
SRF	serum response factor
T3	triiodothyronine
TAD	transcription activation domain

TAZ	PDZ-binding motif
Tb. N.	trabecular number
Tb. Sp.	trabecular separation
Tb. Th.	trabecular thickness
TCF	Ternary Complex Factor
TGFβ	transforming growth factor β
TROG	troglitazone
TV	total volume
TZD	thiazolidinedione
UCP	uncoupling protein
VDR	vitamin D receptor
WASP	Wiskott-Aldrich syndrome protein
WAT	white adipose tissue
Wnt	wingless-int
YAP	Yes-associated protein

INTRODUCTION

Osteoporosis

Osteoporosis is a skeletal disorder characterized by decreased bone mass and deterioration of bone microstructure, which leads to increased fragility fractures in patients even without severe trauma (NIH 2001, Raisz 2005, Rosen and Bouxsein 2006, Kling, Clarke et al. 2014, Montagnani 2014). It is an emerging public health burden affecting more than 10 million American adults and another 34 million people are considered at high risk of developing it due to low bone mass (Melton 2001). In the United States alone, approximately $17 billion was spent on health care for osteoporosis-related mortality and morbidity in 2005 (Burge, Dawson-Hughes *et al*. 2007). The costs for combating osteoporosis are estimated to rise by 50% by 2025 due to the increasing cases of pathological fractures in patients above the age of 65 (Burge, Dawson-Hughes *et al*. 2007).

Osteoporosis was first identified by the English surgeon Sir Astley Cooper in 1822 who described this condition as "the lightness and softness that bones acquire in the most advanced stage of life… and this state of bone… favors much the production of fractures" (Cooper *et al*., 1822). Since then, more and more studies have led to a better understanding of the pathogenesis of osteoporosis. Genetic studies revealed the connection between osteoporosis and various growth factors, receptors and transcription factors. More than 30 genes (including estrogen receptor (ER), vitamin D receptor (VDR), collagen type 1α1 (COL1A1) and transforming growth factor-β1 (TGFB1)) are shown to

be important for maintaining bone mass in human osteoporosis clinical studies (Liu, Liu *et al*. 2003, Baldock and Eisman 2004). Osteoporosis induced fragility fractures in hip and spine often lead to chronic pain and immobility and it is very detrimental for the quality of life for aging patients (Montagnani 2014). In addition, severe medical complications such as thromboembolic disease or pneumonia can develop in long term immobile patients suffering from fragility fractures (Montagnani 2014).

Low peak bone mass during growth, excessive bone resorption and inadequate bone formation during bone remodeling are the three basic pathogenic mechanisms for osteoporosis (Raisz 2005). In humans, the majority of bone mass accumulation happens during the ages of 12-18. If bone formation during this time is hindered by pathological conditions such as inadequate growth hormones, then lower primal bone mass will ensue in adult life and there will be a higher possibility for fragility fractures as the patients age (Recker and Heaney 1993). The pathology of this type of osteoporosis happened earlier in life during growth whereas the phenotype does not manifest itself until decades later. On the other hand, age-related osteoporosis often develops rapidly when patients are in their 50's. The bone loss during aging is inevitable as bone resorption is much more active than formation during this stage of adult life (Brown and Rosen 2003). Post-menopausal patients usually have more severe osteoporosis due to the activation of osteoclasts and the decline in osteoblast functions caused by a marked decrease in estrogen levels (Black, Greenspan *et al*. 2003, Howe, Shea *et al*. 2011). Long-term treatments for some chronic diseases also aggravate bone loss in patients, such as the use

of glucocorticoids or the thiazolidinediones (TZD) family of insulin sensitizers (Gimble, Robinson *et al*. 1996, Ali, Weinstein *et al*. 2005, Lane and Yao 2010).

Current treatments for osteoporosis in clinical practice focus on inhibiting bone resorption and enhancing bone formation (Montagnani 2014). Bisphosphonates are the most commonly prescribed drugs for treating osteoporosis by inhibiting bone resorption. With a high affinity for bone and high efficiency in decreasing the fracture risks in patients, bisphosphonates are used widely in clinical practice (Cummings, Black *et al*. 1998, Harris, Watts *et al*. 1999, Black, Thompson *et al*. 2000, McClung, Geusens *et al*. 2001, Black, Delmas *et al*. 2007). However, long-term use of these drugs leads to osteonecrosis of the jaw amongst other undesirable side effects (Black, Schwartz *et al*. 2006, Rizzoli, Akesson *et al*. 2011). Anabolic treatments promoting osteoblast function are also used clinically such as drugs enhancing parathyroid hormone (PTH) signaling (Horwitz, Tedesco *et al*. 2010) and wingless-int (Wnt) signaling (Baron and Hesse 2012) in bone. Unfortunately, these aforementioned treatments are not sufficient to maintain bone mass in severely osteoporotic patients. Novel therapeutic approaches for osteoporosis are needed for preventing fragility fractures and improving quality of life in an increasing aging population.

Bone Remodeling

To fully understand the mechanism of osteoporosis caused by excessive bone resorption and inadequate bone formation, it is essential to understand the bone

remodeling process in the adult skeleton. To maintain the proper shapes, sizes and integrity, bone is constantly undergoing remodeling by replacing approximately 10% of the bone material annually (Lerner 2006). Bone remodeling is a complicated process, involving both bone formation by osteoblasts and bone resorption by osteoclasts (Hadjidakis and Androulakis 2006, Neumann and Schett 2007).

Bone remodeling occurs in both trabecular and cortical bone (Raisz 2005) and it starts with the activation of osteoclasts differentiation by nuclear factor κ B ligand (RANKL) expressed by pre-osteoblasts (Wada, Nakashima *et al*. 2006). When osteoclasts are fully differentiated, they secrete proteases and other factors that can digest mineralized bone (Hadjidakis and Androulakis 2006, Glass and Karsenty 2007). After a reversal phase when the bone surface is occupied by differentiating osteoblast progenitors, the bone formation phase is initiated by bone matrix production followed by osteoblast maturation. Mature osteoblasts are then embedded in the mineralized bone for transformation into osteocytes (Hadjidakis and Androulakis 2006, Proff and Romer 2009). The resorption and reversal phases during the bone remodeling cycle are much shorter than the bone formation phase (Raisz 2005, Proff and Romer 2009). Therefore, a slight increase of bone remodeling rate will result in excessive bone resorption and eventually excessive bone loss.

It is intriguing that osteoblasts and osteoclasts collaborate so closely during bone remodeling by secreting factors to regulate the differentiation of one another (Raisz 2005, Matsuo and Irie 2008). RANKL is expressed by pre-osteoblasts and resides on the

surface of these cells. The binding of osteoclast progenitors to RANKL is essential for the activation of signaling cascades regulating osteoclast differentiation (Wada, Nakashima *et al*. 2006). Tumor necrosis factor α (TNF-α), interleukin-1 (IL-1) and vitamin D have been shown to promote RANKL expression, whereas estrogens suppress it (Matsuo and Irie 2008). On the other hand, during bone resorption, growth factors including bone morphogenetic proteins (BMPs) released from degrading bone matrix are crucial for the osteoblast progenitor's fate commitment (Matsuo and Irie 2008).

Osteoporosis and Obesity

Obesity and osteoporosis are two major public health issues becoming more and more prevalent in recent years. Although these two diseases appear to develop in different ways, previous investigations revealed common characteristics between them such as genetic predisposition and environmental factors (Rosen and Bouxsein 2006). The underlying mechanism these two conditions share is the dysregulation of a common progenitor cell (Rosen and Bouxsein 2006, Cao 2011). The relationship between osteoporosis and obesity is a very active area of research since potential drugs targeting the common pathological mechanisms can be developed for treating these diseases simultaneously (Rosen and Bouxsein 2006, Cao 2011, Colaianni, Brunetti *et al*. 2014).

Obesity is a condition defined as having excessive body fat accumulation [characterized by a body mass index (BMI) $\geq$ 30 kg/m^2] and it often associates with several metabolic co-morbidities (WHO 2000). Obesity is caused by excessive energy

intake and inadequate energy expenditure (Ogden, Carroll *et al*. 2006, Bessesen 2008). The number of obese patients has doubled since 1980 and about 33% of American adults are obese (Bessesen 2008, Cao 2011). Obesity associated co-morbidities including hypertension, type II diabetes, dyslipidemia and coronary heart diseases are also leading causes of mortality (Messerli, Christie *et al*. 1981). In the United States, the healthcare expenditure related to obesity is approximately $100 billion per year (Wolf and Colditz 1998). With increasing global prevalence and rising adolescence obesity, treating obesity and its associated co-morbidites will be a tremendous burden on the healthcare system (Bessesen 2008).

Various studies are aiming to understand the connection between obesity and osteoporosis. Traditionally, obesity is considered a positive factor for maintaining bone mass due to the excessive mechanical loading conferred to the bone (David, Martin *et al*. 2007, Sen, Xie *et al*. 2008). However, recent evidence contradicted this notion by demonstrating that the obese condition is detrimental to bone health (Goulding, Taylor *et al*. 2000, Cao, Sun *et al*. 2010). Obesity promotes excessive bone loss via various mechanisms. Since adipocytes and osteoblasts are originated from a common progenitor mesenchymal stem cell (MSC), obesity may induce adipogenesis and inhibit osteoblastogenesis in the bone marrow, thereby inhibiting bone formation (Beresford, Bennett *et al*. 1992). Obesity induced inflammation increases the levels of circulating cytokines and leads to the enhancement of osteoclast activity (Wellen and Hotamisligil 2003, Mundy 2007), thus promoting excessive bone loss in obese individuals (Cao 2011). In addition, high levels of leptin and decreased adiponectin secretion by adipose tissue in

obese patients appear to impair bone formation directly and indirectly through up-regulating cytokine levels systemically (Hamrick, Pennington *et al*. 2004). Understanding the underlying connection between obesity and osteoporosis may facilitate identification of new drug targets that can inhibit adipogenesis and enhance osteoblastogenesis at the same time.

Multipotent Mesenchymal Stem Cells (MSCs)

MSCs are multipotent bone marrow stromal cells that possess the ability to self-renew and develop into different lineages (Caplan and Bruder 2001, Jackson, Nesti *et al*. 2012). Given the appropriate milieu of growth factors and microenvironment, MSCs can differentiate into chondrogenic, adipogenic, myogenic or osteoblastogenic lineages (Figure 1) (Aubin 1998, Chamberlain, Fox *et al*. 2007). Multiple signaling pathways and regulatory factors are reported to strictly regulate commitment and terminal differentiation of MSCs to each of these lineages; however the molecular mechanisms underlying the switches between them remain to be investigated (Caplan and Bruder 2001, Chamberlain, Fox *et al*. 2007).

MSCs are very scarce in the total cells population in the bone marrow, consisting about 0.001-0.01% of the total cells (Pittenger, Mackay *et al*. 1999). Despite that MSCs were first identified in the bone marrow stromal fraction, they can also be isolated from skeletal muscle and adipose tissue according to recent reports (Levi and Longaker 2011, James, Zara *et al*. 2012, Mizuno, Tobita *et al*. 2012). The perivascular stromal fraction of

adipose provided a more accessible source for MSCs that can potentially be used in tissue engineering (Crisan, Yap *et al*. 2008, James, Zara *et al*. 2012, Corselli, Crisan *et al*. 2013).

Figure 1. MSCs are multipotent bone marrow stromal cells that possess the ability to self-renew and develop into different lineages.

Given the appropriate milieu of growth factors and micro-environment, MSCs can differentiate into chondrogenic, adipogenic, myogenic or osteoblastogenic lineages. Each of these differentiation processes is strictly regulated to ensure to the proper development of these cells so that they can serve specialized functions in different tissues.

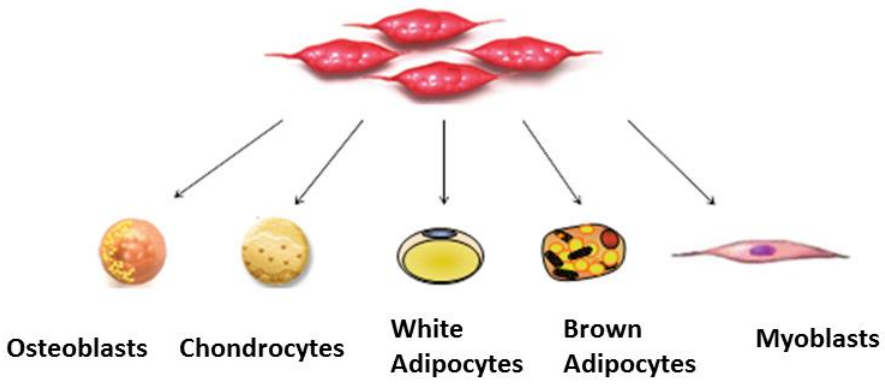

Adipogenesis

Adipogenesis of MSCs can be roughly separated into two phases: determination phase and terminal differentiation phase. During the determination phase, MSCs commit to the adipose lineage with a shift in gene expression but without morphological differentiation (Muruganandan, Roman *et al*. 2009). During the terminal differentiation phase, preadipocytes undergo morphological changes (round up) to accommodate new functions such as lipid synthesis and storage. Lipid droplets will form during this phase and the mature adipocytes also secrete an array of adipokines (Rosen, Walkey *et al*. 2000, Rosen and MacDougald 2006).

Investigations of the transcriptional cascade of adipogenesis have revealed several essential factors for different stages of adipocyte differentiation. The initiation of the adipogenesis starts with the induction of the early regulating factors, two members of the CCAAT enhancer binding protein (C/EBP) family, C/EBPβ and C/EBPδ. These two C/EBPs are expressed earlier than C/EBPα and peroxisome proliferator-activated receptor γ (PPARγ) and they regulate the expression of C/EBPα and PPARγ (Cao, Umek *et al*. 1991, Yeh, Cao *et al*. 1995). Upon induction by C/EBPs, PPARγ hetero-dimerizes with retinoid X receptor (RXR) and turns on the adipogenic transcription program to initiate adipocyte differentiation (Farmer 2006, Ali, Hochfeld *et al*. 2013). PPARγ and C/EBPα then activate the expression of each other in a positive feedback loop to maintain the expression of both genes in mature adipocytes. They also activate a variety of adipogenic genes that are important for adipocyte metabolic functions (Farmer 2006, Vernochet, Peres *et al*. 2009).

It is widely accepted that PPARγ expression is both sufficient and necessary for the commitment and differentiation phases of adipogenesis (Farmer 2006). Studies from transgenic mice of PPARγ confirmed its central role in adipogenesis. Knocking out PPARγ in white adipose tissue (WAT) leads to severe lipodystrophy in mice and these mice do not survive due to the failure to form adipose tissue (Koutnikova, Cock *et al*. 2003).

Osteoblastogenesis

The osteoblast differentiation starts with commitment of progenitor cells and differentiation of pre-osteoblasts (Chamberlain, Fox *et al*. 2007). These cells form mature and functional osteoblasts which would eventually embed in mineralized bone as osteocytes (Neve, Corrado *et al*. 2011) The transcription factor Runt-related transcription factor 2 (Runx2) is indispensable for osteoblast differentiation (Komori, Yagi *et al*. 1997). Signaling pathways such as Wnt/β-catenin and the TGFβ/BMP pathways are also very important in regulating osteoblastogenic transcription factors (Hogan 1996, Gaur, Lengner *et al*. 2005).

Previous studies showed that Runx2 null mutant mice fail to form any bone due to the ablation of osteoblast differentiation (Komori, Yagi *et al*. 1997). Ectopically expressing Runx2 in non-osteoblastic cells is sufficient to activate osteoblast protein including osteocalcin, osteopontin, alkaline phosphatase and type I collagen (Ducy, Zhang *et al*. 1997). Runx2 is the central transcription factor for osteoblast differentiation.

In addition, osterix, a zinc finger containing transcription factor is also shown to be critical for osteoblastogenesis. Osterix-null mice showed a similar phenotype to Runx2 null mice: an absence of bone formation due to blockage of osteoblast differentiation (Nakashima, Zhou *et al*. 2002). Although the osterix null and WT mice have similar levels of Runx2 transcription, the bone formation was completely inhibited in the osterix null mice. In Runx2 null mice, however, there is a complete abolishment of osterix transcription, which suggests osterix is acting downstream of Runx2 in the osteoblastogenesis transcription cascade (Nakashima, Zhou *et al*. 2002, Nakashima and de Crombrugghe 2003).

The Balance between Adipogenesis and Osteoblastogenesis

Adipogenesis and osteoblastogenesis are mutually exclusive yet closely associated processes during MSC development in the bone marrow. The delicate balance between two processes is essential for the maintenance of bone homeostasis. Once the precisely regulated balance between adipogenesis and osteoblastogenesis is disturbed, various metabolic-related diseases develop (James 2013).

Because adipocytes and osteoblasts are originated from the same bone marrow MSC progenitor, the conditions or agents that inhibit osteogenesis will promote adipogenesis and *vice versa* (Ali, Weinstein *et al*. 2005, David, Martin *et al*. 2007, Sen, Xie *et al*. 2008). For example, in age related osteoporosis, there is often an infiltration of adipose contents in the bone marrow due to a switched balance between adipocytes and

osteoblast formation (Meunier, Aaron *et al*. 1971, Rosen and Bouxsein 2006). On the other hand, the pharmacologic therapy for osteoporosis is shown to inhibit fat formation besides maintaining bone mass. In post-menopausal osteoporotic patients treated with sex hormone replacement therapy, there is also a reversal of menopause-related obesity in addition to inhibition of bone loss (Manson and Martin 2001, Sorensen, Rosenfalck *et al*. 2001).

Secondary osteoporosis is frequently observed in type II diabetic patients treated with Avandia, a member of the TZD family of insulin sensitizers and PPARγ agonists, resulting in an infiltration of adipocytes in the bone marrow in both males and females (Rzonca, Suva *et al*. 2004, Ali, Weinstein *et al*. 2005). The excessive adiposity in this condition is caused by the dysregulation of early MSC commitment leading to a switch from the osteoblastogenic to adipogenic lineages induced by TZDs through PPARγ activation (Lecka-Czernik, Moerman *et al*. 2002, Lazarenko, Rzonca *et al*. 2006). The long-term use of glucocorticoids has also been demonstrated to accelerate bone remodeling and enhance bone marrow adiposity and obesity (de Gregorio, Lacativa *et al*. 2006, Faienza, Brunetti *et al*. 2009, Brunetti, Faienza *et al*. 2013, Ventura, Brunetti *et al*. 2013). These findings further confirmed the reverse relationship between adipogenesis and osteogenesis.

On the other hand, activating mutations of lipoprotein related receptor 5 (LRP5), a co-receptor for Wnt signaling pathway, leads to higher bone mass formation in humans (Boyden, Mao *et al*. 2002, Little, Carulli *et al*. 2002, Van Wesenbeeck, Cleiren *et al*.

2003). Qiu and coworkers showed that the biopsies of iliac bones from high bone mass individuals exhibited significantly enhanced bone mass but decreased fat mass (Qiu, Andersen *et al*. 2007). They further confirmed this finding with cell lines harboring LRP5 mutations and showed that different levels of LRP5- Wnt signaling activation leads to different osteoblast and adipocyte differentiation abilities (Qiu, Andersen *et al*. 2007). These discoveries are consistent with the reverse correlation of adipogenesis and osteoblastogenesis demonstrated in osteoporosis patients as described before (Rosen and Bouxsein 2006).

Interestingly, several pathways have been shown to both positively regulate osteoblastogenesis and adipogenesis. BMPs and insulin like growth factor (IGF) signaling are well documented to induce both adipogenic and osteoblastogenic differentiation in MSCs (Wabitsch, Hauner *et al*. 1995, Chen, Ji *et al*. 1998, Kang, Song *et al*. 2009, Xian, Wu *et al*. 2012). The mechanisms that dictate MSCs commitment to one lineage *versus* the other when activated by common positive regulator are not well characterized. Our hypothesis is that cytoskeletal signaling is involved in controlling MSCs fate commitment to adipose *versus* osteoblastogenic lineage by dictating which transcription cascades will be turned on by BMP signaling.

In conclusion, adipogenesis and osteoblastogenesis are reversely correlated processes in the bone marrow and the balance between them is essential for maintaining bone homeostasis (Figure 2). Studying the mechanism of the regulation of MSCs fate

commitment may provide insights for drug targets that enhance osteoblastogenesis and inhibit adipogenesis simultaneously.

Figure 2. A brief summary of signaling pathways regulating the fate commitment of MSCs to adipose *versus* osteoblastic lineages.

The signaling pathways regulating the fate commitment of MSCs to adipose versus osteoblastic lineages are summarized in the scheme below. BMPs and IGF1 activate both adipogenesis and osteoblastogenesis. Wnt signaling and estrogen stimulate osteoblastogenesis but inhibit adipogenesis; while the TZDs and glucocorticoids (GCs) have the opposite effects. BMPs induce osteoblastogenesis through activating Smad signaling, which subsequently turns on the osteoblastogenic transcriptional cascade (Runx2 and osterix activate various osteoblastic proteins). Adipogenesis is initiated by the activation of PPARγ and C/EBPα by C/EBPβ and C/EBPδ, which act in a positive feedback loop to maintain one another's expression, thereby turning on the expression of various adipogenic proteins.

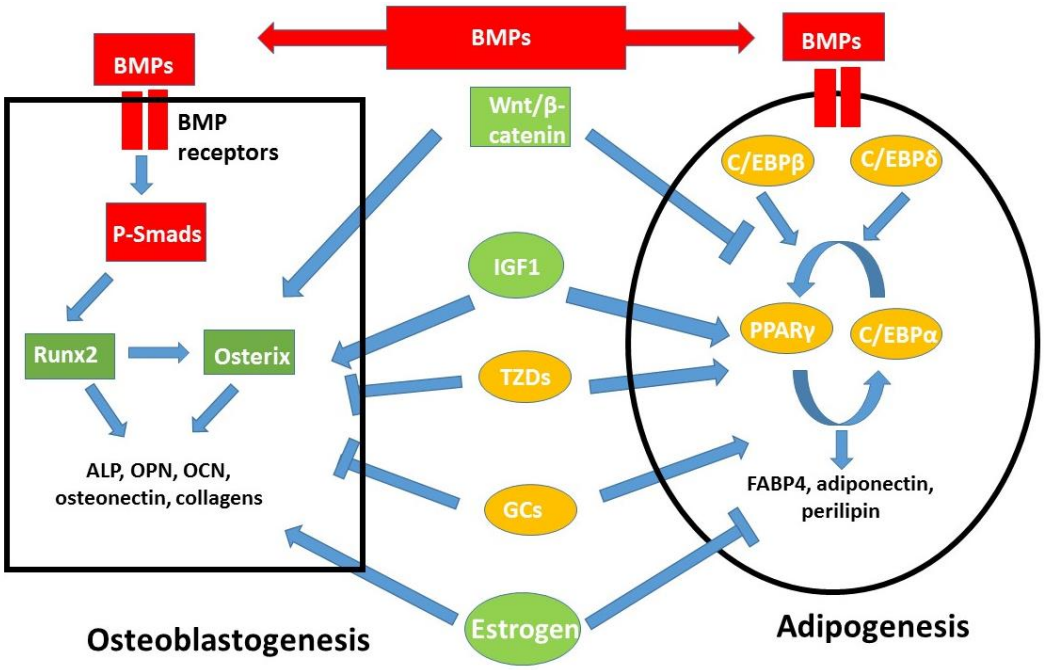

Bone Morphogenetic Proteins (BMPs) Signaling in Adipogenesis and Osteoblastogenesis

BMPs belong to the TGFβ superfamily, which is a large group of growth factors that includes about 50 genes (Ducy and Karsenty 2000, Chen, Deng *et al*. 2012). BMPs were first discovered in 1965 as osteo-inductive factors isolated from demineralized bone matrix. With the cloning of BMP2 and BMP4 in 1988 (Wozney, Rosen *et al*. 1988), multiple studies have been conducted to elucidate the function of the BMPs in skeletal tissue repair. As of 2005, BMP2 and BMP7 have already been approved for clinical uses to facilitate bone fractures healing in several countries (Reddi 2005).

BMPs are essential in embryogenesis, cartilage development and bone formation (Hogan 1996, Ducy and Karsenty 2000, Luu, Song *et al*. 2007). Knocking out BMPs in mice results in severe skeletal defects during development (Hogan 1996, Zhao 2003). *In vitro* studies also showed that BMPs promote osteoblastogenesis in myoblasts by up-regulating various osteoblastogenic proteins such as Runx2, osterix, alkaline phosphatase and osteocalcin (Katagiri, Imada *et al*. 2002, Zhao, Katagiri *et al*. 2006).

BMPs induce osteoblast differentiation through a small mothers against decapentaplegic (Smad) dependent pathway (Derynck and Zhang 2003, Shi and Massague 2003, Guo and Wu 2012). Secreted dimers of BMPs bind cooperatively to the heterodimeric complex of type I and type II BMP receptors (two transmembrane serine/threonine kinase receptors). The phosphorylated type I receptor kinase then activates Smad proteins (Smad 1/5/8) *via* phosphorylation. Phosphorylated Smad1/5/8

binds with Smad4 to form a heterodimeric complex for nuclear translocation (Kretzschmar, Liu *et al*. 1997). This complex interacts directly with Runx2, the central transcription factor for the osteoblastogenesis cascade, and regulates osteoblast gene expression (Xiao, Gopalakrishnan *et al*. 2002, Phimphilai, Zhao *et al*. 2006).

On the other hand, BMPs are also important for adipogenesis in the MSCs. Several lines of evidence have shown that BMP2, BMP4 and BMP7 bind cooperatively with other factors, can induce adipogenic differentiation through the activation of Smad signaling (Wang, Israel *et al*. 1993, Bowers, Kim *et al*. 2006). Recent investigations revealed a novel role for BMP7 in mediating the commitment of progenitors to the brown fat lineage (Tseng, Kokkotou *et al*. 2008). Different from white fat tissue, brown fat tissue is characterized by smaller adipocytes filled with multi-locular lipid droplets and abundant mitochondria, which catabolize lipid in response to cold stimulation (Cannon and Nedergaard 2004).

Kang and associates conducted a thorough study of the importance of BMPs in regulating osteoblastogenesis and adipogenesis of MSCs. BMP2, BMP4, BPM6, BMP7 and BMP9 are all shown to effectively induce both processes when over-expressed in the C3H/10T1/2 line of MSCs (Kang, Song *et al*. 2009). BMPs-induced MSCs fate commitment to each of these lineages was shown to be mutually exclusive both *in vitro* and *in vivo* (Kang, Song *et al*. 2009). Elucidation of the mechanisms underlying the BMP-regulated MSCs lineage divergence may lead to the development of preventative and therapeutic strategies for both obesity and osteoporosis. The role of BMP7 in

inducing brown fat differentiation should also be taken into consideration for combating co-development of obesity and osteoporosis.

Insulin Like Growth Factor 1 (IGF1) Signaling in Osteoblastogenesis and Adipogenesis

IGF1 was originally characterized as an insulin-like soluble growth factor that is primarily expressed in the liver, but it is also found in most peripheral tissues (Yakar, Kim *et al*. 2005, Giustina, Mazziotti *et al*. 2008, Livingstone 2013). IGF1 activates downstream cascades *via* IGF1 receptor (IGFIR) and IGF binding proteins (IGFBPs) and this signaling was shown to contribute to bone formation and remodeling (Peng, Xu *et al*. 2003, Kawai and Rosen 2009, Govoni 2012). IGF1 induces osteoblastogenesis by activating mammalian target of rapamycin (mTOR) downstream pathways (Xian, Wu *et al*. 2012). Ablation of IGF1R in mice inhibited bone formation and led to an osteoporotic phenotype (Xian, Wu *et al*. 2012). A recent study showed that serum response factor (SRF) regulates bone formation through IGF1 expression and Runx2 transcription activity (Chen, Yuan *et al*. 2012).

Interestingly, IGF1 has also been found to promote adipogenesis by promoting the proliferation of adipogenic progenitors (Wabitsch, Hauner *et al*. 1995). IGF1 also regulates adipogenic differentiation through the phosphorylation of Akt1 (Protein Kinase B 1) and Akt2 (Protein Kinase B 2) (Peng, Xu *et al*. 2003). IGF1R has been demonstrated

to act downstream of advanced glycation end product (AGEs) signaling to promote adipogenesis in 3T3-L1 cells (Yang, Chen *et al*. 2013).

Cell Shape Regulates MSCs Fate Commitment

During the differentiation of MSCs, the cell morphology changes significantly in order to serve the specialized functions in different tissues (McBeath, Pirone *et al*. 2004). The adipocytes are round and lipid laden, a source of stored energy (Gregoire, Smas *et al*. 1998), while the osteoblasts become spread and flattened for bone remodeling and mineral deposition (Sikavitsas, Temenoff *et al*. 2001). These differences of cellular morphologies are reported to be caused by the differences in the expression and organizations of cadherins, integrins and cytoskeleton proteins (Gumbiner 1996).

While some reports state that differentiation of MSCs affects cell shape (Spiegelman and Farmer 1982), previous studies have also demonstrated that it is the changes in cell morphology that affect the differentiation of adipogenic 3T3-422A fibroblasts to mature adipocytes (Spiegelman and Farmer 1982, Spiegelman and Ginty 1983). When pre-committed adipogenic 3T3-422A cells are allowed to attach to fibronectin-coated surfaces, the adipogenic differentiation is impaired as shown by inhibition of adipogenic gene expression and poor lipid droplet formation. These effects are rescued by disturbing the actin cytoskeleton organization (Spiegelman and Ginty 1983). In contrast, an increase in cell spreading has been found to enhance

osteoblastogenesis with increased osteocalcin and osteopontin expression (Carvalho, Schaffer *et al*. 1998, Thomas, Collier *et al*. 2002).

The role of cell morphological changes in regulating early commitment of MSCs has also been investigated by manipulating the degree of cell spreading and cell shape. McBeath used a micro-patterning technique to produce adhesive surfaces with different surface areas to manipulate the spreading of single human bone marrow MSCs (hMSCs) (McBeath, Pirone *et al*. 2004). HMSCs preferentially differentiate into adipocytes *versus* osteoblasts when attached to smaller fibronectin islands segregated by non-adhesive materials when given both adipogenic and osteoblastogenic growth factors. In contrast, the hMSCs on larger fibronectin islands differentiate into osteoblasts rather than adipocytes (McBeath, Pirone *et al*. 2004). This switch of lineage commitment is regulated by Ras homolog gene family, member A (RhoA) activity through the Rho-associated protein kinase (ROCK) pathway. In fact, over-expression of RhoA in hMSCs enhances osteoblastogenesis, while over-expression of dominant-negative RhoA reverses this phenotype. The change in the activity of RhoA is sufficient to bypass the effects of differentiation inducers and dictate the commitment of MSCs to osteoblasts *versus* adipocytes (McBeath, Pirone *et al*. 2004).

The transcriptional coactivator of Yes-associated protein (YAP), PDZ-binding motif (TAZ), has also been shown to regulate MSC commitment by inhibiting adipogenesis and enhancing osteogenesis (Hong, Hwang *et al*. 2005). Because the activity of TAZ-YAP signaling is closely associated with actin cytoskeleton polymerization (Kanai, Marignani *et al*. 2000), there may be a potential indirect

interaction between MRTFA (Myocardin-Related Transcription Factor A) –SRF (Serum Response Factor) and TAZ-YAP through actin dynamics in the regulation of MSCs fate commitment (Mendez and Janmey 2012). In summary, cell shape and cytoskeleton signaling regulate the early commitment of MSCs but the molecular mechanisms of these regulations remain to be elucidated.

Rho ROCK Signaling Pathway

The Rho family of GTPases are central regulators of cell motility functions such as cell migration, adhesion, spreading and polarization. This family includes Rho, Ras-related C3 botulinum toxin substrate (Rac) and cell division control protein 42 homolog (Cdc42) subfamilies, (Jaffe and Hall 2005). They regulate the polymerization dynamics of G-actin (globular actin) and F-actin (filamentous actin) *via* several downstream effectors (Pollard 2007, Le Clainche and Carlier 2008). Rho GTPases promote actin polymerization through two mechanisms. Rac and Cdc42 can activate actin-related protein 2/3 (Arp2/3) through Wiskott-Aldrich syndrome protein (WASP) family members to initiate new branched actin filament formation (Ho, Rohatgi *et al*. 2004, Millard, Sharp *et al*. 2004). The other mechanism is mediated by Rho to activate formin family members, thereby increasing linear polymerization of actin filaments by adding monomers to the barbed ends (Zigmond 2004).

Extracellular stimuli activate Rho GTPases through Rho guanine nucleotide exchange factors (GEFs) (Jaffe and Hall 2005). Rho GTPases are activated by the exchange of GDP for GTP, which leads to conformational changes in inactive

downstream effectors (Schmidt and Hall 2002). Well-characterized downstream effectors of Rho GTPase include serine/threonine kinases and tyrosine kinases (Jaffe and Hall 2005).

Activation of Rho GTPases promotes polymerization of G-actin into F-actin filaments mainly through ROCK and formins (Zigmond 2004). When cytoplasmic G-actin levels decrease, myocardin-related transcription factors (MRTFs) are released from their association with G-actin for translocation into the nucleus. MRTFs bind and co-activate SRF, thereby inducing cytoskeletal gene expression (Sotiropoulos, Gineitis *et al*. 1999, Schratt, Philippar *et al*. 2002, Posern and Treisman 2006). These target genes are characterized as SRF class II target genes, including actin itself as well as several actin-binding proteins which can regulate actin dynamics and cell motility (Norman, Runswick *et al*. 1988, Miralles, Posern *et al*. 2003). These newly synthesized proteins then elevate the cytoplasmic G-actin levels thereby providing a negative feedback loop by retaining MRTFs in the cytoplasm where it binds to G-actin (Vartiainen, Guettler *et al*. 2007). This regulatory circuit consisting of RhoA-ROCK-actin-MRTF-SRF is essential for the actin polymerization based cell motility functions (Olson and Nordheim 2010).

Serum Response Factor (SRF)

SRF is ubiquitously expressed in many cell types and it's encoded by a single gene (Treisman 1986, Norman, Runswick *et al*. 1988). As a member of MADS-box (a conserved sequence motif found in MADS-box family genes) family, SRF is highly conserved from yeast to humans (Norman, Runswick *et al*. 1988, Shore and Sharrocks

1995). Homodimers of SRF regulate gene expression by specifically binding to CC (A/T)$_6$GG *cis* elements, identified as CArG-boxes (Treisman 1986, Norman, Runswick *et al*. 1988, Sun, Chen *et al*. 2006).

Although the basal transcriptional activity of SRF is relatively low in cells, the binding and interaction with over 60 co-activators strongly potentiates target gene activation (Miano 2003, Benson, Zhou *et al*. 2011). These co-activators can be categorized into two classes according to the functions of their target genes: Ternary complex factor (TCF) co-activators (Shaw, Schroter *et al*. 1989) and the myocardin family co-activators (Chang, Rickers-Haunerland *et al*. 2001, Wang, Chang *et al*. 2001). These two classes of co-factors bind to SRF and potently co-activate approximately 300 target genes (Gineitis and Treisman 2001).

mitogen activated protein (MAP) kinase phosphorylation activates members of the TCF family (Treisman 1986) E26 transformation-specific (Ets) type co-activators, including ETS-domain protein-1 (Elk-1), SRF accessory protein 1 (SAP1) and SRF accessory protein 2 (SAP2) (Hipskind, Rao *et al*. 1991, Dalton and Treisman 1992). These co-activators bind to SRF and strongly activate the immediate early genes including c-fos when induced with serum stimulation (Shaw, Schroter *et al*. 1989, Janknecht, Ernst *et al*. 1993). The second type of co-activators is the myocardin family, myocardin and MRTFs. Myocardin is mostly expressed in smooth muscle and cardiac tissue (Wang, Chang *et al*. 2001, Wang, Wang *et al*. 2003, Creemers, Sutherland *et al*. 2006), while MRTFA and MRTFB are more universally expressed (Ma, Morris *et al*. 2001, Wang, Li *et al*. 2002). These co-activators have been shown to strongly potentiate

SRF-induced transcriptional activation of multiple smooth muscle and contractile genes *in vivo* and *in vitro* (Wang, Li *et al*. 2002, Du, Ip *et al*. 2003, Li, Wang *et al*. 2003, Small, Warkman *et al*. 2005). In addition, the Nkx2-5 family of homeodomain proteins and the GATA family of zinc finger transcription factors positively regulate SRF transcription activity as co-factors (Chen and Schwartz 1996, Belaguli, Sepulveda *et al*. 2000, Sepulveda, Vlahopoulos *et al*. 2002). How these different co-activators work together to orchestrate SRF transcription activity during complex differentiation and development processes remains to be elucidated (Posern and Treisman 2006).

The functions of SRF have been studied extensively in different model organisms and different organs in mice (Miano, Long *et al*. 2007). The SRF global deletion mice are not viable due to impaired gastrulation and defects in embryonic tissue layer migration before organogenesis even initiates (Arsenian, Weinhold *et al*. 1998). Deletion of SRF conditionally in mice has demonstrated essential functions of SRF in almost all organs (Miano 2010). For example, deletion of SRF in embryonic hearts inhibits cardiogenesis by reducing the transcription of cardiogenic genes (Niu, Yu *et al*. 2005). Mosaic inactivation of SRF specifically in cardiac myocytes leads to significant inhibition of smooth muscle protein and contractile protein expression resulting in focal lesions and heart failure in mice (Parlakian, Charvet *et al*. 2005, Gary-Bobo, Parlakian *et al*. 2008). Deletion of SRF in skeletal muscle leads to marked decrease in muscle mass and disrupted sarcomeres (Charvet, Houbron *et al*. 2006). Tissue specific deletion of SRF in hepatocytes causes an abnormality in liver regeneration following partial hepatectomy, although the livers of SRF deletion mice are normal at birth (Latasa, Couton *et al*. 2007,

Sun, Battle *et al*. 2009). SRF deletion in neurons results in compromised neuronal migration due to disrupted actin cytoskeleton (Alberti, Krause *et al*. 2005, Knoll, Kretz *et al*. 2006). *In vivo* and *in vitro* results suggest an essential role for SRF in T-cell maturation and megakaryocytes functions as well (Fleige, Alberti *et al*. 2007, Halene, Gao *et al*. 2010). The functions of SRF in these tissues are mostly associated with the regulation of cell motility and contractility by regulating the actin cytoskeleton dynamics (Miano 2010).

A previous study identified SRF as a positive regulator of bone mass maintenance (Chen, Yuan *et al*. 2012). The tissue specific deletion of SRF in mice leads to a significant decrease in bone mineral density and compromised bone formation. SRF is regulating skeletal homeostasis *via* IGF-1 expression and RUNX2 trans-activation activity (Chen, Yuan *et al*. 2012). Whether MRTFA is also involved in SRF regulated bone formation is still not determined. On the other hand, by transducing 3T3-L1 cells with shRNA, SRF was shown to be a negative regulator for adipogenesis. Knocking down SRF enhances lipid droplet formation and adipogenic gene expression (Mikkelsen, Xu *et al*. 2010).

In summary, SRF is an essential transcription factor that is potently co-activated by two classes of co-factors to activate the downstream immediate response genes or smooth muscle contractile genes (Figure 3). Previous evidence identified SRF as a positive regulator of bone formation but a negative regulator of adipogenesis, thus we propose that SRF important for the regulation of early MSC commitment downstream of

Rho-ROCK-actin and that MRTFs might be involved in this regulation as co-activators of SRF.

Figure 3. MRTFs and TCFs potentiate SRF transcriptional activity in response to different signaling pathways.

RhoA promotes actin polymerization through ROCK and formin, while Rac and Cdc42 achieve the same effect *via* WASP-Arp2/3 pathway. The polymerization of G-actin liberates G-actin bound MRTFs which translocate into the nucleus and co-activate SRF target genes such as actin itself and actin binding proteins (ABPs) to regulate actin dynamics. On the other hand, upon activation by the Ras-Raf-MEK-Erk pathway, TCF complexes bind to SRF to co-activate immediate response genes such as c-fos.

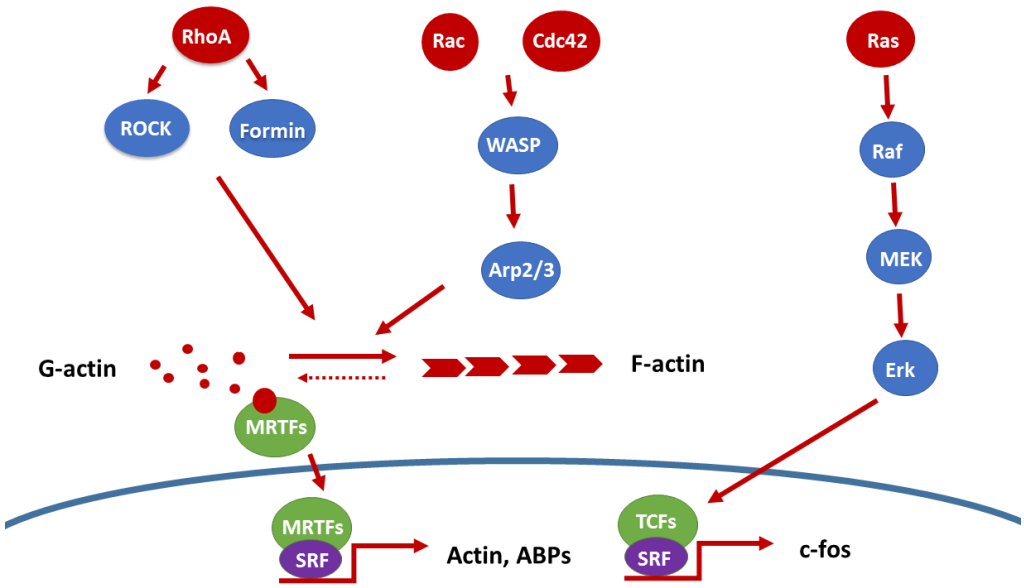

Myocardin-related Transcription Factors (MRTFs)

MRTFs belong to the myocardin family that includes myocardin, MRTFA and MRTFB (Wang, Li *et al*. 2002, Olson and Nordheim 2010). While the expression of myocardin is primarily in cardiac myocytes and smooth muscle cells (Wang, Chang *et al*. 2001, Du, Ip *et al*. 2003), MRTFA and MRTFB are more widely expressed in different cell types (Wang, Li *et al*. 2002). MRTFA gene expression has been observed in embryonic stem cells and fibroblasts and it is highly abundant in MSCs, muscle cells and epithelial cells during embryogenesis. MRTFA has also been demonstrated to co-express with myocardin in human heart (Wang, Li *et al*. 2002, Du, Chen *et al*. 2004). MRTFB is enriched in the epithelial cells of the kidney, lung and testis during embryogenesis (Wang, Li *et al*. 2002).

There is about 35% similarity for the amino acid sequences of the three family members, with several common conserved domains (Wang, Li *et al*. 2002). The most conserved domain is the RPxxxEL (RPEL) motif-containing domain in the N-terminus of the proteins. RPEL domains have been shown to regulate the interaction between MRTFs and G-actin monomers (Miralles, Posern *et al*. 2003, Posern, Miralles *et al*. 2004, Guettler, Vartiainen *et al*. 2008, Mouilleron, Guettler *et al*. 2008). The divergence of the sequence in the RPEL domain of myocardin abolishes its ability to bind with G-actin. As a result, the cellular localization of myocardin is not regulated by G-actin levels. In fact, myocardin is only present in the nucleus without nucleus-cytoplasm shuttling (Pipes, Creemers *et al*. 2006). Nevertheless, the activity of myocardin can be regulated indirectly by actin polymerization through heterodimerization with MRTFs through a conserved

leucine zipper domain (Wang, Wang *et al*. 2003). The B1 domain (a conserved domain found in the sequences of myocardin family members), located in between a basic domain and a glutamine-rich domain, is responsible for binding to SRF (Wang, Chang *et al*. 2001). SAF-A/B, Acinus, and PIAS (SAP) domain is also a conserved region in myocardin and MRTFs that promote the induction of SRF target gene expression (Aravind and Koonin 2000, Wang, Chang *et al*. 2001). The transcription activation domain (TAD) in the C-terminus of these proteins is essential for the co-activation activity (Wang, Li *et al*. 2002). The dominant negative variants of MRTFs and SRF used in previous studies are truncated variants without the TAD domain (Chang, Wei *et al*. 2003, Luchsinger, Patenaude *et al*. 2011).

Myocardin and MRTFs are shown to be essential for development of various tissues by genetic studies using myocardin and MRTFs knockout mice (Oh, Richardson *et al*. 2005, Li, Chang *et al*. 2006, Sun, Boyd *et al*. 2006, Huang, Cheng *et al*. 2008, Huang, Min Lu *et al*. 2009). Previous studies conducted by Huang and coworkers showed the importance of myocardin in regulating the transcription of cell contractility genes in both cardiomyocytes and smooth muscle cells (Huang, Cheng *et al*. 2008, Huang, Min Lu *et al*. 2009). MRTFB deletion in mice results in embryonic death due to severe defects in cardiac neuronal crest development (Oh, Richardson *et al*. 2005). The MRTFA null mice are viable, fertile and appear normal compared to the WT mice. However, the female MRTFA KO mice fail to nurse their pups normally due to an inability to produce milk, which is caused by defects in the mammary myoepithelial cell development and premature apoptosis in these cells (Li, Chang *et al*. 2006, Sun, Boyd *et al*. 2006).

The nucleus-cytoplasm shuttling of MRTFs is an essential component of the regulation the MRTF transcriptional activation functions. Recent studies showed that MRTFA is a negative regulator of adipogenesis *via* regulation of actin cytoskeleton dynamics (Nobusue, Onishi *et al*. 2014, McDonald, Li *et al*. 2015). MRTFA may play a similar role in the early lineage commitment of the bone marrow MSCs to osteoblasts *versus* adipocytes.

Summary

Osteoporosis is a pressing public health issue consequent to the loss of bone mass and deterioration of bone micro-structure. Bone marrow adiposity often develops simultaneously with osteoporosis due to inappropriate MSCs fate switching to adipose *versus* osteoblastic lineage. Understanding the underlying mechanisms of early MSCs fate commitment may lead to the identification of potential drug targets for both obesity and osteoporosis.

Cell shape has been shown to regulate the commitment of MSCs through Rho-ROCK signaling pathway (McBeath, Pirone *et al*. 2004). In this study, we investigated whether the actin-MRTFA-SRF circuit acts downstream of the Rho-ROCK pathway to promote osteoblastogenesis and inhibit adipogenesis. By evaluating the phenotypes of MRTFA KO (MRTFA KO) mice, we investigated the role of MRTFA in bone formation. Furthermore, we used bone marrow derived MSCs from these mice to study whether MRTFA regulates the early commitment of MSCs. Finally, to further demonstrate the role of MRTFA-actin-SRF in MSCs fate switch, we investigated how adipogenesis and

osteoblastogenesis are affected in C3H/10T1/2 MSC lines that stably over-express MRTFA, SRF and their dominant negative variants.

MATERIALS AND METHODS

Materials

Dulbecco's Modified Eagle's Medium (DMEM) with 4.5 g/L glucose (Mediatech, Inc; Herndon, VA) was supplemented with 10% fetal bovine serum (Life Technologies, Grand Island, NY) and 1% penicillin/streptomycin (Mediatch, Inc; Manassas, VA). Minimum Essential Medium, Alpha 1X (α-MEM) with Earle's salts, ribonucleosides, deoxyribonucleosides & L-glutamine was obtained from Mediatch, Inc. (Manassas, VA) and was also supplemented with 10% fetal bovine serum and 1% penicillin/streptomycin as mentioned above. Dexamethasone, indomethacin, 3-isobutyl-methylxanthine, T3, 2-Phospho-L-ascorbic acid trisodium salt and Alizarin Red S powder was obtained from Sigma-Aldrich (St. Louis, MO). β-Glycerophosphate, Disodium Salt, Pentahydrate were purchased from Santa Cruz Biotechnology (Dallas, TX). Recombinant insulin and TRIzol reagents were purchased from Life Technologies (Carlsbad, CA). Recombinant BMP7 and TGFβ1 proteins were purchased from R&D Technologies (North Kingstown, RI). Halt protease inhibitor cocktail was purchased from Pierce (Rockford, IL). CCG1423 compound was purchased from Cayman Chemical Company (Ann Arbor, MI). C3H10T1/2 cells were purchased from the American Type Culture Collection (Manassas, VA).

Animals

All the studies and experimental procedures were approved and supervised by the Institutional Animal Care and Use Committee of Boston University. The breeding and experimental procedures were set up properly according to the Guidelines for Care and Use of Laboratory Animals by the National Institute of Health. The MRTFA$^{+/-}$ and WT mice (mixed C57BL/6J 129 genetic background generated by Dr. Barbara Smith's Laboratory, Boston University School of Medicine) were originally generated by Dr. Eric Olson, UT Southwestern Medical Center (Li, Chang *et al*. 2006) and were given to us as a kind gift. All mice were kept in a 12 hour light/dark cycle at 23°C with free access to normal chow in the Boston University Laboratory Animal Science Center (McDonald, Li *et al*. 2015). Age-, strain- and sex- matched WT mice were used in all experiments as controls for the MRTFA KO mice.

For the micro-computed tomography (Micro-CT) studies, the femur samples were isolated from adult males between the ages of 15-17 weeks old and adult females between the ages of 23-24 weeks. Some of these femur samples were then decalcified for histological studies. All the bone marrow-derived MSCs used for *ex vivo* studies, mRNA and protein samples of total femurs were isolated from matched male and female mice between the ages of 8 to 12 weeks old.

For the diet studies, 4-6 week old male WT and MRTFA KO mice were fed with a diet with 10% kcal% fat [low fat diet (LFD), Research Diets Inc., D12450B] or a diet with 60% kcal% fat [high fat diet (HFD), Research Diets Inc., D12492] for 6 weeks. The

femurs of these mice were then harvested for Micro-CT studies. Serum samples were also collected from these mice by placing the blood drawn from the hearts into anti-coagulate blood collection tubes. These blood samples were placed on ice for 30 minutes and then spun for 90 seconds at 1,500 x g to separate the serum for ELISA assays.

Quantitative Micro-Computed Tomography (Micro-CT) Analysis

Mice femurs were harvested, fixed in 4% formaldehyde for 5 days and then placed in PBS at 4°C for experiments. Scans were performed using a Scanco micro-CT 40 system (Scanco Medical, Basserdorf, Switzerland) located in the Orthopedic and Developmental Biomechanics Laboratory at Boston University (assisted by Dr. Elise Morgan, Zackery Webster and Gabriel McDonald). These scans were performed using 12 micron voxel size resolution with 200 ms integration time, under conditions of 55 E (KVp) and 145 I (μA). Transverse images scanned by the micro-CT were then traced manually with a computer program and stacked to render a 3D image of the cortical and trabecular femurs from WT or MRTFA KO mice (Bouxsein, Boyd *et al*. 2010).

For trabecular bone analysis, the metaphysis was identified by starting the scans 4 mm from the distal end of the femurs and taking 130 slices (at 12 μm per slice) distally for a total scanned region of 1.6 mm. The trabecular bone was quantitatively analyzed using a semi-automated segmentation protocol with a fixed threshold of 225 (for male mice) or 188 (for female mice). The total volume, bone volume, trabecular thickness,

trabecular number, connectivity density, trabecular separation, average bone mineral density and total tissue mineral density were calculated according to the standard algorithms provided by the system manufacturer.

For cortical bone analysis, the mid-diaphyseal region was located half way along the length of the bone and a total of 50 slices (12 μm/slice) within a region of 0.6mm (25 slices above and below the mid-point) were scanned. The cortical bone was separated for quantitative analysis using a semi-automated segmentation protocol with a fixed threshold of 250 (for male mice) or 220 (for female mice). The total bone volume, cortical bone volume, cortical thickness and average bone mineral density were calculated according to the standard algorithms provided by the system manufacturer. 3D images of both the trabecular and cortical bone of the mentioned mice were then generated for comparison of bone morphology between WT and MRTFA KO mice.

DNA Isolation and Genotyping by PCR

Mouse tails were cut (approximately 2mm) and digested in 300 μl of 50 mM NaOH at 95°C for 90 minutes to 120 minutes (vortex vigorously every 20-30 minutes). 30μl of 1M Tris (PH=8) and 250 μl of Phenol: Chloroform were added followed by vigorous vortexing. The samples were centrifuged at 15000 x g at 4°C for 5 minutes and the supernatant was collected. To the supernatant, 300 μl of isopropanol and 30 μl sodium acetate (PH 5.2) were added followed by vigorous vortexing. These samples were then centrifuged at maximum speed for 20 minutes. The supernatant was discarded and

the precipitation was washed with 500 μl of cold 70% ethanol (spin at maximum speed for 5 minutes). After the second centrifugation, the supernatant was discanted and the pellet was left in the chemical hood for air-drying. The genome DNA was then re-suspended in 250 μl of Tris-low-EDTA buffer and the DNA concentration was measured by spectrophotometry.

To screen for MRTFA WT and KO alleles, primers were designed to amplify the WT fragment (600bp) and KO fragment (350bp). For PCR, 120ng of DNA was added to 10 μl of GoTaq Green Master Mix (Promega), 4 μl H_2O, 2 μl of 1 μM GT5 sense primer, 1 μl of 1 uM GT6 anti-sense primer and 1 μl anti-sense primer LacZ3-QB for 2 minutes at 94°C and then followed by 30 cycles of 20 seconds at 94°C, 30 seconds at 57°C and 45 seconds at 72°C. Finally, after 1 minute of incubation at 72°C, WT allele fragment of about 600 nucleotides and KO allele fragment of about 350 nucleotides were generated and then detected by electrophoresis on a 1% agarose gel to determine the genotypes of the mice.

Histology

Mice femurs and tibiae were dissected, fixed in 4% formaldehyde for 5 days and then decalcified in 14% w/v EDTA dissolved in water for another 5 days. These samples were embedded in paraffin and sectioned (5 um section thickness) by Boston University's Experimental Pathology Laboratory Services Core (Cheryl Spencer) (Carroll, Wigner *et al*. 2012). Sections of the femurs and tibiae were then de-paraffinized, rehydrated and

stained with Hematoxylin & Eosin to visualize the bone mass and marrow contents. Bright field images were obtained by light microscope.

ELISA Assays

The Enzyme-Linked Immunosorbent Assay (ELISA) Kit (SEA957Mu 96 tests) for Procollagen I N-Terminal Propeptide (PINP) for mouse serum was purchased from Cloud-Clone Corp. (Houston, TX). The assays were performed according to the manufacturer's instructional manual. Both the freshly diluted standards and diluted serum samples were incubated in the provided ELSA kit wells for 2 hours at 37°C. Liquid was removed without washing and 100 μl biotinylated detection antibody were added to each well for 1 hour incubation at 37°C. After adequate washing, 100 μl HRP (Horseradish Peroxidase) conjugate were added for 30 minutes at 37°C. Following adequate washing, 90 μl of substrate solution were added to the wells for 15 -25 minutes at 37°C and then 50 μl of stop solution was added for optical density (OD) values reading using a micro-plate reader set to 450 nm. Using the best fitting curved created with the values generated from the diluted standards, the concentrations of PINP in each sample were calculated. The ELISA assay (E-EL-M0366 96 tests) for the Mouse Cross Linked C-telopeptide of Type I Collage (CTX-1) (Purchased from Elabscience, Wuhan, P.R.C.) was also performed according similar instructions provided by the manufactures.

Cell Culture and Treatments

C3H/10T1/2 cells were obtained from the American Type Culture Collection and maintained at 37°C and 5% CO_2 in a cell culture incubator. For adipogenic induction, at confluence, cells were induced to differentiate in DMEM supplemented with 10% FBS, 5 μM dexamethasone, 0.5 mM isobutylmethylxanthine (IBMX), 860 nM insulin, 1 nM 3, 3, 5-triiodo-L-thyronine (T3), and 125 μM indomethacin. 48 hours post induction; the cells were maintained in medium containing 10% FBS, 860 nM insulin, and 1 nM T3 for another 6 days (McDonald, Li *et al*. 2015). For osteoblastogenic induction, after the cells reached confluence, they were treated with DMEM supplemented with 10%FBS, 5 nM dexamethasone, 50μM L-ascorbic acid and 8 mM β-glycerophosphate, disodium salt for 21 days (Carroll, Wigner *et al*. 2012) (Figure 4).

Figure 4. A scheme for adipogenic and osteoblastogenic differentiation in C3H/10T1/2 cells.

For adipogenic differentiation, the cells were induced at confluence with 5 µM dexamethasone, 0.5 mM IBMX, 860 nM insulin, 1 nM 3, 3, 5-triiodo-L-thyronine (T3), and 125 µM indomethacin. 48 hours post induction; the cells were kept in medium containing 860 nM insulin, and 1 nM T3 for another 6 days. BMP4 or BMP7 were added to the cells three days prior to adipogenic induction for activating brown fat genes. For osteoblastogenic induction, after the cells reached confluence, they were induced with 5 nM dexamethasone, 50µM L-ascorbic acid and 8 mM β-glycerophosphate, disodium salt for 21 days (Caplan and Bruder 2001).

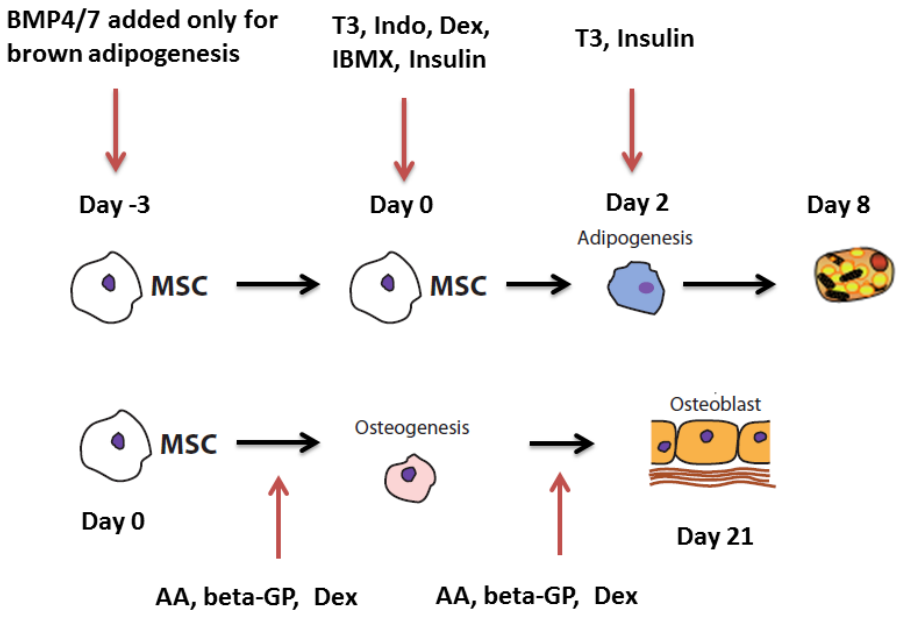

Adopted from Caplan et al., 2010

Plasmids and Viral Transduction

MRTFA, DN-MRTFA, SRF and DN-SRF cDNAs (Chang, Wei *et al*. 2003, Luchsinger, Patenaude *et al*. 2011) were kind gifts from Dr. Matthew Layne (Boston University School of Medicine). The fragments of these cDNAs were enzymatically digested out of the original plasmids at Hind III sites and then sub-cloned into the pMSCV retroviral vector (Clontech) by ligation at the Hind III sites. MRTFA, DN-MRTFA cDNA were tagged with FLAG-tag at the C-Terminus. FLAG tags were also added *via* PCR to the C-Terminus of SRF and DN-SRF cDNA (Figure 5).

EcoPack (Clontech) packaging cells were used for retrovirus production. These cells were transfected at 70% confluence by using Lipofectamine LTX and Plus Reagent (Invitrogen) and 8 μg of the respective pMSCV vectors. The viral supernatant was harvested and filtered with 0.45um filters 48 hours after the transfection. 50% confluence C3H/10T1/2 cells were incubated for 12 hours with the viral supernatant containing 10 μg/mL polybrene. These cells were then selected with 350 μg/mL hygromycin over 3-4 passages to establish stable over-expression cell lines of the mentioned proteins.

Figure 5. MRTFA, DN-MRTFA, SRF and DN-SRF over-expressing plasmids.

MRTFA, SRF and their truncated variants without the transcription activation domain (TAD) in the C-terminus were sub-cloned in pMSCV retroviral vector (Clontech). Retro virus was produced to infect C3H/10T1/2 cells to establish stable over-expression cell lines. The DN-MRTFA has 630 amino acids, while DN-SRF has 266 amino acids (Olson and Nordheim 2010).

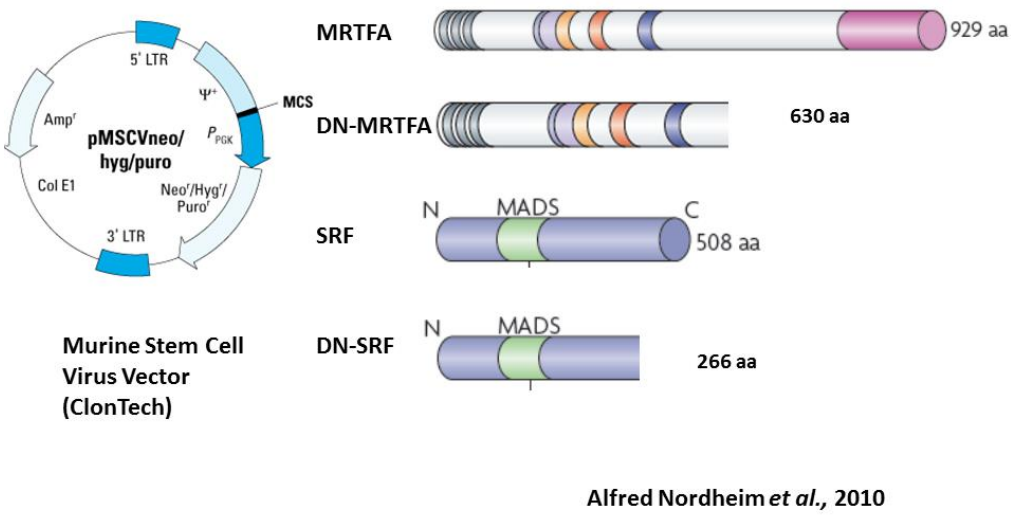

Isolation and Differentiation of Bone Marrow Mesenchymal Stem Cells (BM-MSCs)

WT and MRTFA KO mice were euthanized and their femurs and tibiae were extracted without the soft tissues. The bone marrow cavity contents were flushed out with a 23G needle attached to a 10ml syringe containing αMEM growth media. The bone marrow contents were re-suspended and filtered using 100um cell strainers. The cells, which passed through the strainers, were counted and plated without being disturbed until day 4 of culture when half of the media was replaced. On day 6 of culture, for the osteoblastogenic induction, these cells were treated with αMEM containing 10%FBS, 5 nM dexamethasone, 50 µM L-ascorbic acid and 8 mM β-glycerophosphate, disodium salt for 21 days (Carroll, Wigner *et al*. 2012). For the adipogenic induction, the cells were treated with αMEM supplemented with 10% FBS, 5 µM dexamethasone, 0.5 mM isobutylmethylxanthine, 860 nM insulin, 1 nM 3, 3, 5-triiodo-L-thyronine (T3), and 125 µM indomethacin. 48 hours post induction; the cells were maintained in medium containing 10% FBS, 860 nM insulin, and 1 nM T3 for another 6 days. For SRF inhibition experiments, 1 mM CCG1423 (Cayman Chemicals) was added to the cells for 3 days prior to induction of adipogenic induction, while 1mM CCG1423 were supplemented in the osteoblastogenic induction media for 21 days.

Quantitative Reverse Transcription-based Polymerase Chain Reaction (RT-PCR)

Total RNA was isolated from C3H10T1/2 cells or tissues using TRIzol reagent (Life Technologies), chloroform was added to the TRIzol extracted samples followed with vigorous vortexing. The milky mixture was then centrifuged at 14,000 X g for 15

minutes, after which the aqueous phase of the mixture was removed without disturbing the white protein layer. Isopropanol was then added to the aqueous phase followed by vigorous vortexing and then the mixture was placed at -20°C for 2 hours for RNA precipitation. After 10 minutes of centrifugation at 14,000 X g, the supernatant was discarded and the RNA pellets were left behind for air-drying in the chemical fume hood (McDonald, Li *et al*. 2015). The RNA pellets were then dissolved in 14-20 µl nuclease-free water and quantified with a Nano Drop machine (Varelas Laboratory, BUSM) for RT-PCR reactions.

Mice femurs were dissected and the soft tissues were removed as much as possible. These femurs were snap-frozen in liquid nitrogen after sample collection and then pulverized in liquid nitrogen using a mortar and pestle. The pulverized samples were then placed in RNA extraction buffer RLT buffer (RNeasy Mini Kit) and the RNA extraction process was performed according to the manufacturer's instruction.

Reverse Transcriptase (RT) reactions were performed using 2 µg RNA from either C3H10T1/2 cells or tissues and a high-capacity cDNA RT Kit (Applied Biosystems) according to the manufacturer's instructions. RT random primers, RT buffer provided by the kit, high-capacity reverse transcriptase and dNTP were added to each RT reaction according to the suggested concentrations provided by the instructional manual.

Diluted cDNA was used for Quantitative RT-PCR in 96-well plates performed with the Fermentas Maxima SYBR Grenn RT-PCR Master Mix (Fermentas Life Sciences) in the ABI Prism 7300 sequence detector. The PCR program used was consisted of with an initial denaturation step at 95°C for ten minutes, followed with a

denaturation step for 15 seconds at 95℃, a 20 second annealing step at 60℃, and a 30 second elongation step for 30 seconds for a total of 40 cycles. SYBR green fluorescence emissions were quantified at the end of each cycle for evaluating the mRNA levels. mRNA levels of genes were calculated by normalizing to the level of Gapdh. Primer sequences used for RT-PCR analysis are listed as follows:

Acta-F: 5’-GTCCCAGACATCAGGGAGTAA-3’

Acta-R: 5’-TCGGATACTTCAGCGTCAGGA-3’

Adipoq-F: 5’-TGTTCCTCTTAATCCTGCCCA-3'

Adipoq-R: 5’-CCAACCTGCACAAGTTCCCTT-3’

Alpl-F: 5’- GCACCTGCCTTACCAACTCT-3’

Alpl -R: 5’-TGGAGTTTCAGGGCATTTTT-3’

Bglap-F: 5’-CTGACCTCACAGATGCCAAG-3’

Bglap-R: 5’-GTAGCGCCGGAGTCTGTTC-3’

Cebpa-F: 5’-CAAGAACAGCAACGAGTACCG-3’

Cebpa-R: 5’-GTCACTGGTCAACTCCAGCAC-3’

Cidea-F: 5’-TGCTCTTCTGTATCGCCCAGT-3’

Cidea-R: 5’-GCCGTGTTAAGGAATCTGCTG-3’

Col1a1-F: 5’-GCTCCTCTTAGGGGCCACT-3’

Col1a1-R: 5’-CCACGTCTCACCATTGGGG-3’

Col3a1-F: 5’-CTGTAACATGGAAACTGGGGAAA-3’

Col3a1-R: 5’-CCATAGCTGAACTGAAAACCACC-3’

Cox7a1-F: 5’-GCTCTGGTCCGGTCTTTTAGC-3’

Cox7a1-R: 5’-GTACTGGGAGGTCATTGTCGG-3’

Elovl3-F: 5’-TTCTCACGCGGGTTAAAAATGG-3’

Elovl3-R: 5’-GAGCAACAGATAGACGACCAC-3’

Fabp3-F: 5’-AGTCACTGGTGACGCTGGACG-3’

Fabp3-R: 5’-AGGCAGCATGGTGCTGAGCTG-3’

Fabp4-F: 5’-AAGGTGAAGAGCATCATAACCCT-3’

Fabp4-R: 5’-TCACGCCTTTCATAACACATTCC-3’

Gapdh-F: 5’-AGGTCGGTGTGAACGGATTTG-3’

Gapdh-R: 5’-TGTAGACCATGTAGTTGAGGTCA-3’

Igf1-F: 5’- TGACATCCGCAACGACTATCA-3’

Igf1-R: 5’- CCAGTGCGTAGTTGTAGAAGAGT-3’

Igf1r-F: 5’- TGACATCCGCAACGACTATCA-3’

Igf1r-R: 5’- CCAGTGCGTAGTTGTAGAAGAGT-3’

Mrtfa-F: 5’- AGGACCGAGGACTATTTGAAACG-3’

Mrtfa-R: 5’-CCACAATGATAGCCTCCTTCAG-3’

Mrtfb-F: 5’-ATGCCTTGAGGGAAGCAACC-3’

Mrtfb-R: 5’-GCTCGCTCCAGGCTTTTTATC-3’

Plin-F: 5’-ATGTCAATGAACAAGGGCCCAACC-3’

Plin-R: 5’-TGGTGCTGTTGTAGGTCTTCTGGA-3’

Pparg-F: 5’-TCAGCTCTGTGGACCTCTCC-3’

Pparg-R: 5’-ACCCTTGCATCCTTCACAAG-3’

Runx2-F: 5’-CGAGACCAACCGAGTCATTT-3’

Runx2-R: 5’-ACGCCATAGTCCCTCCTTTT-3’

Sp7-F: 5’-TTTCTCATTAACTCGTTGCCATCT-3’

Sp7-R: 5’-CTTCGGGAAAACGGCAAATA-3’

Spp1-F: 5’- AAGGCGCATTACAGCAAACACTCA-3’

Spp1-R: 5’- CTCATCGGACTCCTGGCTCTTCAT-3’

Spock-F: 5’- ACCCCCGGCAATTTCATGG-3’

Spock-R: 5’- TGTCTTCCCAGCTCTTGATGTAA-3’

Srf-F: 5’-GGCCGCGTGAAGATCAAGAT-3’

Srf-R: 5’-CACATGGCCTGTCTCACTGG-3’

Ucp1-F: 5’-ACTGCCACACCTCCAGTCATT-3’

Ucp1-R: 5’-CTTTGCCTCACTCAGGATTGG-3’

Western Blot Analysis

Total cellular protein was extracted from primary bone marrow stem cells or C3H10T1/2 cells with RIPA protein extraction buffer containing 10% proteinase inhibitor (McDonald, Li *et al*. 2015). MRTFA KO and WT mice femurs were dissected, snap-frozen in liquid nitrogen after sample collection and then pulverized in liquid nitrogen using a mortar and pestle in 600ul RIPA protein extraction buffer (Carroll, Wigner *et al*. 2012).

The mentioned samples were then homogenized with sonication to break up the genome DNA. The lysates were vortexed and centrifuged at 14,000 X g for 10minutes after incubating on ice for 30 minutes. The supernatant was collected from these

centrifuged samples without disturbing the cells or tissue debris. After quantification of the supernatant using the BCA (bicinchoninic acid) Protein Assay Reagent kit (Pierce), all the protein samples were normalized in 5X reducing buffer containing 200mM Tris pH 6.8, 8% SDS, 0.4% bromophenol blue, 40% glycerol and 400 mM DTT. The protein samples were subsequently fractionated by 10% -12% SDS-PAGE and transferred to PVDF (polyvinylidene difluoride) membranes purchased from BioRad at 120 mA voltage for overnight. PVDF membranes containing the protein samples were blocked with 5% non-fat milk powder dissolved in 1x PBST buffer and incubated with various primary antibodies specific to different proteins. Secondary antibodies (Sigma) conjugated with horseradish peroxidase and an ECL substrate kit (purchased from Denville) were used to develop the membranes for comparing the levels of target proteins (McDonald, Li *et al*. 2015).

The primary antibodies against the following proteins were obtained from the indicated vendors: MRTFA, Osteopontin, C/EBPα, SRF (Santa Cruz, CA), adiponectin (Pierce, Rockford, IL) and cyclophilin A (Cyc A) (Millipore, Billerica, MA). Monoclonal antibodies against FABP4 (aP2), and polyclonal antibodies against Perilipin were obtained from Cell Signaling (Danvers, MA). Monoclonal antibodies against αSMA were obtained from Sigma-Aldrich (St. Louis, MO).

Alizarin Red S Staining

Bone marrow stromal derived MSCs were allowed to differentiate into mature osteoblasts for 21 days as described before. To assess mineralized nodules, the differentiated cells were washed with PBS, and then fixed with 10% formaldehyde at room temperature for 10 minutes. The 2% (w/v) Alizarin Red S staining solution was made by dissolving 2 grams of Alizarin Red S powder in 100ml H2O (adjust the pH to 4.1-4.3 with ammonium hydroxide) and the solution was filtered with 0.45μm filters. Following the fixation, cells were washed with water and stained with 2% alizarin red solution at room temperature for 30 minutes. Following staining, cell layers were rinsed with deionized water until washes were clear (Carroll, Wigner *et al*. 2012). Digital photographs of stained cells were then captured.

Statistical Analysis

Data are presented as mean values +/- standard error of means (SEM). Unpaired 2-tail Student's t-test was conducted to assess statistical significance and $p \leq 0.05$ was considered significant.

RESULTS

MRTFA KO Mice have Reduced Trabecular Bone Mass

Introduction

Osteoporosis is a skeletal disorder characterized by excessive bone loss and increased fragility fractures. And it often results in poor quality of life predominantly in the aging population (Raisz 2005). Several previous reports suggested that a possible mechanism for age-related osteoporosis is the inappropriate bone marrow MSC fate switch to adipocytes versus osteoblasts (Beresford, Bennett *et al*. 1992, Justesen, Stenderup *et al*. 2001). McBeath identified the RhoA-ROCK pathway as a crucial regulator for MSC fate commitment through regulation of cell morphology and spreading (McBeath, Pirone *et al*. 2004). As downstream effectors of RhoA-ROCK signaling, MRTFA and SRF potently activate the expression of actin and proteins regulating actin turnover and polymerization. Therefore, we hypothesize that the actin-MRTFA-SRF circuit is acting downstream of RhoA-ROCK to regulate the early commitment of MSCs.

The original MRTFA KO mice were generated by Dr. Eric Olson's laboratory where workers identified MRTFA as an essential regulator of mammary myoepithelial cell development and survival (Li, Chang *et al*. 2006). Dr. Barbara Smith's laboratory also studied the role of MRTFA in regulation of collagen gene expression in myofibroblasts using the MRTFA KO mice. They discovered that MRTFA regulates collagen gene expression in pulmonary fibroblasts through a novel MRTFA Sp1 interaction to enhance collagen expression independent of SRF (Luchsinger, Patenaude *et al*. 2011). We collaborated with Dr. Barbara Smith and Dr. Matthew Layne to further

characterize the phenotype of MRTFA KO mice. McDonald and Li from our group showed that knocking out MRTFA enhances the development of beige adipocytes in white adipose tissue. Moreover, the MRTFA KO mice are resistant to diet-induced insulin resistance and obesity (McDonald, Li *et al*. 2015).

Because the importance of MRTFA in bone mass maintenance and bone formation has never been investigated before, we are the first to document the effects of MRTFA on bone morphometry. In this study, we compared body weight, femur and tibia length in MRTFA KO and WT mice. We also measured bone morphometric parameters in both cortical and trabecular bone using Micro-CT analysis. Cortical bone, also known as compact bone, forms the cortex of most of the bones. Trabecular bone is more porous and it often has more bone remodeling activity, therefore it is more severely affected in osteoporosis than cortical bone.

We mainly focused on the pathological relevant bone morphometric parameters including bone volume fraction (BV/TV) in both cortical and trabecular bone, cortical thickness, estimated bone density and trabeculae parameters. The osteoblastogenic gene expression in femurs and the levels of serum markers for osteoblast and osteoclast activity were also measured in the MRTFA KO and WT mice.

Recent studies demonstrate that obesity can lead to excessive bone loss by enhancing adipogenesis and inhibiting osteoblastogenesis in the bone marrow MSCs (Cao 2011). To investigate whether MRTFA deletion can potentiate bone loss under adipogenesis-inducing conditions, we analyzed the bone morphometric parameters of WT

and MRTFA KO mice fed with LFD or HFD, the latter causing adipose expansion, in part through hyperplasia.

MRTFA KO Mice have Significantly Lower Whole Body Weight, Shorter Tibia and Femur Lengths than WT Controls.

Dr. Matthew Layne's laboratory first discovered that the MRTFA KO mice appear to be smaller than the WT mice. To confirm this finding and further explore whether this is due to the compromised skeletal development in the MRTFA KO mice, we measured whole body weight, femur and tibia length in both male and female WT and MRTFA KO mice. The femurs and tibiae were dissected from 17 week old matched male WT and MRTFA KO mice and their lengths compared (Figures 6 and 7). Both the femurs and tibiae from MRTFA KO mice were significantly shorter than those from the WT mice (Figure 6 and 7).

We then gathered one cohort of male mice (WT n=7, MRTFA KO n=7) and one cohort of female mice (WT n=7, MRTFA KO n=7) to measure their whole body weight and femur and tibia length for comparison. For the male mice (15-17 weeks old), MRTFA KO mice have significantly lower body weights averaging 29.9 grams as compared to the controls averaging 32.2 grams (Figure 7). The femurs and tibiae are also significantly shorter in the MRTFA KO male mice (Figure 7). The female mice (24 weeks old) also showed similar phenotypes: the weights of WT mice averaged 27.1 grams, while the MRTFA KO mice averaged 24.4 grams (Figure 8). The female MRTFA

KO mice also had significantly shorter femurs and tibiae when compared with the controls (Figure 8).

From these observations, we speculate that the shorter femurs and tibiae in the MRTFA KO might be due to compromised osteoblast differentiation during skeletal development, although other mechanisms such as defects in chondrocyte differentiation or growth plate development should also be taken into consideration. Due to aforementioned defects in the female MRTFA KO mammary myoepithelial cells development, we only used $MRTFA^{+/-}$ female mice for breeding purpose and the selected WT and MRTFA KO mice for experiments were all nursed by the same $MRTFA^{+/-}$ mother.

Figure 6. MRTFA KO Mice have shorter femurs and tibiae as compared to the controls.

Both femurs and tibiae were dissected from 17 week old matched male WT and MRTFA KO mice. The upper and lower orange line mark the beginning and end of the WT mouse femurs to show the differences in the lengths of WT and MRTFA KO mice.

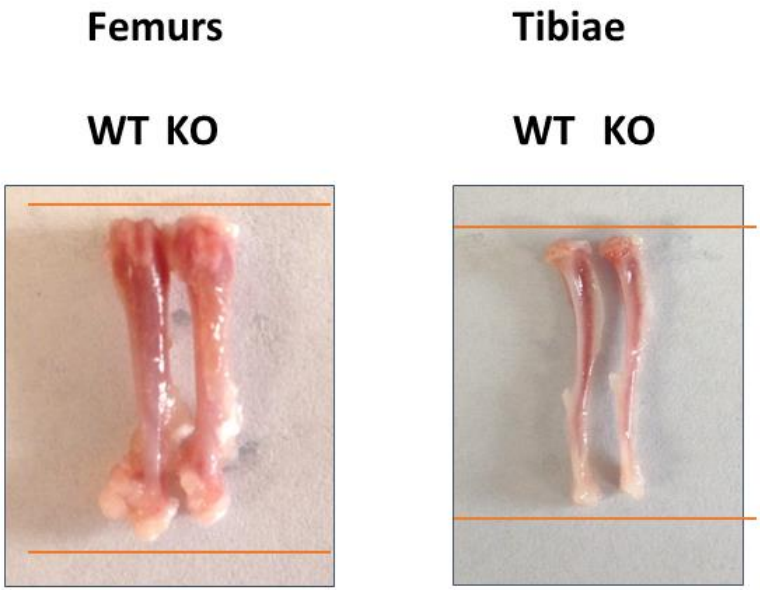

Figure 7. Male MRTFA KO mice have lower body weight, shorter femur and tibia length as compared to the controls.

WT (n=7) and MRTFA KO (n=7) male mice (15-17 weeks old) were euthanized and then weighed. The femurs and tibiae of the mice were then dissected and the bone lengths were measured with a caliper. The data are expressed as mean +/- SEM (Standard Error of Deviation). Data were analyzed by Student's t-test (** $p \leq 0.01$).

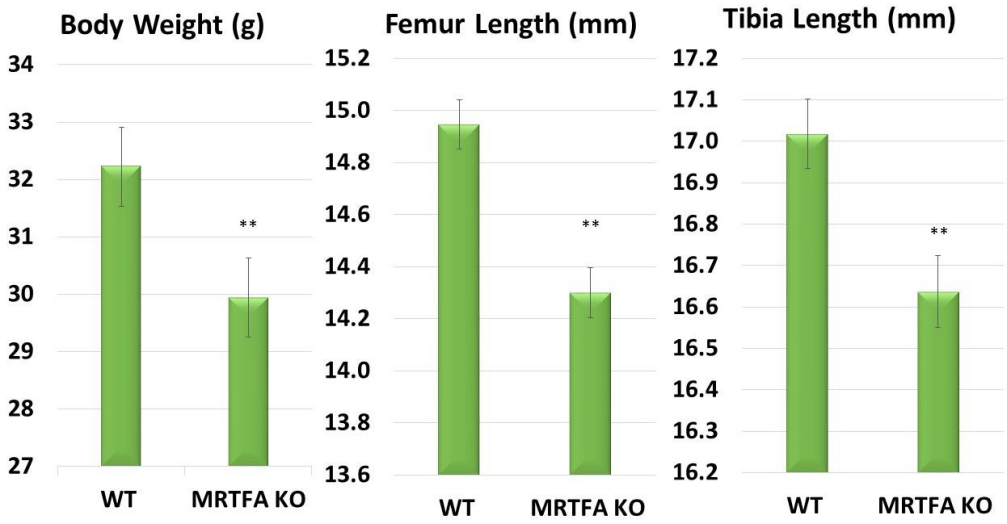

Figure 8. Female MRTFA KO mice have lower body weight, shorter femur and tibia length as compared to the controls.

The whole body weight, femur and tibia length for female WT (n=7) and MRTFA KO (n=7) mice were measured as described in Figure 7. The age of these mice range from 22 to 24 weeks old (* $p \leq 0.05$, ** $p \leq 0.01$).

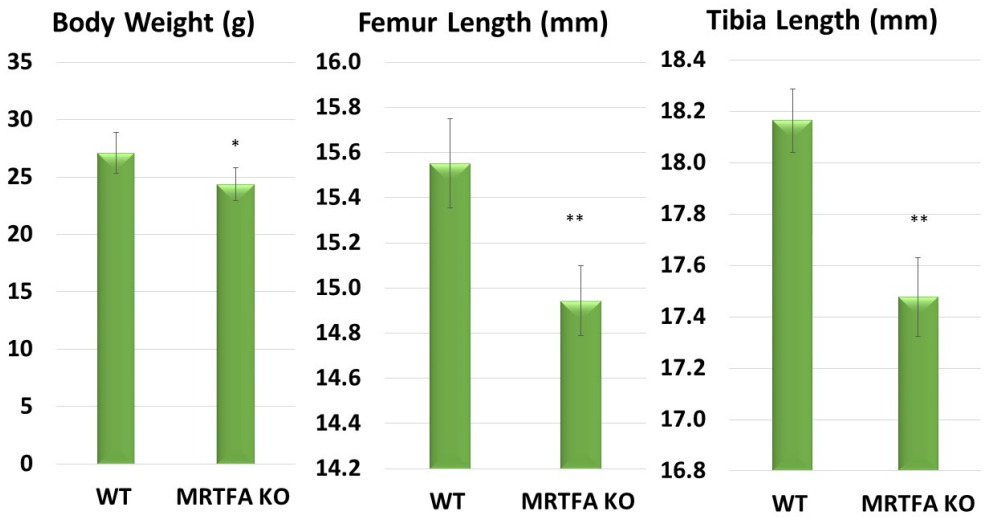

MRTFA KO Mice Showed Marked Decrease in Bone Mass in the Trabecular Region of Femurs

Micro-CT analysis has been used widely to evaluate trabecular and cortical bone structures in different animal models. The Micro-CT scanning system offers a non-destructive method to acquire high-resolution images of the micro-structures of *ex vivo* samples and it allows accurate quantification of the micro-architectural parameters of the samples as well (Bouxsein, Boyd *et al*. 2010).

Micro-CT analysis was performed on the femur samples of 17 week old male and 24 week old female WT and MRTFA KO mice. High-resolution 3D images of the bone microstructures were generated from the scans. Various trabecular and cortical bone morphometric parameters were quantified and compared. The overall morphology and size of the bone can be observed from the 3D images. Additionally, microstructural characteristics including cortical thickness and the morphology of trabeculae can be observed. Trabeculae are the small rod or beam like bone structures in the trabecular bone. The size, morphology, density and degree of separation of trabeculae usually represent the quantity and quality of bone.

The 3D images of the mid-diaphyseal region of cortical femur from male WT and MRTFA KO mice showed no obvious morphological differences (Figure 9A). The shape and size of the bones from WT and MRTFA KO were similar (Figure 9A). However, the 3D images of trabecular regions of proximal femurs showed a marked reduction in trabecular bone volume in the MRTFA KO mice as compared to WT controls (Figure 9B).

There was more spacing volume and less bone volume in the trabecular femurs from the MRTFA KO mice. The trabeculae appeared to be thinner in the MRTFA KO mice as well.

Figure 9. Representative Micro-CT images of mid-diaphyseal cortical bone and trabecular bone of WT and MRTFA KO male mice.

Mouse femurs were harvested when the male mice were about 17 weeks old (WT n=7, MRTFA KO n=7). Representative three-dimensional images of mid-diaphyseal cortical regions (A) and trabecular regions (B) of femurs generated by Micro-CT analysis are shown. Transverse images scanned by the Micro-CT were traced manually with a computer program and stacked to render 3D images.

Figure 9A

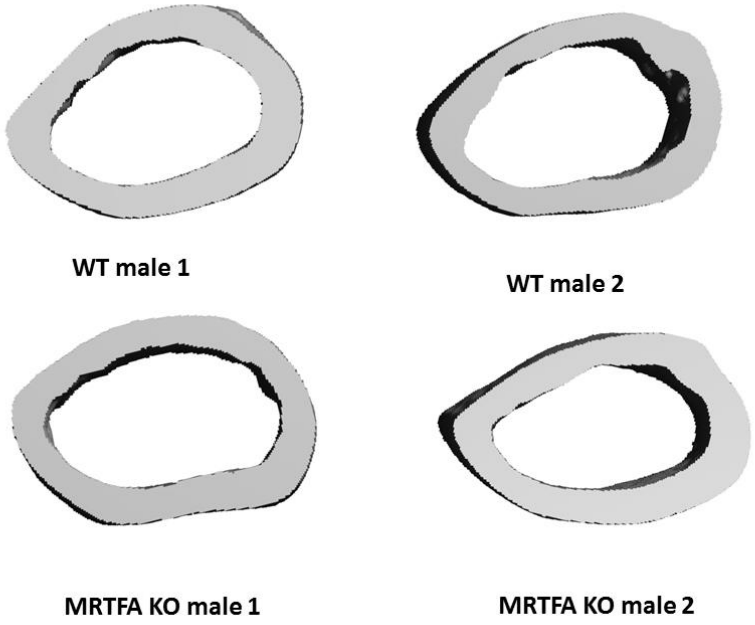
WT male 1
WT male 2
MRTFA KO male 1
MRTFA KO male 2

B

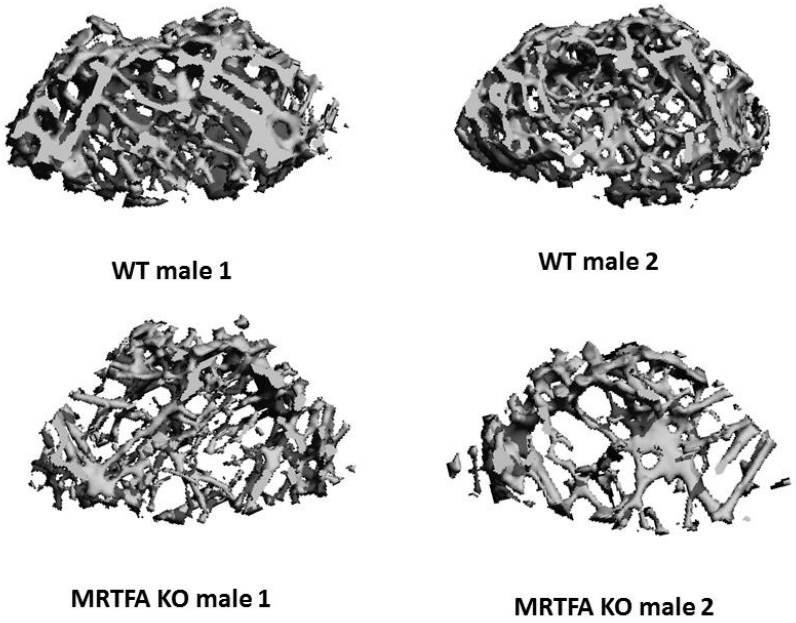
WT male 1
WT male 2
MRTFA KO male 1
MRTFA KO male 2

The 3D images of the scans generated from WT and MRTFA KO female mice showed similar trends as those observed in the male mice (Figure 10). Some of the MRTFA KO mouse cortical bone appeared to have thinner cortical thickness than in the WT bone. For the trabecular bone of the female mice, the MRTFA KO mice demonstrated a remarkable decrease in bone volume as shown in Figure 10B. There was significantly less bone volume in the MRTFA KO mice with more trabecular spacing and much thinner trabeculae.

The 3D images generated from male and female mice consistently showed that the MRTFA KO mice have significantly less bone volume and thinner trabeculae in the trabecular femurs. The female MRTFA KO mice seem to have a more severe osteoporotic phenotype than the male mice.

Using software provided by the Scanco micro-CT 40 system, we quantified various bone morphometric parameters based on the 3D models of the area of interest in the above mentioned bone samples. One of the pathological relevant cortical bone parameters we studied was cortical thickness, which is calculated as the average thickness of the femoral cortex (Bouxsein, Boyd *et al*. 2010). As shown in both Figure 11 and Table 1, there was no statistically significant difference in cortical thickness between male WT and MRTFA KO mice, despite a non-significant trend of thinner cortical thickness in MRTFA KO mice (Table 1, Figure 11 $p=0.09$). There was no significant difference between the bone volume fraction (BV/TV) of WT and MRTFA KO mice (Table 1, Figure 11). On the other hand, there was a marked decrease in total tissue

volume and bone volume (Table 1, Figure 11 lower panel), which is likely due to smaller overall bone size in MRTFA KO mice.

Figure 10. Representative Micro-CT images of mid-diaphyseal cortical bone and trabecular bone of WT and MRTFA KO female mice.

Representative 3D images of mid-diaphyseal cortical regions (A) and trabecular regions (B) of femurs generated by Micro-CT analysis are shown (as described in Figure 9). Mice femurs were harvested when the female mice were about 24 weeks old (WT n=7, MRTFA KO n=7). The images of two pairs of WT and MRTFA KO female mice are shown to represent the remaining data.

Figure 10A

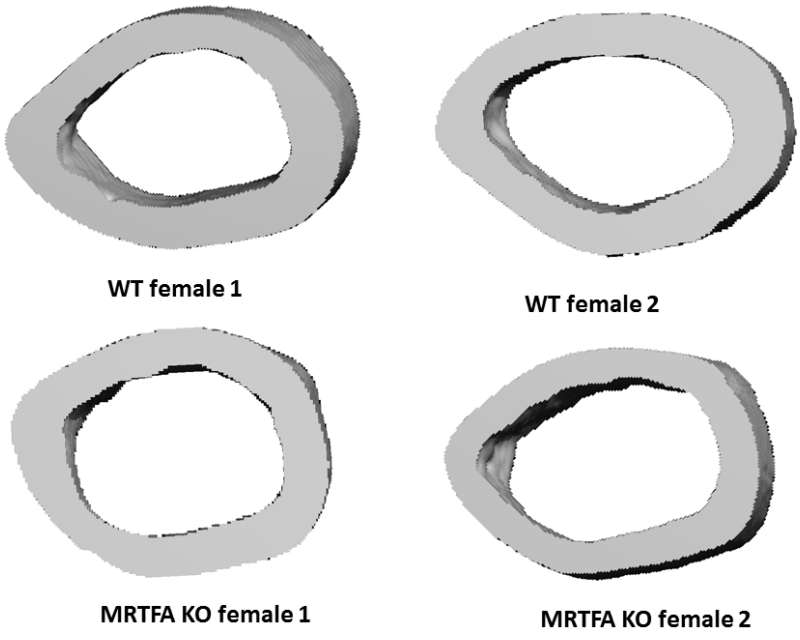
WT female 1
WT female 2
MRTFA KO female 1
MRTFA KO female 2

B

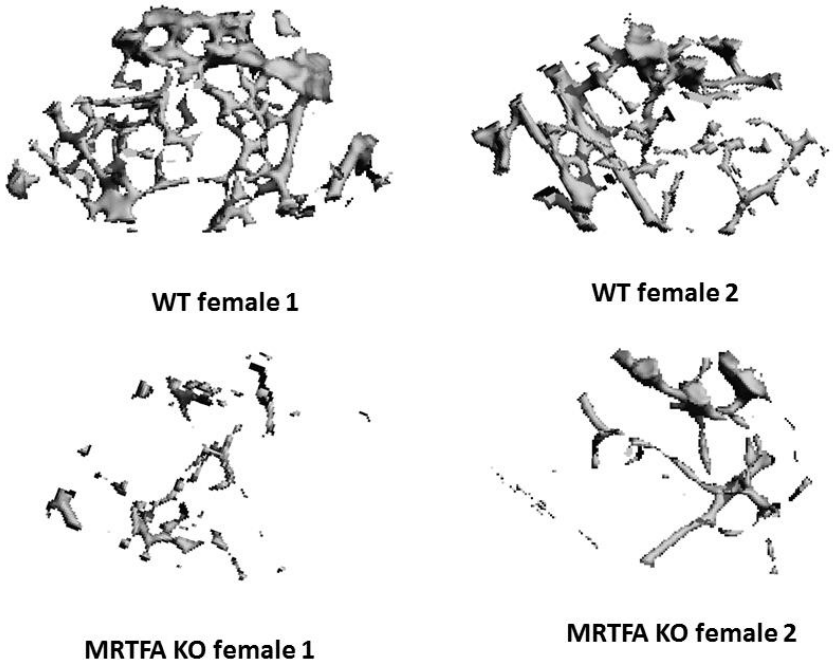
WT female 1
WT female 2
MRTFA KO female 1
MRTFA KO female 2

Figure 11. MRTFA KO mice have smaller cortical bone but there is no significant difference in cortical thickness between male WT and MRTFA KO mice.

The femur samples were harvested from 17 week old male mice (WT n=7, MRTFA KO n=7) and fixed in 10% formalin for 5 days before Micro-CT scanning. Software provided by the Scanco micro-CT 40 system was used to generate quantitative bone microstructural parameters shown in this figure. The cortical thickness, cortical bone volume fraction (BV/TV), total volume (TV) and bone volume (BV) of the mid-shaft area of femurs are shown. The data is expressed as the mean values of the 7 mice in each group with standard error of deviation. (*$p<0.05$).

Figure 11

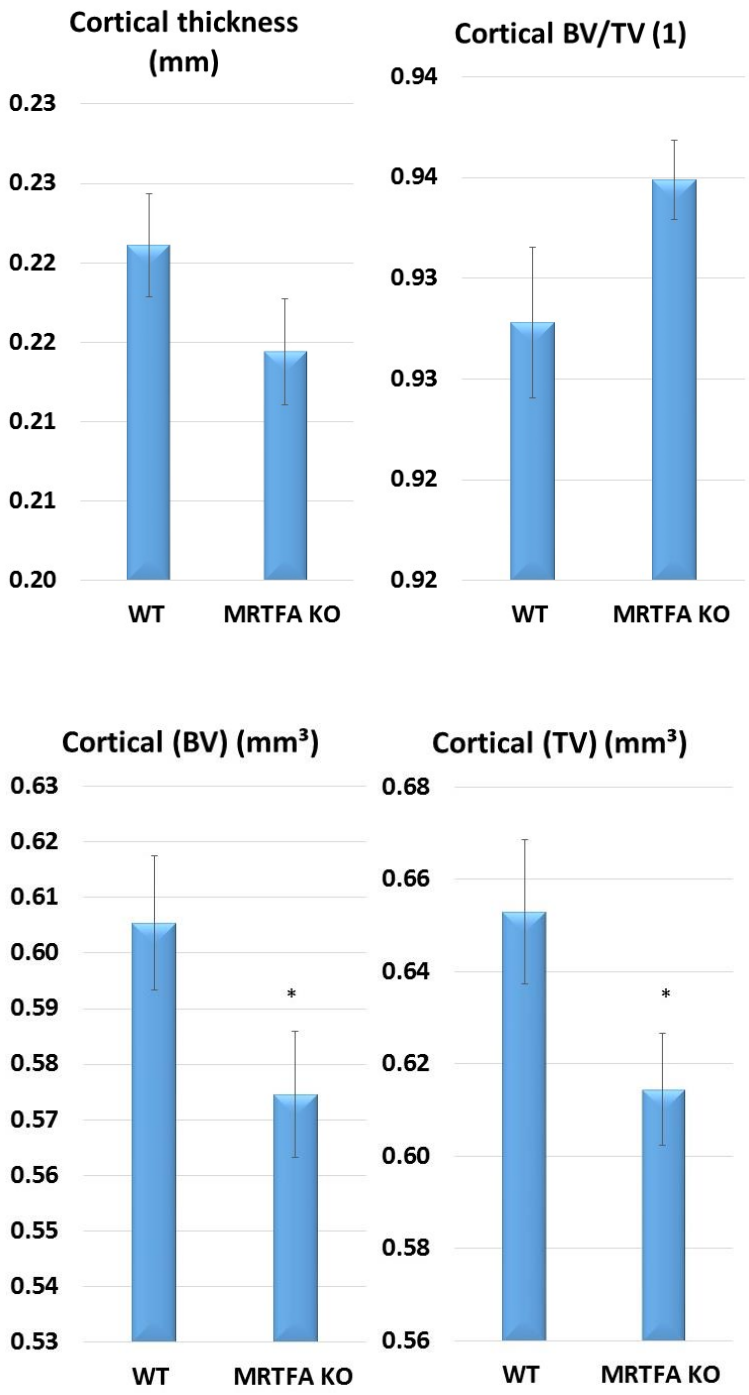
Cortical thickness (mm)
0.23
0.23
0.22
0.22
0.21
0.21
0.20
WT
MRTFA KO
Cortical BV/TV (1)
0.94
0.94
0.93
0.93
0.92
0.92
WT
MRTFA KO
Cortical (BV) (mm³)
0.63
0.62
0.61
0.60
0.59
0.58
0.57
0.56
0.55
0.54
0.53
*
WT
MRTFA KO
Cortical (TV) (mm³)
0.68
0.66
0.64
0.62
0.60
0.58
0.56
*
WT
MRTFA KO

The same analytical approaches were used for the female mice samples to generate bone morphometric indices. As shown in both Figure 12 upper panel and Table 2, the cortical thickness of the female MRTFA KO mice was significantly thinner than the controls. However, there was no significant difference found between the BV/TV of WT and MRTFA KO female mice (Table 2, Figure 12 upper panel). Similar to the male mice, there was a marked decrease in both total tissue volume and bone volume in the mid-diaphyseal femurs of female MRTFA KO mice (Table 2, Figure 12 lower panel).

The Micro-CT analysis of the trabecular region of male MRTFA KO mice showed that they had significantly less bone volume fraction (about 20% reduction when compared to the controls) (Figure 13C and Table 1). The BV of the MRTFA KO was lower than that of the WT controls (Figure 13B and Table 1), which might lead to lower bone volume fraction, given that there was no difference in the TV (Figure 13A and Table 1).

The mean apparent mineral density of the total tissue was also significantly lower in the MRTFA KO mice (Figure 13E and Table 1), but no difference was found in mean density of the bone volume (Figure 13D and Table 1). The total bone tissue density was reduced in the MRTFA KO mice due to loss of bone mass since bone has a much higher density than the non-bone soft tissues. In summary, the male MRTFA KO showed a small but significant reduction in trabecular bone mass when compared to the controls.

Figure 12. Female MRTFA KO have smaller cortical bone and thinner cortical thickness.

As in figure 11, the femur samples were harvested from 24 week old female mice (WT n=7, MRTFA KO n=7) and scanned with Micro-CT. The cortical thickness, cortical bone volume fraction (BV/TV), total volume (TV) and bone volume (BV) of the mid-shaft area of femurs are presented as mentioned in Figure 9 (**$p<0.01$).

Figure 12

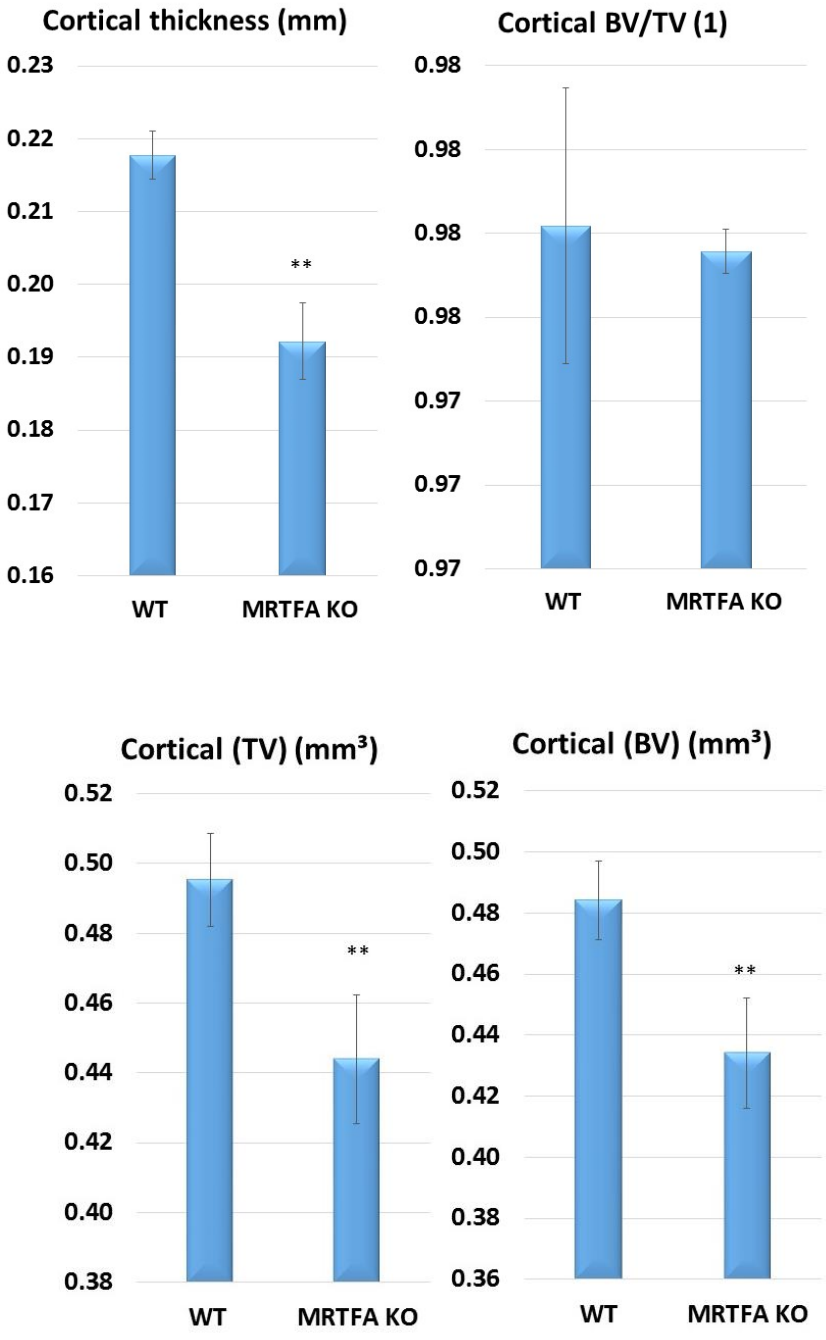
Cortical thickness (mm)
0.23
0.22
0.21
0.20
0.19
0.18
0.17
0.16
**
WT
MRTFA KO
Cortical BV/TV (1)
0.98
0.98
0.98
0.98
0.97
0.97
0.97
WT
MRTFA KO
Cortical (TV) (mm³)
0.52
0.50
0.48
0.46
0.44
0.42
0.40
0.38
**
WT
MRTFA KO
Cortical (BV) (mm³)
0.52
0.50
0.48
0.46
0.44
0.42
0.40
0.38
0.36
**
WT
MRTFA KO

Figure 13. Trabecular bone morphometric parameters comparison in male WT and MRTFA KO mice.

The same samples were analyzed as described in Figure 11. The trabecular total volume (Trabecular TV) (A), trabecular bone volume (Trabecular BV) (B), trabecular bone volume fraction (BV/TV) (C), bone volume density (D) and total volume density (E) of the trabecular femurs are shown. The data are presented as described in Figure 9 (*$p<0.05$).

Figure 13.

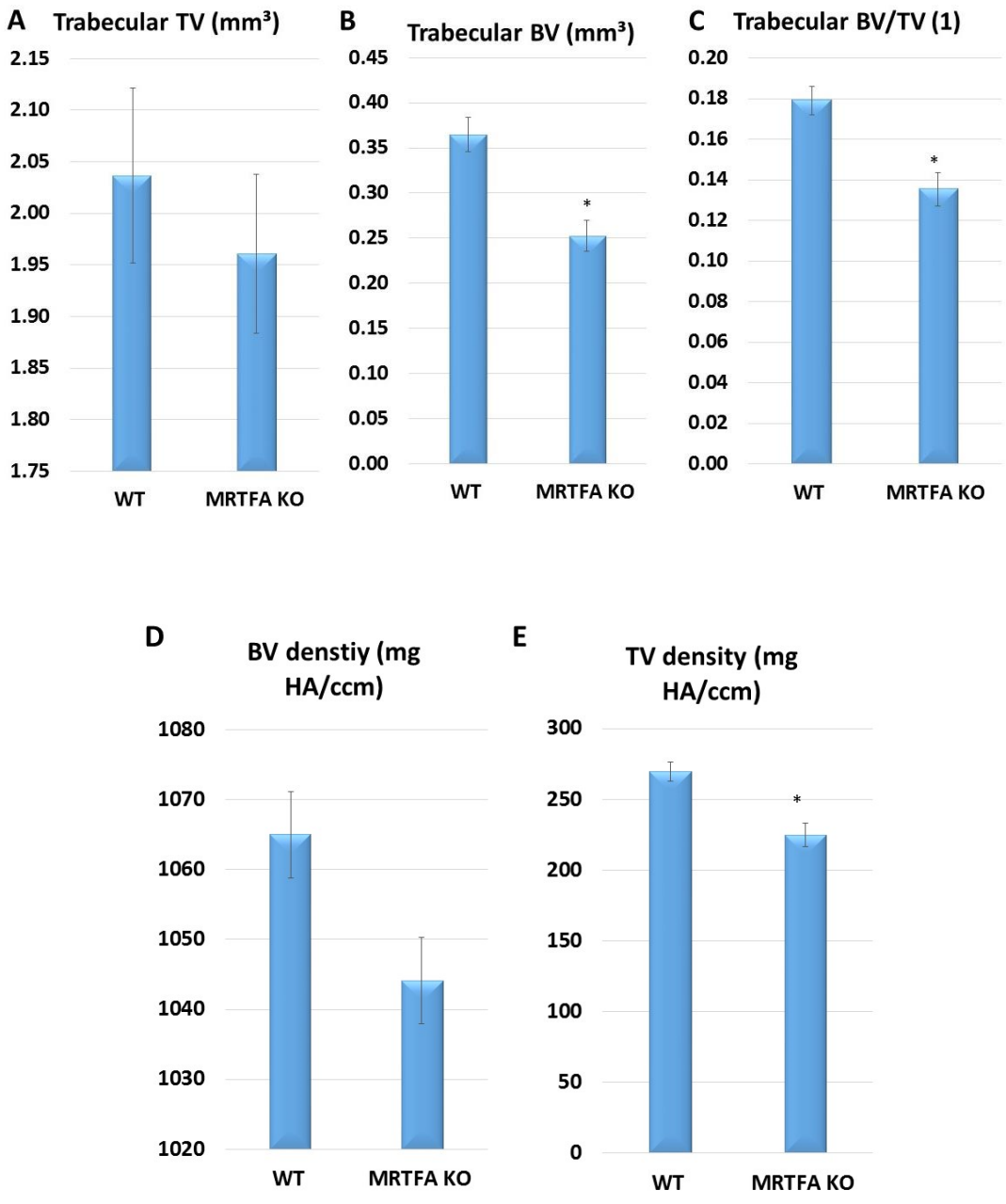
A
Trabecular TV (mm³)
2.15
2.10
2.05
2.00
1.95
1.90
1.85
1.80
1.75
WT
MRTFA KO
B
Trabecular BV (mm³)
0.45
0.40
0.35
0.30
0.25
0.20
0.15
0.10
0.05
0.00
*
WT
MRTFA KO
C
Trabecular BV/TV (1)
0.20
0.18
0.16
0.14
0.12
0.10
0.08
0.06
0.04
0.02
0.00
*
WT
MRTFA KO
D
BV denstiy (mg HA/ccm)
1080
1070
1060
1050
1040
1030
1020
WT
MRTFA KO
E
TV density (mg HA/ccm)
300
250
200
150
100
50
0
*
WT
MRTFA KO

The Micro-CT analysis for the female mice demonstrated a more severe osteoporotic phenotype in the trabecular bone of the MRTFA KO mice. The trabecular bone volume fraction (BV/TV) was approximately 50% lower in MRTFA KO female mice as compared to the controls (Figure 14C and Table 2). This appeared to be due to the drastic reduction in the trabecular bone volume in the MRTFA KO mice as shown in Figure 14B and Table 2, although there were no significant difference in the total volume (Figure 14A and Table 2).

Moreover, the mean density of the total tissue was lower in the MRTFA KO mice due to reduced bone mass fraction of the total tissue (Figure 14E and Table 2). However, there was no difference in the mineral density of the bone mass itself (Figure 14D and Table 2). Consistent with the results we discovered in the male mice, MRTFA KO mice displayed an osteoporotic phenotype in both genders and this phenotype was more prominent in the female mice.

Based on the 3D calculations, the mean trabecular number (Tb. N.), mean trabecular thickness (Tb. Th.), mean trabecular separation (Tb. Sp.), mean connectivity density (Conn. D.) and structure model index (SMI) were determined for comparison. There was no significant difference in the male WT and MRTFA KO mice except for SMI (Table 1), which is an indicator of the shapes of the trabeculae. The values of SMI varied from 0 to 3: 0 represents perfectly parallel plates and 3 represents perfectly cylindrical rods. The mean SMI of WT mice was 1.54 and the MRTFA KO was 1.94, which indicates the trabeculae of the mice was more plate-like whereas those of the

MRTFA KO mice were more rod-like. This may suggest that the trabeculae in the MRTFA KO mice are thinner than the WT controls. However, the quantification of trabecular thickness did not show a significant difference between MRTFA KO and the controls.

Figure 14. Trabecular bone morphometric parameters: comparison of female WT and MRTFA KO mice.

The same samples from Figure 12 were analyzed as described in Figure 11. The trabecular total volume (Trabecular TV) (A), trabecular bone volume (Trabecular BV) (B), trabecular bone volume fraction (BV/TV) (C), bone volume density (D) and total volume density (E) of the trabecular femurs are shown. The data are presented as described in Figure 9 (**$p<0.01$).

Figure 14.

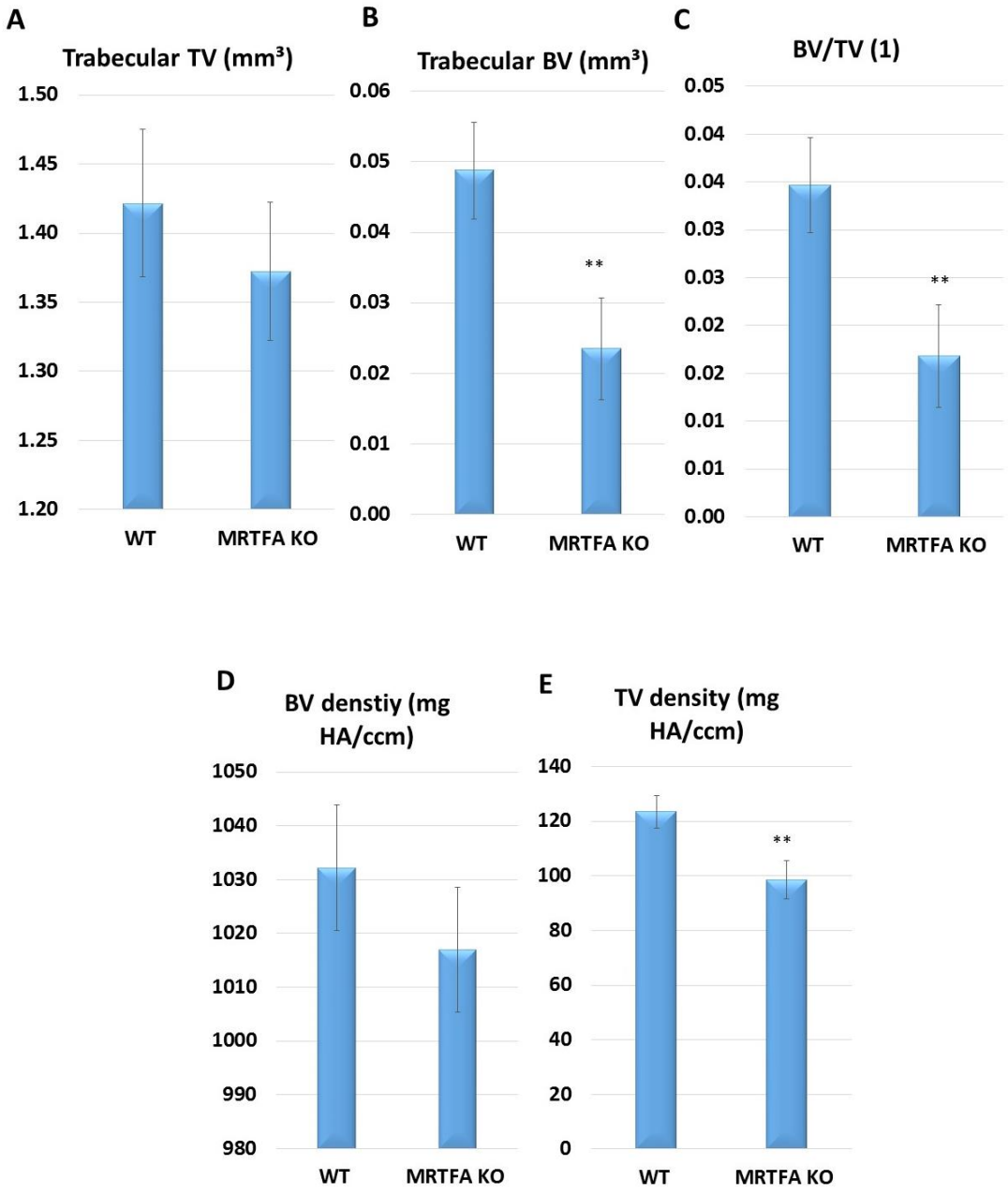
A
Trabecular TV (mm³)
1.50
1.45
1.40
1.35
1.30
1.25
1.20
WT
MRTFA KO
B
Trabecular BV (mm³)
0.06
0.05
0.04
0.03
0.02
0.01
0.00
**
WT
MRTFA KO
C
BV/TV (1)
0.05
0.04
0.04
0.03
0.03
0.02
0.02
0.01
0.01
0.00
**
WT
MRTFA KO
D
BV denstiy (mg HA/ccm)
1050
1040
1030
1020
1010
1000
990
980
WT
MRTFA KO
E
TV density (mg HA/ccm)
140
120
100
80
60
40
20
0
**
WT
MRTFA KO

On the other hand, the trabecular morphometric indices mentioned above were drastically different between female MRTFA KO mice and controls. The trabecular number (Tb. N.), which represents the measurement of mean number of trabeculae per unit length, was significantly lower in the female MRTFA KO mice (Figure 15A, Table 2). However, no significant difference was found in the trabecular thickness (Tb. Th.) (mean thickness of trabeculae) and SMI (Figure 15B, E and Table 2) between MRTFA KO and control mice. The trabecular separation (Tb. Sp.), the mean distance between trabeculae, increased significantly in the female MRTFA KO mice (Figure 15C and Table 2). The connectivity density (Figure 15D and Table 2), a measure of the degree of connectivity of trabeculae, was much lower in the female MRTFA KO mice. The increase of trabecular separation and decrease of connectivity density collectively indicates less bone mass and more non-bone soft tissue in the trabecular bone of the MRTFA KO mice.

Interestingly, several bone structure parameters such as bone volume fraction, trabecular number, trabecular separation, connectivity density and the mean tissue density were all significantly lower in the female WT and MRTFA KO mice as compared to the males (Table 3). The mean values of the female mice were approximately 50% to 90% less than that of the males (Table 3). With age and gender differences, both WT and MRTFA KO female mice were much more osteoporotic than the males. This may explain the severity of the osteoporotic phenotype in the female mice.

In conclusion, MRTFA KO mice had reduced bone mass in the trabecular femurs as compared to the WT controls and the female MRTFA KO mice have a more severe osteoporotic phenotype than the males.

Figure 15. Trabecular bone morphometric parameters representing bone mass were compared in female WT and MRTFA KO mice.

The same samples from Figure 12 were analyzed as described in Figure 11. The trabecular number (Tb. N) (A), trabecular thickness (Tb. Th.) (B), trabecular separation (Tb. Sp.) (C), connectivity density (Conn. D.) (D) and trabecular structure model index (SMI) (E) of the trabecular femurs are shown. The data are presented as described in Figure 9 (*$p<0.05$, **$p<0.01$).

Figure 15.

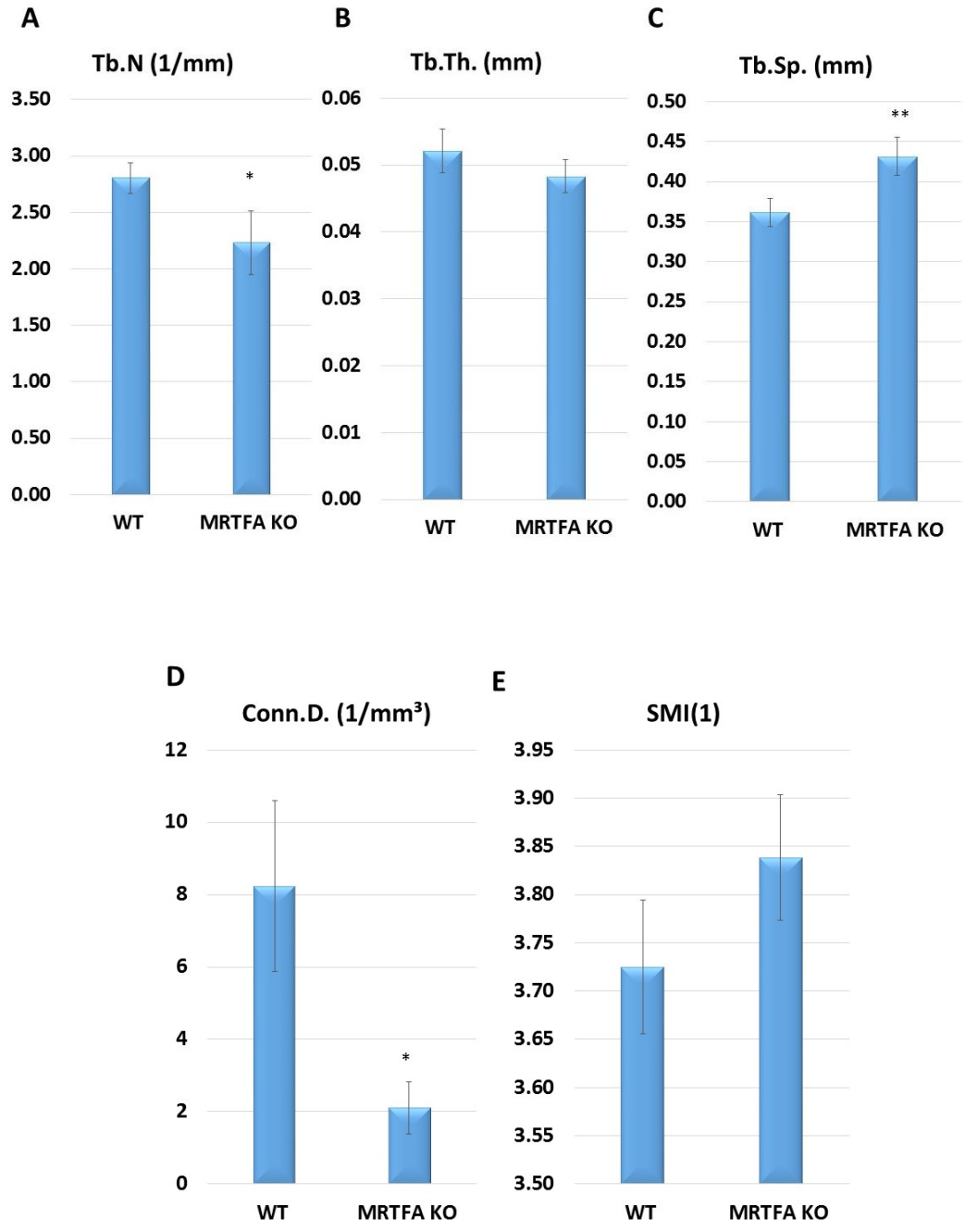
A
Tb.N (1/mm)
3.50
3.00
2.50
2.00
1.50
1.00
0.50
0.00
*
WT
MRTFA KO
B
Tb.Th. (mm)
0.06
0.05
0.04
0.03
0.02
0.01
0.00
WT
MRTFA KO
C
Tb.Sp. (mm)
0.50
0.45
0.40
0.35
0.30
0.25
0.20
0.15
0.10
0.05
0.00
**
WT
MRTFA KO
D
Conn.D. (1/mm³)
12
10
8
6
4
2
0
*
WT
MRTFA KO
E
SMI(1)
3.95
3.90
3.85
3.80
3.75
3.70
3.65
3.60
3.55
3.50
WT
MRTFA KO

Table 1. MRTFA KO male mice have significant trabecular bone loss as compared to the WT mice.

The femurs were obtained from male mice as described in Figure 11 and 13. The data is expressed as the mean values ± standard error of deviation for each group (*$p<0.05$, **$p<0.01$). The cortical thickness, cortical BV/TV, TV and BV of cortical femurs are included. The trabecular bone morphometric parameters shown in this table are as follows: trabecular BV/TV, trabecular TV, trabecular BV, connectivity density, structure model index, trabecular number, trabecular thickness, trabecular density, mean density of total volume and mean density of bone volume.

Table1.

	WT (n=7)	MRTFA KO (n=7)	P value
Body Weight (g) **	32.1±1.7	29.9±1.2	0.01
Femur Length (mm) **	16.3±0.3	15.8±0.3	0.01
Tibia Length (mm) **	18.2±0.2	17.9±0.2	0.002
Cortical Total Volume (TV) (mm^3) *	0.65±0.04	0.61±0.03	0.04
Cortical Bone Volume (BV) (mm^3) *	0.61±0.03	0.57±0.0.03	0.04
Cortical BV/TV (1)	0.93±0.01	0.93±0.01	0.06
Cortical Thickness (mm)	0.22±0.01	0.21±0.01	0.09
Trabecular Total Volume (TV)(mm^3)	3.2±0.4	2.9±0.4	0.13
Trabecular Bone Volume (BV) (mm^3) *	0.68±0.1	0.52±0.2	0.05
Trabecular BV/TV (1)*	0.21±0.01	0.17±0.05	0.05
Connectivity Density ($1/mm^3$)	157±22	126±65	0.13
Structure Model Index (1) *	1.54±0.2	1.94±0.5	0.03
Trabecular Number(1/mm)	4.84±0.4	4.44±0.9	0.15
Trabecular Thickness (mm)	0.058±0.004	0.058±0.004	0.47
Trabecular Separation (mm)	0.20±0.2	0.22±0.05	0.12
Mean/Density of TV (Apparent) (mg HA/ccm) *	301±23	253±48	0.02
Mean/Density of BV (Material) (mg HA/ccm)	1053±23	1040±29	0.18

Table 2. MRTFA KO female mice showed an osteoporotic phenotype as compared to the WT mice.

The femurs were obtained from female mice as in Figure 10, 12 and 13. The data is shown as described in Table 1 (*p<0.05, **p<0.01). All the bone parameters shown are listed in Table 1.

	WT (n=7)	MRTFA KO (n=7)	P value
Body Weight (g) *	28.2±3.2	24.7±3.4	0.04
Femur Length (mm) **	15.6±0.5	15.0±0.5	0.006
Tibia Length (mm) **	18.2±0.4	17.5±0.4	0.0003
Cortical Total Volume (TV) (mm^3) **	0.50±0.04	0.44±0.05	0.01
Cortical Bone Volume (BV) (mm^3) **	0.48±0.03	0.43±0.05	0.01
Cortical BV/TV (1)	0.98±0.009	0.98±0.001	0.41
Cortical Structure Model Index (1) **	0.70±0.03	0.61±0.05	0.0002
Cortical Thickness (mm) **	0.22±0.009	0.19±0.013	0.00001
Cortical Mean/Density of TV (Apparent) (mgHA/ccm)**	1412±9	1384±20	0.0003
Cortical Mean/Density of BV (Material) (mg HA/ccm)**	1531±9	1513±17	0.004
Trabecular Total Volume (TV)(mm^3)	1.42±0.1	1.37±0.1	0.18
Trabecular Bone Volume (BV) (mm^3) **	0.05±0.1	0.02±0.01	0.004
Trabecular BV/TV (1)**	0.04±0.01	0.02±0.007	0.004
Connectivity Density ($1/mm^3$) *	8.2±6.3	2.1±1.9	0.01
Structure Model Index (1)	3.72±0.2	3.84±0.2	0.14
Trabecular Number(1/mm) *	2.80±0.4	2.23±0.6	0.02
Trabecular Thickness (mm)	0.052±0.01	0.048±0.01	0.25
Trabecular Separation (mm) **	0.36±0.05	0.43±0.04	0.006
Trabecular Mean/Density of TV (Apparent) (mg HA/ccm)**	123±16	98±18	0.009
Trabecular Mean/Density of BV (Material) (mg HA/ccm)	1032±31	1017±76	0.32

Osteoblastogenic Gene Expression was reduced in MRTFA KO Mouse Femurs.

To study whether the decreased bone mass in the MRTFA KO mice is caused by the inhibition of osteoblastogenesis, we compared the mRNA levels of osteoblastogenic genes in the femurs of MRTFA KO mice with the WT controls. The mRNA level of Mrtfa was consistently reduced in the MRTFA KO mice (Figure 16A) and the Mrtfa mRNA signal detected in the MRTFA KO mice might be from the incomplete fragments of Mrtfa mRNA.

Expression of the osteoblastogenic transcription factor Runx2 mRNA was lower in the MRTFA KO mice compared to the WT mice (Figure 16A). mRNA levels of osteoblastogenic genes such as Alpl (Alkaline phosphatase), Spp1 (secreted phosphoprotein 1) and Bglap (bone gamma-glutamate protein) were also reduced in some of the MRTFA KO femurs (Figure 16A). Alpl levels are positively associated with bone formation, thus the decreased Alpl mRNA indicates inhibited osteoblastogenic activity (Komori, Yagi *et al*. 1997). Osteopontin is an extracellular structural protein in bone that is very important for bone remodeling. Osteocalcin is a secretory protein that is important for mineralization and calcium homeostasis in bone (Komori, Yagi *et al*. 1997). The reduction of the mRNA levels of these genes suggests inhibited osteoblast differentiation in the MRTFA KO mouse femurs. The protein level of osteopontin was also significantly lower in the MRTFA KO mouse femurs (Figure 17B), which was consistent with the mRNA levels.

Insulin-like growth factor 1 (IGF1) is proven to be essential for bone formation during maintenance of bone homeostasis in adult life (Peng, Xu *et al*. 2003). A previous study showed that SRF regulates bone formation *via* the IGF1 and IGF1R signaling pathway (Chen, Yuan *et al*. 2012, Xian, Wu *et al*. 2012). We measured the mRNA levels of Igf1 and Igf1r in the MRTFA KO mice since MRTFA is a known co-activator of SRF target genes. Interestingly, mRNA levels of Igf1 and Igf1r in the MRTFA KO mouse femurs were also reduced, similar to the SRF knockout mice (Figure 16B). This might be partially responsible for the shorter femurs and tibiae and reduction of trabecular bone mass seen in the MRTFA KO mice. The trabecular region of the proximal femurs from WT and MRTFA KO mice was sectioned and stained with H&E. There is more non-bone soft tissue spacing (purple) and less mineralized bone mass (pink) in the MRTFA KO mice as shown in Figure 17A.

The balance between bone formation and resorption is essential for proper bone remodeling. Based on the aforementioned results, we still cannot rule out that the osteoporotic phenotype in MRTFA KO mice is due to both inadequate osteoblastogenesis and excessive osteoclast activity. To further elucidate the mechanism of the bone loss in MRTFA KO mice, we measured the levels of the widely used clinical osteoporotic markers, PINP and CTX-1, in sera of WT and MRTFA KO mice. PINP is a cleaving by-product produced during Type I collagen synthesis and it is positively correlated with osteoblastogenesis activity. CTX-1 is the by-product of enzymatic cleavage of Type I collagen occurring during bone resorption by osteoclasts, thus serves as a marker for bone breakdown. PINP levels were significantly lower in MRTFA KO mouse serum as

compared to the controls in Figure 16A. Reduced PINP levels also indicate that osteoblastogenesis in other types of bone such as vertebrae are likely compromised in the MRTFA KO mice. On the other hand, there is no significant difference in CTX-1 levels between WT and MRTFA KO mice, which suggests the osteoporotic phenotype in MRTFA KO mice is most likely due to the inhibition of osteoblastogenesis instead of excessive bone resorption by osteoclasts.

Collectively, the Micro-CT analysis, osteoblastogenic gene mRNA levels and ELISA results showed that MRTFA KO mice have reduced bone mass in the trabecular femurs. The reduced bone mass in MRTFA KO mice is likely due to reduced osteoblastogenesis.

Figure 16. mRNA levels of select osteoblastogenic genes, IGF1 and IGF1R are lower in MRTFA KO femurs.

The femurs of WT (n=3) and MRTFA KO mice (n=3) were dissected and pulverized in liquid nitrogen for mRNA extraction. Mrtfa, Runx2, Alpl, Spp1, Bglap (A), Igf1 and Igf1r levels (B) [WT (n=4) and MRTFA KO mice (n=4)] were probed with corresponding primers and the relative levels of these genes are presented. The fold change of these genes was normalized to Gapdh mRNA levels and the mean value of WT samples was set at 1. The dots of same colors represent matched WT and MRTFA KO mice samples. Alpl: alkaline phosphates, Igf1: insulin like growth factor 1, Igf1r: insulin like growth factor 1 receptor.

Figure 16

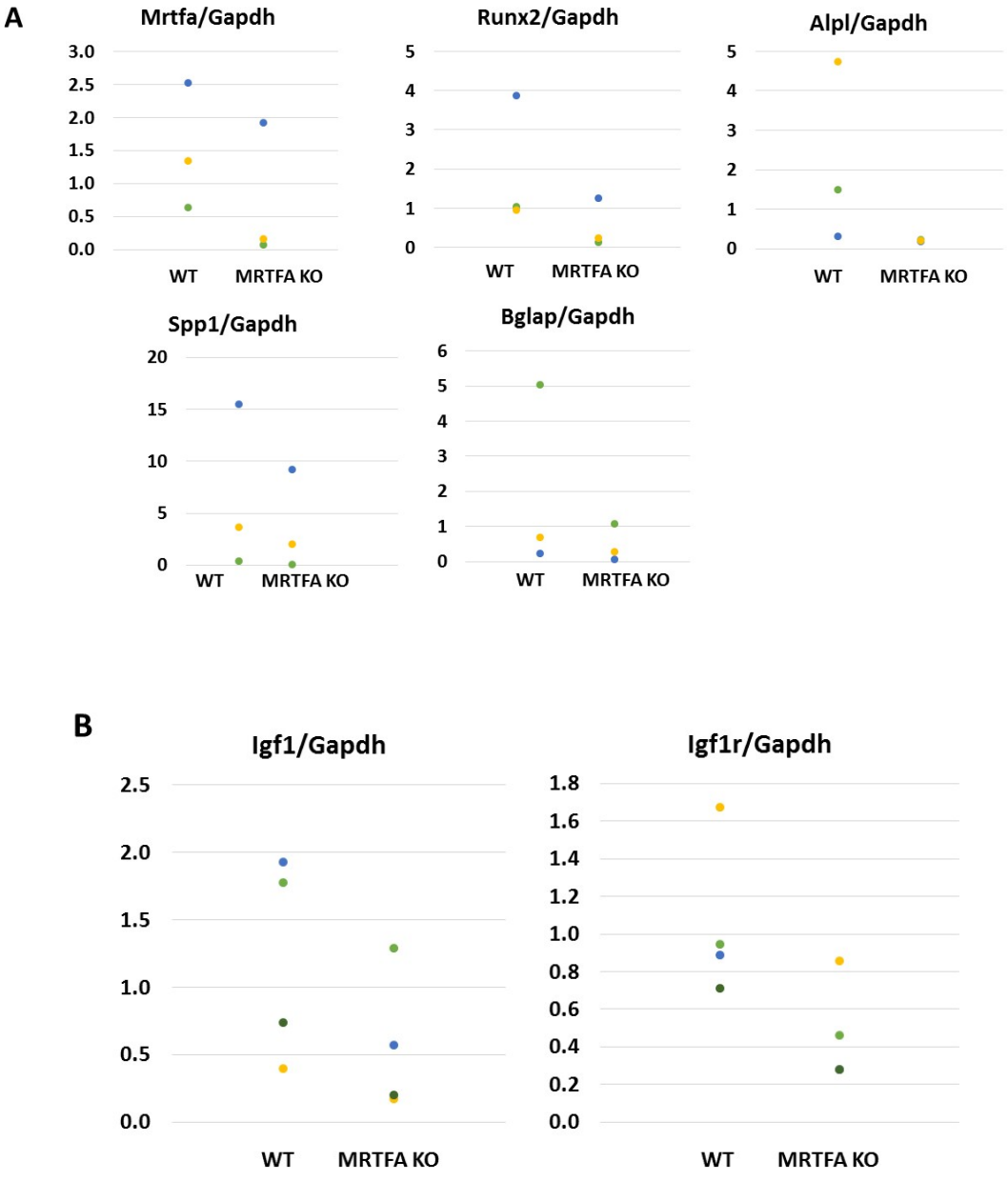
A
Mrtfa/Gapdh
3.0
2.5
2.0
1.5
1.0
0.5
0.0
WT
MRTFA KO
Runx2/Gapdh
5
4
3
2
1
0
WT
MRTFA KO
Alpl/Gapdh
5
4
3
2
1
0
WT
MRTFA KO
Spp1/Gapdh
20
15
10
5
0
WT
MRTFA KO
Bglap/Gapdh
6
5
4
3
2
1
0
WT
MRTFA KO
B
Igf1/Gapdh
2.5
2.0
1.5
1.0
0.5
0.0
WT
MRTFA KO
Igf1r/Gapdh
1.8
1.6
1.4
1.2
1.0
0.8
0.6
0.4
0.2
0.0
WT
MRTFA KO

Figure 17. There is less bone mass in MRTFA KO femur in H&E staining and osteopontin protein is lower in MRTFA KO mice.

Histological sections of proximal femur were stained with H&E to visualize the bone structures (A). The area with pink color and purple dots is mineralized bone mass, whereas the purple part is bone marrow cavity and contents (A). Femurs were obtained from WT and MRTFA KO mice for protein extraction in RIPA buffer. Western blots for osteopontin in 3 WT and 2 MRTFA KO mice are shown (B).

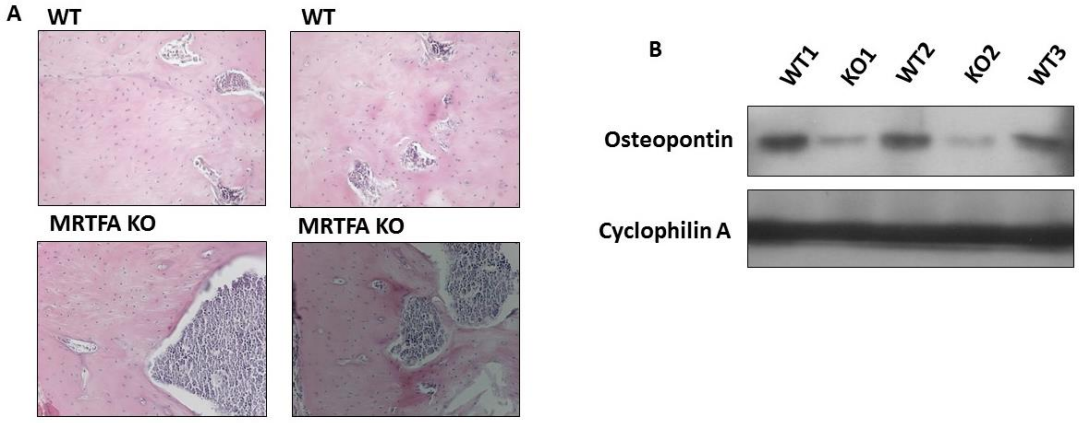

Figure 18. MRTFA KO mice have lower osteoblasts activity marker levels in the serum.

Blood samples were collected from the hearts of matched WT (n=6) and MRTFA KO (n=7) mice. ELISA assays were performed in diluted serum to measure the levels of procollagen I N-terminal propeptide (PINP) (A) and cross linked C-telopeptide of Type I collagen (CTX-1) (B). The data is expressed as described before (*p<0.05).

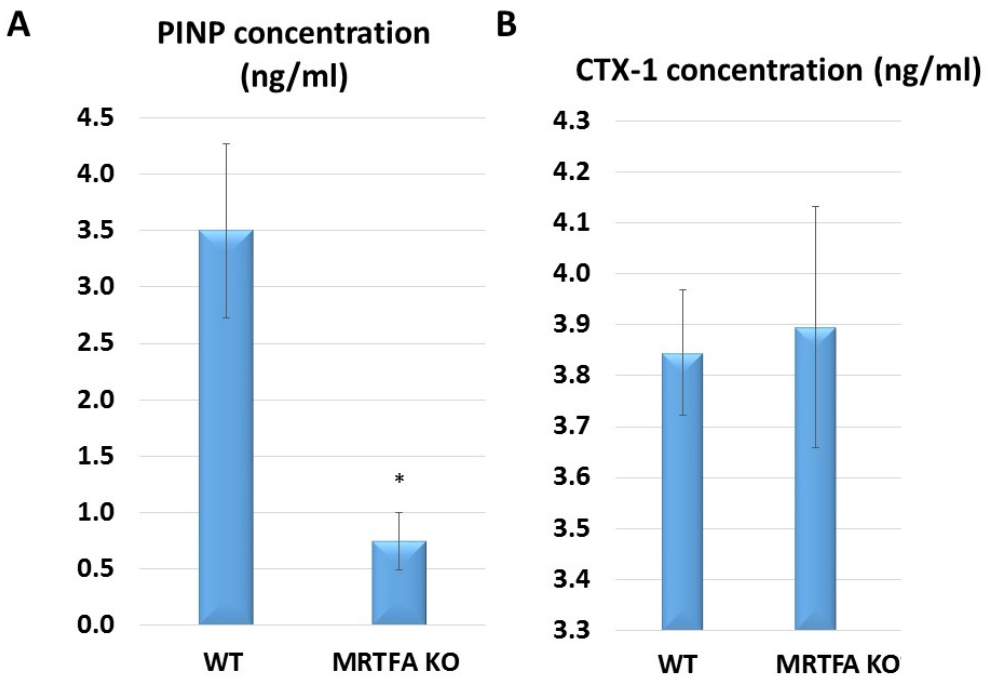

The Loss of MRTFA Potentiates Bone Mass Loss When Mice are Challenged with a High Fat Diet (HFD).

Representative 3D images of the cortical and trabecular femurs from each group of mice (WT LFD, WT HFD, KO LFD and KO HFD) are shown in Figure 19. No significant difference was observed in the cortical thickness amongst the 4 groups in Figure 19A. On the other hand, the bone mass of MRTFA KO mice fed with either LFD or HFD appeared to be reduced compared to their WT counterparts (Figure 19B). There was less bone volume in the MRTFA KO mice and more non-bone soft-tissue spacing as shown in Figure 19B.

The lengths of the femurs and tibiae of the 4 groups of mice were measured. There was no statistically significant difference between WT and MRTFA KO fed with LFD for either femur or tibia length (Figure 20A, B and Table 4). However, the MRTFA KO mice fed with a HFD for 6 weeks had significantly shorter femurs and tibiae (Figure 20A, B and Table 4).

Cortical thickness of HFD MRTFA KO mice was significantly thinner than the HFD controls, while there was no statistically significant difference between LFD WT and MRTFA KO mice (Figure 20C and Table 4). The trabecular BV/TV and connectivity density in HFD MRTFA KO mice were also reduced as compared to the HFD controls (Figure 20D, E and Table 4). These differences were not seen between WT and MRTFA KO mice fed with LFD. In summary, the MRTFA KO mice were more susceptible to bone loss when challenged with a HFD.

Figure 19. Representative 3D images of mid-diaphyseal cortical bone and trabecular bone of WT and MRTFA KO male mice fed with either HFD or LFD.

The femurs were harvested from 12 week old male mice (WT LFD n=6, MRTFA KO LFD n=8, WT HFD n=5, MRTFA KO HFD n=6). These mice were placed on different diets when they were 4-6 weeks old after weaning from $MRTFA^{+/-}$ mothers. WT and MRTFA KO mice were fed with a diet with 10% kcal% fat (low fat diet) or a diet with 60% kcal% fat (high fat diet) for 6 weeks. The representative 3D images of both cortical (A) and trabecular bone (B) of each group are shown to represent the remaining data.

Figure 19

A

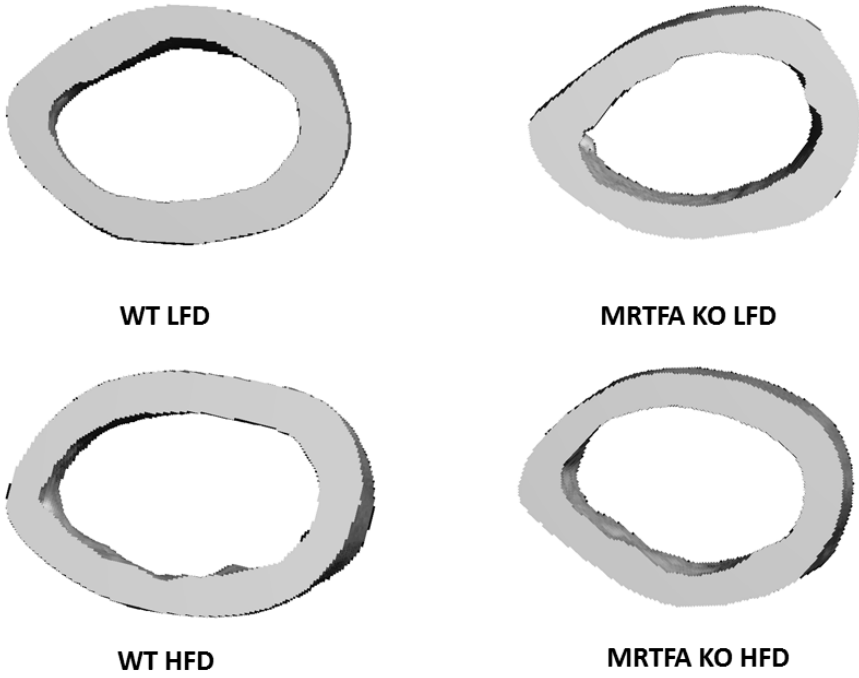
WT LFD
MRTFA KO LFD
WT HFD
MRTFA KO HFD

B

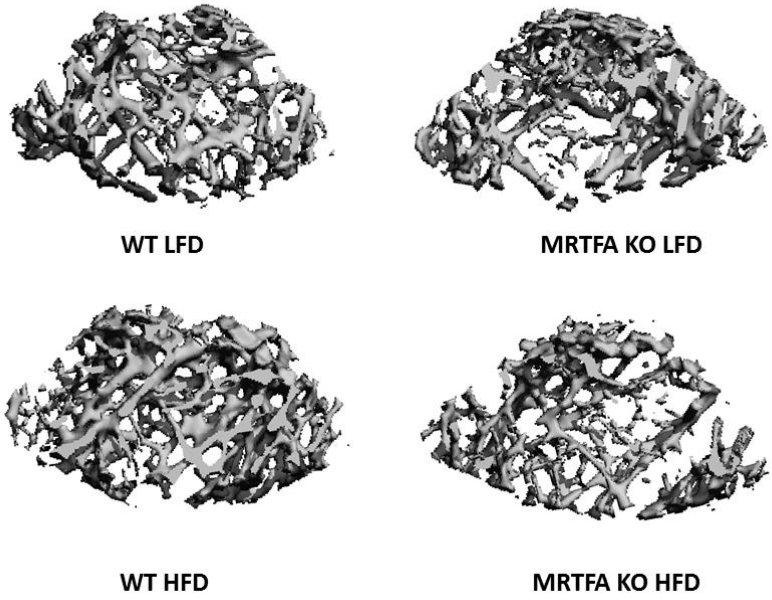
WT LFD
MRTFA KO LFD
WT HFD
MRTFA KO HFD

Figure 20. MRTFA KO mice have an osteoporotic phenotype when challenged with HFD.

The femurs were obtained from the mice as described in Figure 19. The femur length (A), tibia length (B), cortical thickness (C), trabecular BV/TV (D) and connectivity density (E) of the femurs are shown. The data is expressed as in Figure 9. Student's T-tests were performed between WT LFD and MRTFA KO LFD, WT HFD and MRTFA KO HFD, respectively. (*p≤0.05).

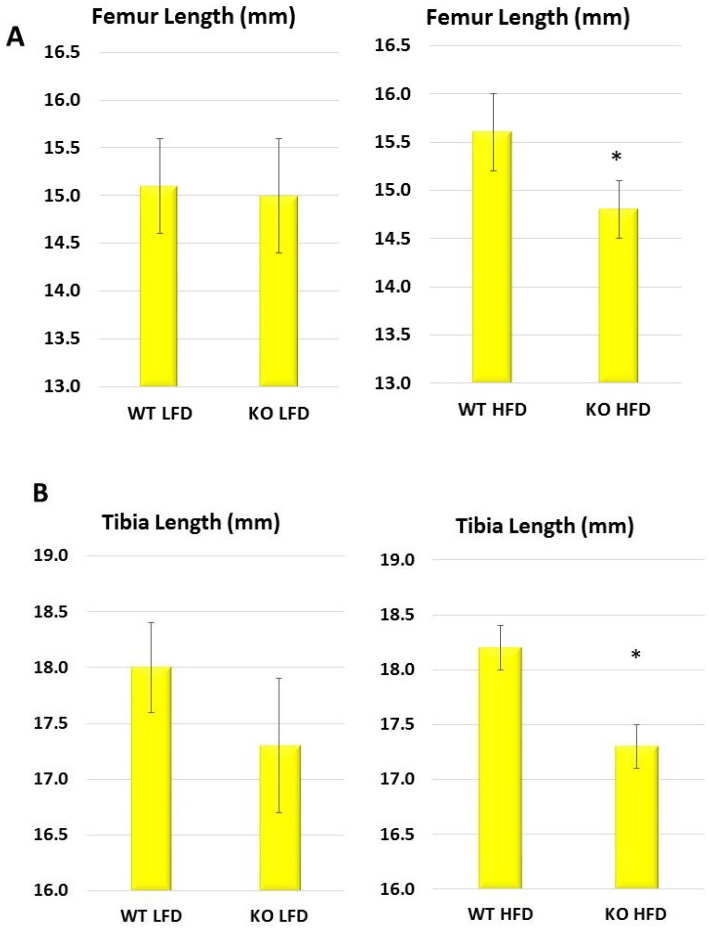

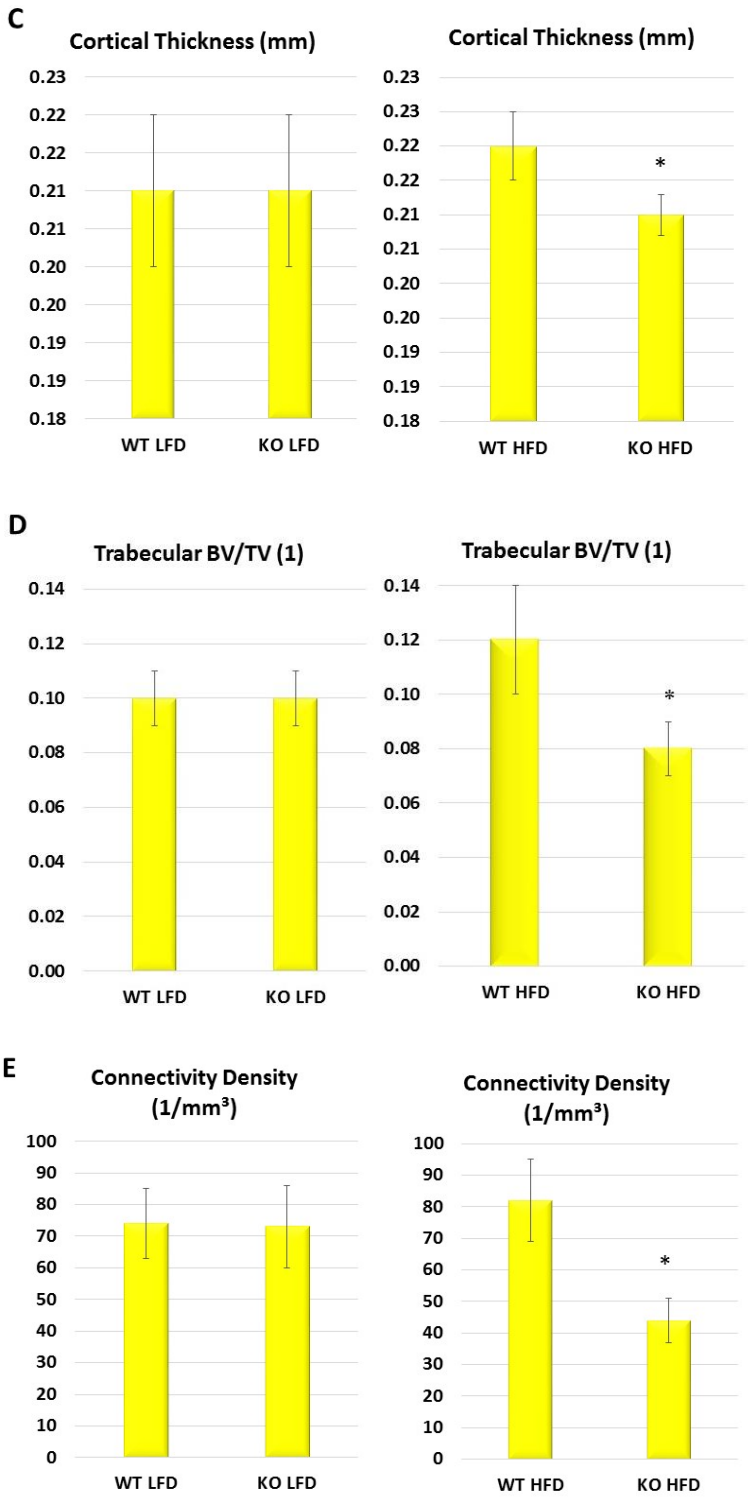
C
Cortical Thickness (mm)
0.23
0.22
0.22
0.21
0.21
0.20
0.20
0.19
0.19
0.18
WT LFD
KO LFD
Cortical Thickness (mm)
0.23
0.23
0.22
0.22
0.21
0.21
0.20
0.20
0.19
0.19
0.18
*
WT HFD
KO HFD
D
Trabecular BV/TV (1)
0.14
0.12
0.10
0.08
0.06
0.04
0.02
0.00
WT LFD
KO LFD
Trabecular BV/TV (1)
0.14
0.12
0.10
0.08
0.06
0.04
0.02
0.00
*
WT HFD
KO HFD
E
Connectivity Density (1/mm³)
100
90
80
70
60
50
40
30
20
10
0
WT LFD
KO LFD
Connectivity Density (1/mm³)
100
90
80
70
60
50
40
30
20
10
0
*
WT HFD
KO HFD

Table 3. MRTFA KO developed an osteoporotic phenotype when challenged with HFD.

The femurs were obtained from mice as in Figure 19 and 20. The values shown in this table are the values of each mice group ± standard error. The bone morphometric parameters included are listed in Table 1.

	WT LFD (n=6)	MRTFA KO LFD (n=8)	WT HFD (n=5)	MRTFA KO HFD (n=6)
Body Weight (g)	31.6±4.5	27.4±3.2	37.9±5.9	35.8±6.8
Femur Length (mm)	15.1±0.5	15.0±0.6	15.6±0.4	14.8±0.3
Tibia Length (mm)	18.0±0.4	17.3±0.6	18.2±0.2	17.3±0.2
Cortical Total Volume (TV) (mm^3)	0.54±0.02	0.54±0.03	0.59±0.02	0.54±0.02
Cortical Bone Volume (BV) (mm^3)	0.53±0.02	0.53±0.03	0.58±0.02	0.53±0.02
Cortical BV/TV (1)	0.98±0.001	0.98±0.001	0.98±0.001	0.98±0.001
Cortical Thickness (mm)	0.21±0.01	0.21±0.01	0.22±0.005	0.21±0.003
Trabecular Total Volume (TV)(mm^3)	1.99±0.1	1.81±0.1	2.1±0.1	1.9±0.1
Trabecular Bone Volume (BV) (mm^3)	0.19±0.02	0.18±0.03	0.26±0.06	0.15±0.02
Trabecular BV/TV (1)	0.10±0.01	0.10±0.01	0.12±0.02	0.08±0.01
Connectivity Density ($1/mm^3$)	74±11	73±13	82±13	44±7
Structure Model Index (1)	3.0±0.2	2.9±0.2	2.6±0.2	3.0±0.1
Trabecular Number(1/mm)	4.3±0.1	4.2±0.2	4.1±0.2	3.7±0.2
Trabecular Thickness (mm)	0.053±0.003	0.052±0.003	0.056±0.003	0.051±0.002
Trabecular Separation (mm)	0.22±0.01	0.24±0.01	0.24±0.01	0.27±0.02
Trabecular Mean/Density of TV (Apparent) (mg HA/ccm)	172±11	170±13	184±20	150±9
Trabecular Mean/Density of BV (Material) (mg HA/ccm)	986±11	996±68	1008±13	995±10

Discussion

Osteoporosis is manifested by excessive loss of bone mass and increased tendency for pathological fractures. Previous studies showed osteoporotic bones have increased bone marrow adiposity in the trabecular region (Meunier, Aaron *et al*. 1971, Justesen, Stenderup *et al*. 2001, Rosen and Bouxsein 2006). Since adipocytes and osteoblasts differentiate from the common progenitors, the disruption of the fate switch between these two lineages will lead to decreased osteoblastogenesis and enhanced adipogenesis and osteoporosis (Rosen and Bouxsein 2006). The aim of thesis was to investigate whether or not the actin-MRTFA-SRF circuit acts downstream of RhoA-ROCK signaling to dictate the MSC fate switch between osteoblasts and adipocytes.

Here, we studied the role of MRTFA in bone formation *in vivo* using a global MRTFA KO mouse model. The MRTFA KO mice had lower whole body weight, shorter femurs and tibiae in both genders. Although the lower whole body weight seen in the MRTFA KO phenotype might be due to the decreased fat mass discovered by others in our group, a reduction in bone size and bone mass might also be contributing to this phenotype (McDonald, Li *et al*. 2015).

The defects of the bone lengths in MRTFA KO mice suggested that osteoblast development and function was impaired. Accordingly, we found that MRTFA KO mice had reduced osteoblastogenic gene mRNA levels. However, other mechanisms for the compromised longitudinal growth of the MRTFA KO bones such as defects in chondrogenesis and growth plate development should be explored in future studies. Since

Runx2 has been shown to regulate chondrocyte maturation and limb growth (Yoshida, Yamamoto et al. 2004), the inhibition of Runx2 in MRTFA KO mice (Figure 16A) might lead to impairment of chondrogenesis and contribute to the defects of longitudinal growth of limbs in the mice.

Micro-CT analysis performed on WT and MRTFA KO mice revealed an osteoporotic phenotype in the MRTFA KO mice. Female MRTFA KO had a thinner cortical thickness in the mid-diaphyseal area of the femurs, although the difference was not seen in the males. The MRTFA KO mice had smaller tissue volume and bone volume due to smaller overall bone sizes in both genders (Figure 11 and 12).

Both male and female MRTFA KO mice consistently exhibited a significant osteoporotic phenotype with decreased bone mass in trabecular femur. BV/TV was approximately 20% lower in the male MRTFA KO mice and approximately 50% lower in the females. The histological images of the trabecular femur validated this finding (Figure 17A). The osteoporotic phenotype was more striking in the female MRTFA KO mice as shown by the marked reduction of trabecular number, connectivity density and increase of trabecular separation. Reduced mRNA levels of osteoblastogenic genes and lower osteopontin protein expression were seen in MRTFA KO mice as well.

Additionally, the serum levels of systemic osteoblasts activity marker PINP was decreased by more than 75% in the MRTFA KO mice. This indicates that the impairment of osteoblastogenesis might also be occurring in other bones, although we have not yet investigated the microstructures in other bones in the MRTFA KO mice. To investigate

whether excessive activation of osteoclasts contributed to the bone loss in the MRTFA KO mice, we measured the serum levels of osteoclast activity marker CTX-1. No significant differences were found in CTX-1 levels between WT and MRTFA KO mice, which suggests that excessive bone resorption is not the mechanism for the osteoporotic phenotype.

To study whether MRTFA is protective against osteoporosis in adipogenic-inducing pathological conditions, we studied the changes of bone mass in WT and MRTFA KO mice fed with either LFD or HFD. The MRTFA KO mice exhibited decreased bone lengths and bone mass when challenged with HFD, but the difference between WT and MRTFA KO mice fed with LFD is not statistically significant despite a trend of decreased bone lengths in MRTFA KO mice. This finding suggests that ablation of MRTFA potentiated bone loss under adipogenic-inducing conditions such as HFD. To confirm whether there is more adipose tissue in the MRTFA KO mice bone marrow, histological examinations and measurements of adipogenic genes expression will be performed in future investigations.

There is a discrepancy in the Micro-CT results of older *versus* younger male mice. The decreased trabecular bone mass as seen in 17 week old MRTFA KO mice was not recapitulated in the 12 week old mice. When the MSC early fate commitment shifts towards adipogenesis over osteoblastogenesis as the mice age, the effect of MRTFA deletion might manifest itself more in bone remodeling. Also, MRTFB might compensate for the loss of MRTFA functionally to maintain a normal bone phenotype in the younger

MRTFA KO mice. We speculate MRTFA might play a more important role in the maintenance of bone mass in adult life.

In summary, MRTFA KO mice exhibited an osteoporotic phenotype with reduced bone mass in the trabecular femurs in both genders. This phenotype appears to be due to inhibited osteoblastogenesis. MRTFA appears to be an important regulator for maintaining bone mass *in vivo*.

Deletion of MRTFA promotes the differentiation of primary bone marrow MSCs to adipocytes *versus* osteoblasts.

Introduction

MSCs are pluripotent bone marrow stromal progenitors which possess the potential to differentiate into chondrocytes, adipocytes, myoblasts or osteoblasts when given the appropriate milieu of growth factors and extracellular microenvironment (Caplan and Bruder 2001) (Figure 1). However, an understanding of the underlying molecular mechanisms of the fate commitment of MSCs to different lineages is still incomplete.

Based on previous studies (McBeath, Pirone *et al.* 2004, Xian, Wu *et al.* 2012) and the osteoporotic phenotype seen in the MRTFA KO mice, we hypothesize that the actin-MRTFA-SRF circuit is acting downstream of RhoA-ROCK pathway to regulate MSC fate commitment. Because the mouse model we used is a MRTFA global knock out, we have not yet been able to definitively confirm that the osteoporotic phenotype is caused by inappropriate fate switch of the MSCs in a cell autonomous manner. In this section, we isolated bone marrow MSCs from WT and MRTFA KO mice to determine whether the fate commitment of these cells is altered by the ablation of MRTFA using an established *ex vivo* system.

The SRF inhibitor, CCG1423, is a small molecule acting downstream of the RhoA-ROCK pathway to inhibit MRTFA-dependent SRF target gene transcription (Evelyn, Wade *et al.* 2007). By treating the MSCs with CCG1423, we can determine

whether MRTFA-SRF-dependent transcriptional activity is important for MSC lineage commitment.

Results

The fate commitment of MSCs isolated from MRTFA KO mice shifted towards adipocytes over osteoblasts.

Bone marrow derived MSCs isolated from MRTFA KO mice exhibited an enhanced capacity to differentiate into adipocytes in comparison to the MSCs from WT mice (Figure 21). The phase contrast microscopic images of the MSCs showed that the MRTFA KO cultures accumulated more lipid droplets during adipogenesis (Figure 21A). Furthermore, the mRNA and protein levels of several important adipogenic genes such as Pparg, Cepba, Adipoq and Fabp4 were significantly increased in the MRTFA KO cells relative to the controls (Figure 21B, C).

Interestingly, mRNA levels of several brown fat genes including beta-3 adrenergic receptor (Adrb3), peroxisome proliferator-activated receptor gamma co-activator 1-α (Ppargc1a) and Ppargc1b also increased in the MRTFA KO cells. These findings are consistent with a recent study conducted by our group showing that MRTFA regulates the commitment of beige adipocytes. In fact, studies by others have identified a subset of brown fat genes in bone marrow fat and referred to it as yellow fat (Krings,

Rahman *et al*. 2012). Whether enhancement of these brown fat genes in the MRTFA KO mice contributes to the whole body metabolism deserves further investigation.

Figure 21. Bone marrow derived MSCs from MRTFA KO mice showed enhanced adipogenic differentiation.

Femurs and tibiae were dissected from WT (n=3) and MRTFA KO mice (n=3). The bone marrow cavity contents were flushed out of these bones with MSC growth media. After the MSCs reach confluence, adipogenic inducers were added to the cells. Dexamethasone, IBMX, insulin, T3 and indomethacin were added for 2 days and T3 and insulin were supplemented in the growth media for another 8 days. The phase contrast microscopic images were acquired at day 10 of adipogenesis (A). The mRNA and protein samples were then extracted from these cells. Adipogenic gene expression was analyzed by RT-PCR using the corresponding primers Pparg, Cebpa, Plin, Adipoq, Fabp4, Ppargc1a, Ppargc1b and Adrb3. The mean relative levels (normalized to Gapdh mRNA levels) of the genes expression are shown in (C) with standard error (*$p<0.05$). Expression of adiponectin and C/EBPα in these differentiated MSCs were probed with western blots analysis as shown in C.

Figure 21

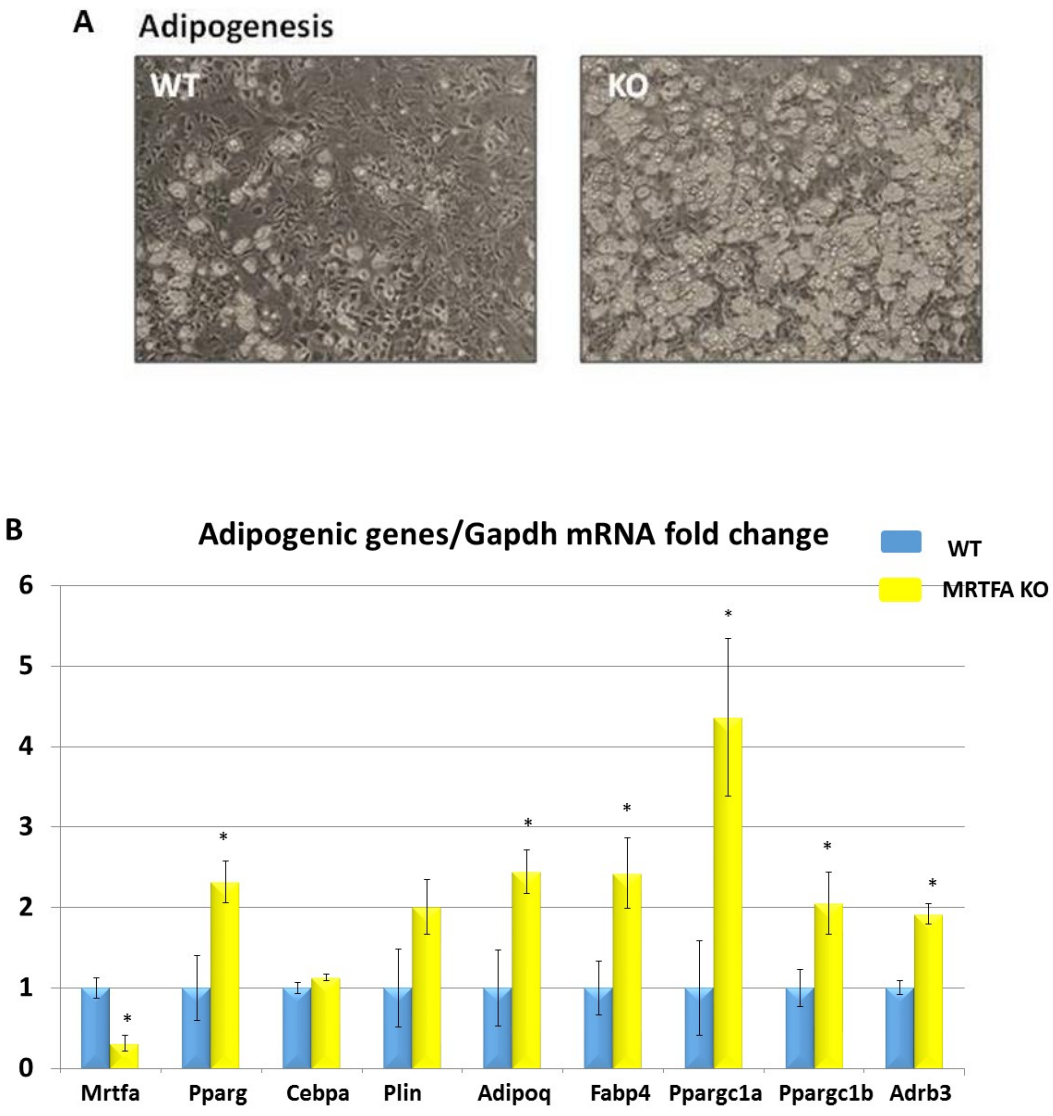
A
Adipogenesis
WT
KO
B
Adipogenic genes/Gapdh mRNA fold change
WT
MRTFA KO
6
5
4
3
2
1
0
Mrtfa
Pparg
Cebpa
Plin
Adipoq
Fabp4
Ppargc1a
Ppargc1b
Adrb3

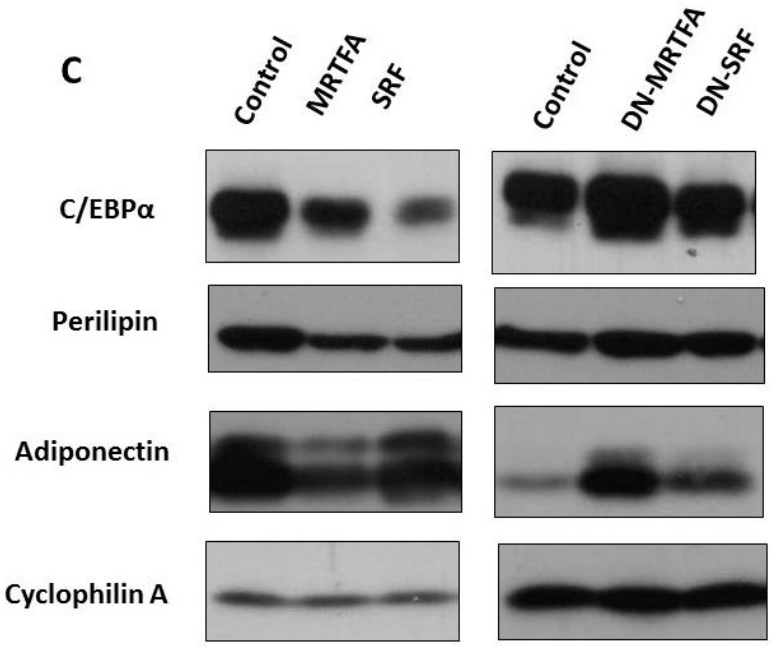
C
Control
MRTFA
SRF
Control
DN-MRTFA
DN-SRF
C/EBPα
Perilipin
Adiponectin
Cyclophilin A

In contrast to WT MSCs, the MRTFA KO cells showed compromised osteoblastogenic differentiation with decreased bone nodule formation and mineral deposition (Figure 22A). Alizarin Red S staining was performed to visualize the calcific deposition in the differentiated WT and MRTFA KO MSCs (Figure 22B). Both male and female MRTFA KO MSCs had less mineral deposition as compared to the controls and this difference was more striking in the females. The mRNA levels of several osteoblastogenic genes such as Runx2, Spp1, Bglap and Spock were reduced in differentiated MRTFA KO mice MSCs (Figure 22C). We hypothesize that the inhibition of these osteoblastogenic genes leads to the reduced mineral deposition during bone formation as described in the last section.

Figure 22. Osteoblastogenesis was attenuated in MRTFA KO mice bone marrow MSCs.

The bone marrow derived MSCs were harvested as described in Figure 21. After the MSCs reached confluence, the cells were treated with osteoblastogenic inducers including L-ascorbic acid, β-glycerophosphate and dexamethasone. This osteo-inducing media were refreshed every 3 days until day 21 of differentiation. The phase-contrast images were acquired at day 21 of osteoblastogenesis (A). Then the differentiated cells were stained with 2% Alizarin Red S to visualize the mineral depositions in mature osteoblasts (B). The mRNA samples were extracted from MSCs at day 21 of osteoblastogenic differentiation. Osteoblastogenic genes were probed by RT-PCR using the following primers: Runx2, Alpl, Spp1, Spock and Bglap. The data are presented C as described in Figure 19 (*$p<0.05$).

Figure 22

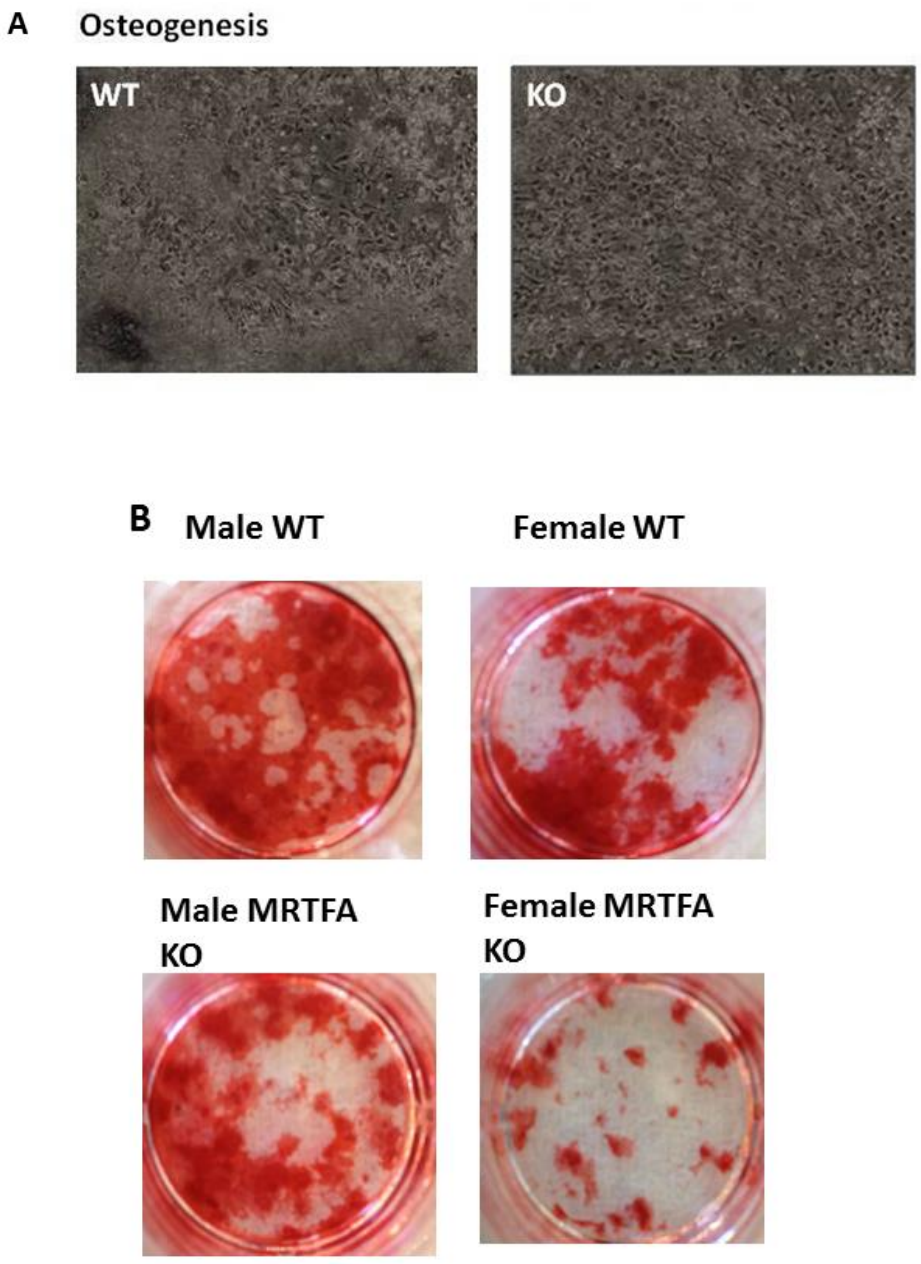
A
Osteogenesis
WT
KO
B
Male WT
Female WT
Male MRTFA KO
Female MRTFA KO

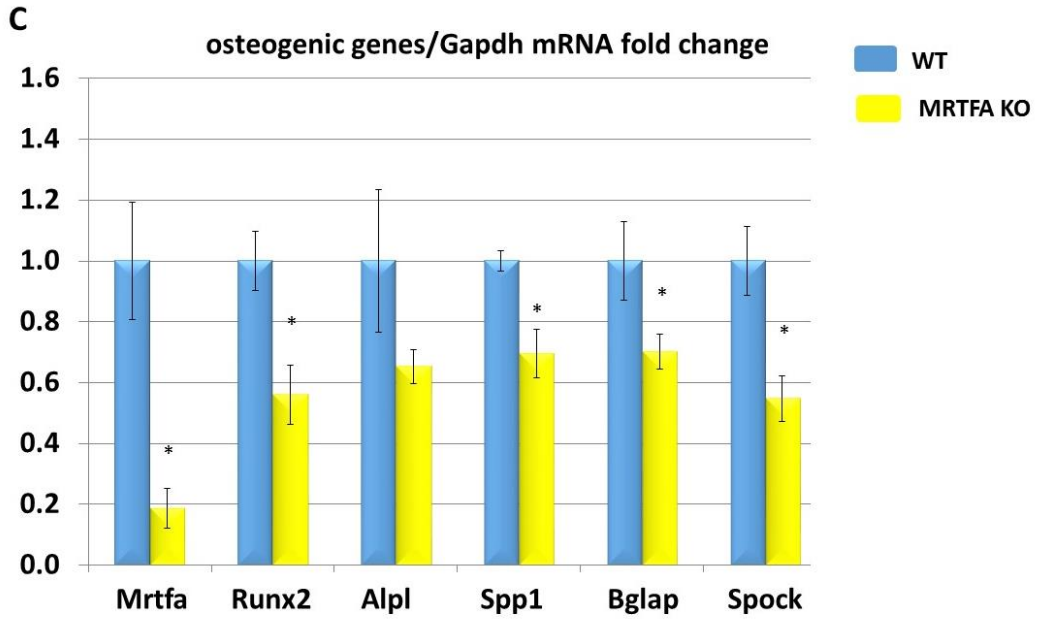
C
osteogenic genes/Gapdh mRNA fold change
WT
MRTFA KO
1.6
1.4
1.2
1.0
0.8
0.6
0.4
0.2
0.0
Mrtfa
Runx2
Alpl
Spp1
Bglap
Spock

The SRF inhibitor CCG1423 attenuated osteoblastogenesis and promoted adipogenesis in bone marrow MSCs

CCG1423 pre-treated MSCs (treated with CCG1423 for 2 days prior to adipogenic induction) had more lipid accumulation (Figure 23A) and increased mRNA levels of adipogenic genes such as Pparg, Cepba and Plin (Figure 23B). When CCG1423 was added for the entire differentiation time frame, there was a similar degree of enhancement of adipogenesis (data not shown).

On the other hand, when CCG1423 was added to the MSCs during osteoblastogenesis, bone nodule formation was inhibited (Figure 24A). Reduced mRNA levels of Alpl, Bglap and Spock genes also confirmed the inhibition (Figure 24B). When CCG1423 was only added to MSCs for 2 days prior to osteoblastogenic induction, there was no inhibitory effect on osteoblastogenic gene expression at day 21 of differentiation. It is likely that after 21 days of osteoblastogenesis, the initial reduction in SRF/MRTFA activity by CCG1423 recovered to levels permissive for osteoblastogenic gene expression.

These data also suggest that SRF/MRTFA activity is required throughout the osteoblastogenic process. In contrast, it appears that SRF/MRTFA activity only needs to be suppressed during the commitment phase of adipogenesis, unless differentiation itself inhibits the activity.

In conclusion, the fate commitment of MSCs was regulated by the SRF/MRTFA activity. Inhibiting the SRF/MRTFA activity led to inhibition of osteoblastogenesis but enhancement of adipogenesis in WT MSCs.

Figure 23. The SRF inhibitor CCG1423 enhanced adipogenesis in WT bone marrow MSCs.

Bone marrow MSCs were isolated from WT mice (n=3). DMSO (vehicle) or 1 mM SRF inhibitor CCG1423 was added to the MSCs when the cells were sub-confluent. CCG1423 was then removed and the adipogenic inducers mentioned in Figure 21 were added at confluence. The phase-contrast images of the cells were captured at day 10 (A). The mRNA levels of adipogenic genes were measured by RT-PCR using primers for Pparg, Cebpa, Plin and Adipoq (B). The data is presented according to Figure 19 (*$p<0.05$).

Figure 23

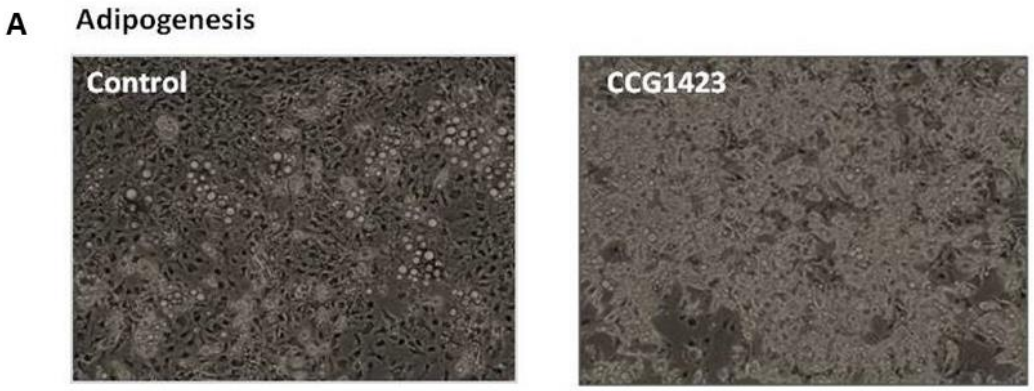
A
Adipogenesis
Control
CCG1423

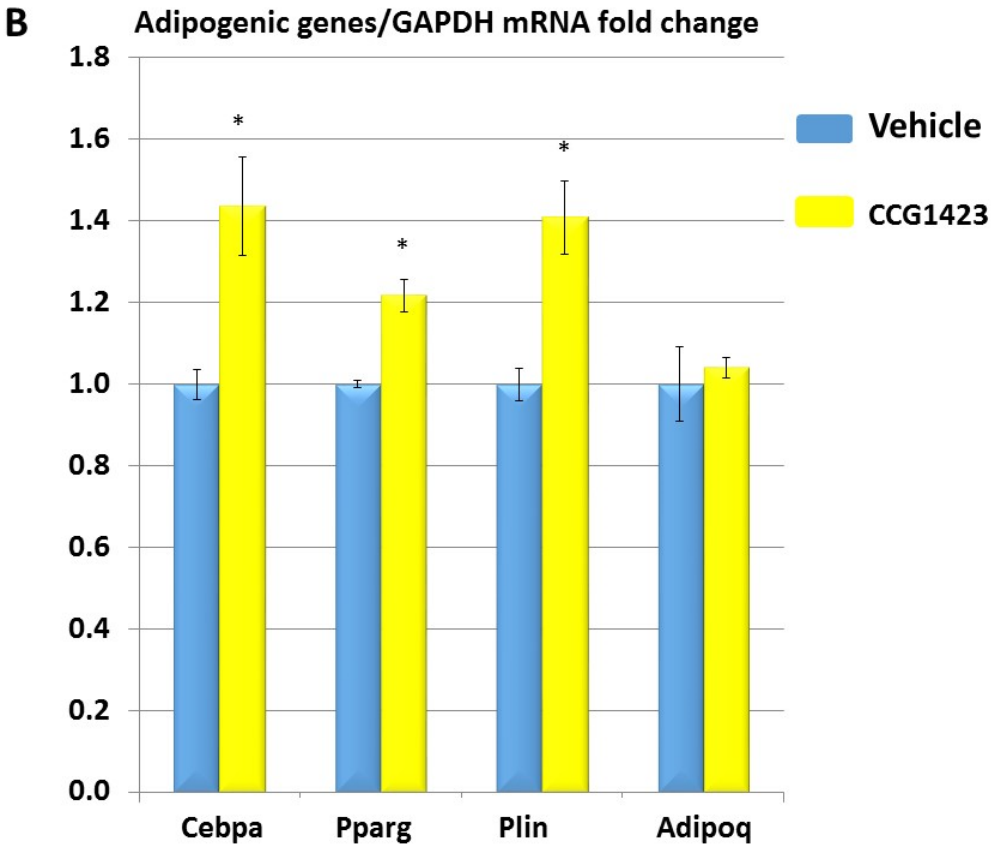
B
Adipogenic genes/GAPDH mRNA fold change
1.8
1.6
1.4
1.2
1.0
0.8
0.6
0.4
0.2
0.0
*
*
*
Vehicle
CCG1423
Cebpa
Pparg
Plin
Adipoq

Figure 24. SRF inhibitor inhibited osteoblastogenesis in WT bone marrow MSCs.

DMSO (vehicle) or 1 mM SRF inhibitor CCG1423 was added to the MSCs when the cells reached confluence, together with the osteoblastogenic inducers as described in Figure 22. The osteoblastogenic inducing media was refreshed every 3 days with either DMSO or CCG1423 for a total of 21 days. The phase-contrast images were captured at day 21 of differentiation (A). Osteoblastogenic gene mRNA levels were measured by RT-PCR using primers against Runx2, Alpl, Spp1, Bglap and Spock (B). That data is presented as in Figure 19 (*$p<0.05$).

Figure 24

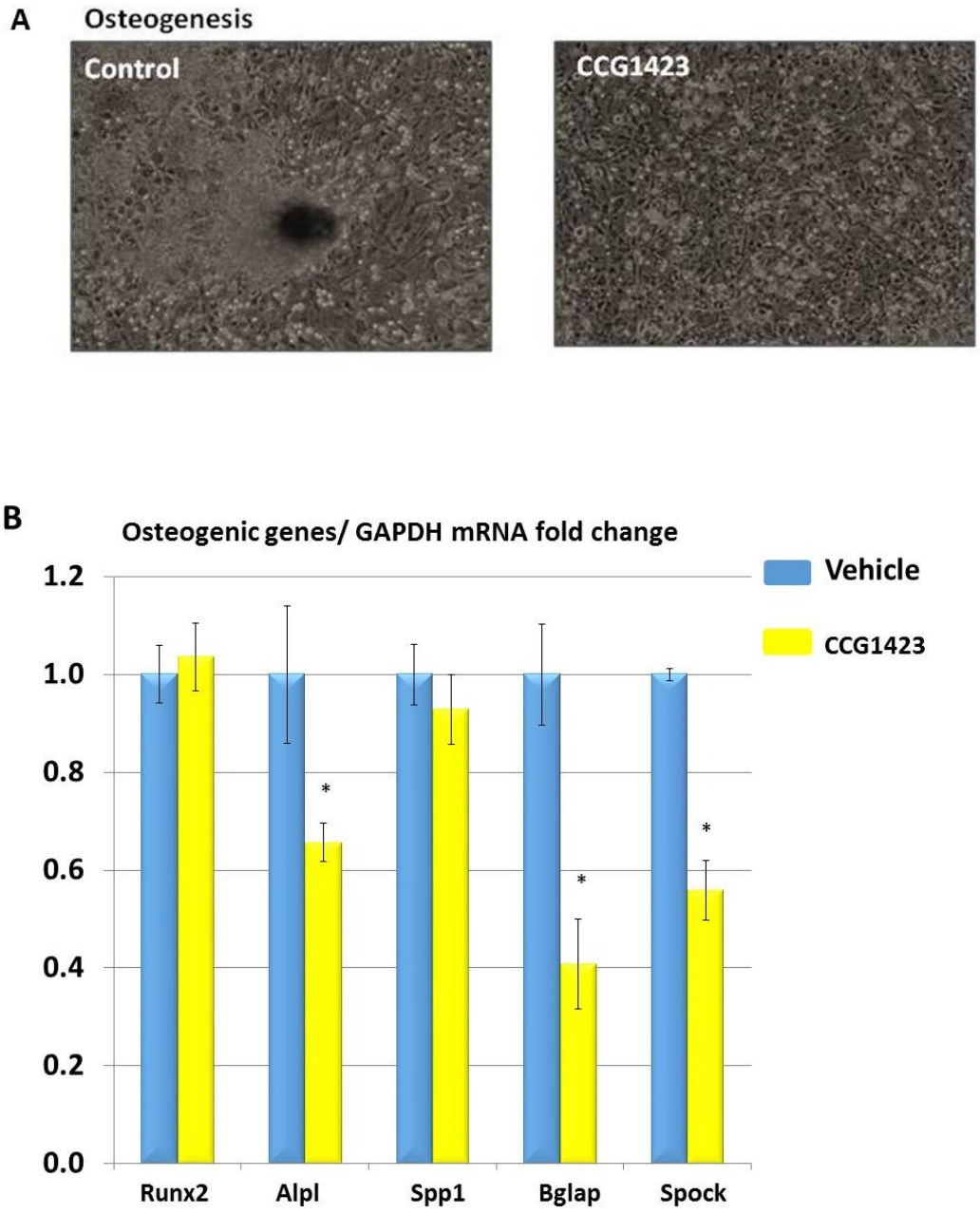
A
Osteogenesis
Control
CCG1423
B
Osteogenic genes/ GAPDH mRNA fold change
Vehicle
CCG1423
1.2
1.0
0.8
0.6
0.4
0.2
0.0
*
*
*
Runx2
Alpl
Spp1
Bglap
Spock

Discussion

In this chapter, we discovered that the ablation of MRTFA in bone marrow MSCs inhibited osteoblastogenesis but enhance adipogenesis in a cell autonomous manner. Isolating and investigating the bone marrow MSCs helped to rule out the possibility that the osteoporotic phenotype seen in the MRTFA KO mice was caused entirely by systemic growth hormone defects (IGF1 and IGF1R). We speculate that the ablation of MRTFA and MRTFA-dependent SRF target genes altered the actin dynamics in the MSCs, which led to cytoskeletal re-organization, becoming more permissive for adipogenic rather than osteoblastogenic differentiation.

Evelyn showed that CCG1423 specifically inhibits SRF/MRTFA-induced target genes such as actin itself and regulators for actin dynamics and turnover (Evelyn, Wade et al. 2007). Despite the fact that CCG1423 was removed once the adipogenic induction was started, the adipogenesis was still increased in the WT MSCs. From this, we can infer that MRTFA/SRF regulated the MSCs fate commitment at a very early stage prior to morphological differentiation.

Although the bone marrow derived MSCs used in the aforementioned studies provided a useful *ex vivo* system to study MSC fate switch, the heterogeneity of these un-sorted bone marrow cells might confound the interpretation of the results. It has been shown that only 0.01%-0.001% of the total bone marrow cells are MSCs (Pittenger, Mackay *et al*. 1999). Although the erythrocytes and unattached immune cells were removed by media change after the MSCs were attached (more than 70%-80% of the

total cells), there were still significant numbers of cells, presumably hematopoietic stem cells, immune cells, endothelial cells, fibroblasts and others in the mixed culture. Some of these cells might respond very differently to the growth factor treatment and confound the results obtained from these experiments. As seen in Figure 21 and 23, the percentage of increase in the mRNA levels of adipogenic genes is milder compared to the differences observed in the phase-contrast images of the cells. The undifferentiated non-MSCs might dilute the adipogenic gene mRNA signal detected by RT-PCR, thus lead to the inconsistencies in the results. This potentially confounding factor of this system should be taken into consideration during data interpretation and the MSCs should be further purified in future studies.

In conclusion, we have showed that the ablation of MRTFA in the MSCs enhanced adipogenesis but inhibited osteoblastogenesis. Treating the WT MSCs with SRF inhibitor CCG1423 mimicked the effects of knocking out MRTFA by inhibiting osteoblastogenesis but enhancing adipogenesis.

MRTF/SRF signaling promotes osteogenesis and inhibits adipogenesis in MSC line C3H10T1/2 cells.

Introduction

Based on the results in the previous sections, we have concluded that MRTFA is important for maintaining bone mass *in vivo* due to its role in regulating the MSC fate switch between adipose and osteoblastic lineages. In this section, we document the changes of MRTFA, SRF and select target genes during adipogenesis. C3H10T1/2 MSCs stably over-expressing MRTFA, SRF and their dominant negative variants were used to manipulate the MRTFA/SRF activity in order to study the role of the actin-MRTFA-SRF circuit in MSC fate determination.

C3H/10T1/2 cells were originally derived from primary cells isolated from a whole C3H mouse embryo as described in a study published in 1973 (Reznikoff, Bertram *et al.* 1973). These cells possess the potential to differentiate into multiple lineages such as adipocytes, chondrocytes, osteoblasts and myoblasts, thus they are widely used for studying MSCs. Because the studies described earlier were conducted in heterogeneous bone marrow cells, the results might be confounded by the presence of other cells types in the bone marrow besides MSCs. Therefore, it is of interest to recapitulate these results in C3H10T1/2 cell lines over-expressing MRTFA, dominant negative MRTFA (DN-MRTFA) to support the conclusions drawn earlier.

Mikkelsen first identified SRF as a negative regulator of adipogenesis (Mikkelsen, Xu et al. 2010). Chen has since showed that SRF regulates bone formation *via* IGF-1 and Runx2 (Chen, Yuan et al. 2012). Based on the aforementioned studies, we hypothesized

that SRF promotes osteoblastogenesis but inhibits adipogenesis in the MSCs through the same mechanisms as described in Chapters I and II. This chapter serves to prove this hypothesis in C3H/10T1/2 cell lines over-expressing SRF and dominant negative SRF (DN-SRF).

MRTFA, SRF and their target genes are down-regulated during adipogenesis

Figure 25 and 27 shown in this chapter have been published in McDonald and Li et al. 2015 (McDonald, Li et al. 2015). Permission to include these figures in this thesis was acquired from Cell Journal.

During the adipogenic differentiation of C3H10T1/2 cells, Mrtfa, Mrtfb, Srf and their select target genes including Acta, Col1a1 and Col3a1 are all down-regulated, thereby allowing the cells to adopt a round morphology for promoting lipid accumulation as shown in Figure 25A and B. This down-regulation of genes happened at an early stage of adipogenesis prior to morphological differentiation. The mRNA levels of these genes decreased at least 60% as compared to baseline between day 0 and day 1 of adipogenesis and this significant reduction continued until day 2 as shown in Figure 25A and B. The levels of these genes remained low throughout adipogenic differentiation and lipid droplets accumulated in the maturing adipocytes. MRTFA and SRF appeared to be negative regulators for adipogenesis. The down-regulation of MRTFA, SRF and their target genes is associated with the dramatic reorganization of cytoskeleton, which is required for proper adipocyte maturation (Spiegelman and Farmer 1982).

Figure 25. MRTFA, SRF and their select target genes were down-regulated during adipogenesis.

C3H/10T1/2 cells were induced for adipogenic differentiation upon confluence with growth media containing dexamethasone, IBMX, insulin, T3 and indomethacin for 2 days. The cells were then maintained in growth media supplemented with T3 and insulin for another 6 days. mRNA and protein samples (n=3) were extracted at different time points at day 0 (D0), day 1 (D1), day 2 (D2), day 4 (D4), day 6 (D6) and day 8 (D8) for RT-PCR (A) and western blot analysis (B). The genes probed in A are Mrtfa, Mrtfb, Srf, Acta, Col1a1, Col3a1, Fabp4 and Ucp1. The fold changes of these genes (shown with standard error) were normalized to Gapdh mRNA levels and the mean value of day 0 samples was set at 1. The protein levels of MRTFA, SRF, SMA and FABP4 are shown in B.

Figure 25

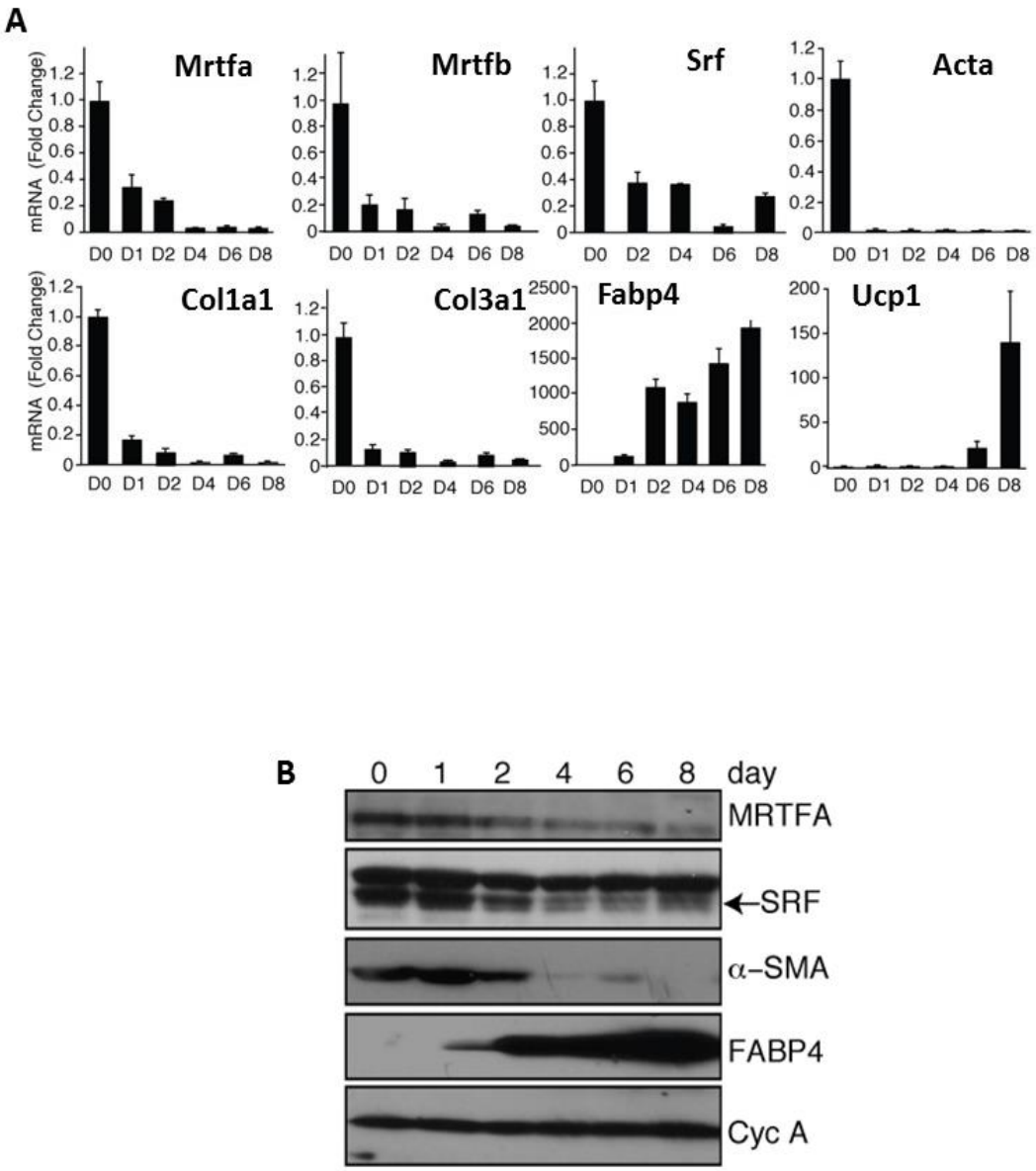
A
Mrtfa
Mrtfb
Srf
Acta
Col1a1
Col3a1
Fabp4
Ucp1
mRNA (Fold Change)
D0 D1 D2 D4 D6 D8
B
0 1 2 4 6 8 day
MRTFA
←SRF
α–SMA
FABP4
Cyc A

MRTFA and SRF promotes osteogenesis and inhibits adipogenesis.

The C3H/10T1/2 stable cell lines over-expressing MRTFA, SRF and their dominant negative variants were generated by retroviral infection as described in the Materials and Methods (Luchsinger, Patenaude *et al*. 2011, Wang, Prakash *et al*. 2012). Western blot analysis was performed on these cells to confirm successful stable over-expression of the relevant proteins. MRTFA and FLAG-tag levels were probed. The MRTFA band migrates as a 150 kilodalton (kDa) band and the SRF band (FLAG-tagged) at approximately 50 kDa (Figure 26), sizes which are consistent with their known molecular weights and the time course results in Figure 26. DN-MRTFA band (FLAG-tagged) migrated as a 70 kDa band and DN-SRF band (FLAG-tagged) at approximately 30 kDa (Figure 26). The sizes of these bands are also consistent with the numbers of amino acids in these dominant negative variants (truncated forms without the transactivation domains). Although the mRNA and the protein level of MRTFA was significantly increased in the MRTFA over-expressing cells, we were unable to detect any signal for FLAG-tag in these cells.

Over-expression of MRTFA or SRF inhibited adipogenesis with reduced lipid droplet accumulation and inhibited adipogenic genes expression; whereas the over-expression of DN-MRTFA or DN-SRF enhanced adipogenesis. As shown in Figure 27A, MRTFA or SRF over-expressing MSCs had significantly less lipid-laden cells, while the cultures of dominant negative variants MSCs had many more mature adipocytes (Figure 27A). These observations were confirmed by the mRNA levels of adipogenic genes in the mentioned cell lines. Over-expression of either MRTFA or SRF inhibited mRNA

accumulation of Pparg, Cebpa, Plin, Adipoq and Fabp4 (Figure 27B); whereas over-expression of their dominant negative forms increased expression of some of these genes (Figure 27B). The consequent changes in protein levels of C/EBPα, perilipin and adiponectin were consistent with these results (Figure 27C).

Interestingly, brown fat genes fatty acid binding protein 3 (FABP3), cell death activator CIDE-A (Cidea), ELOVL fatty acid elongase 3 (Elovl3) and cytochrome c oxidase polypepetide 7A1 (Cox7a1) (Figure 27D) were also significantly inhibited in the MRTFA or SRF over-expressing cells during BMP7-induced adipogenesis. These results are consistent with the findings in the earlier study on bone marrow MSCs and our previous study showing that MRTFA KO adipose stromal fraction cells have enhanced brown fat genes (McDonald, Li *et al*. 2015).

The over-expression of MRTFA, SRF or their dominant negative variants, on the other hand, resulted in very different cell shapes for the MSCs during osteoblastogenesis (Figure 28A). The MRTFA or SRF over-expressing MSCs exhibited spread and elongated shapes in response to the osteoblastogenic inducers (Figure 28A). In contrast, the shapes of the cells over-expressing either DN-MRTFA or DN-SRF were rounder and more irregular (Figure 28A). These observed changes in the cell shapes correlated with changes in osteoblastogenic mRNA levels. MRTFA or SRF over-expression enhanced osteoblastogenic genes such as Spp1 and Bglap (Figure 28B); while dominant negative variants inhibited the expression of these genes (Figure 28C).

Figure 26. Over-expression of MRTFA, SRF and their dominant negative variants in C3H/10T1/2 cells.

The stable C3H/10T1/2 cells lines were harvested for western blot analysis to confirm the successful over-expression of MRTFA, SRF and their dominant negative variants. Probes against MRTFA and FLAG-tag were used for these samples. The MRTFA band is around 150 kDa and the SRF band is around 50 kDa. DN-MRTFA FLAG tag band is around 70 kDa and DN-SRF FLAG tag band is around 30 kDa.

Figure 26

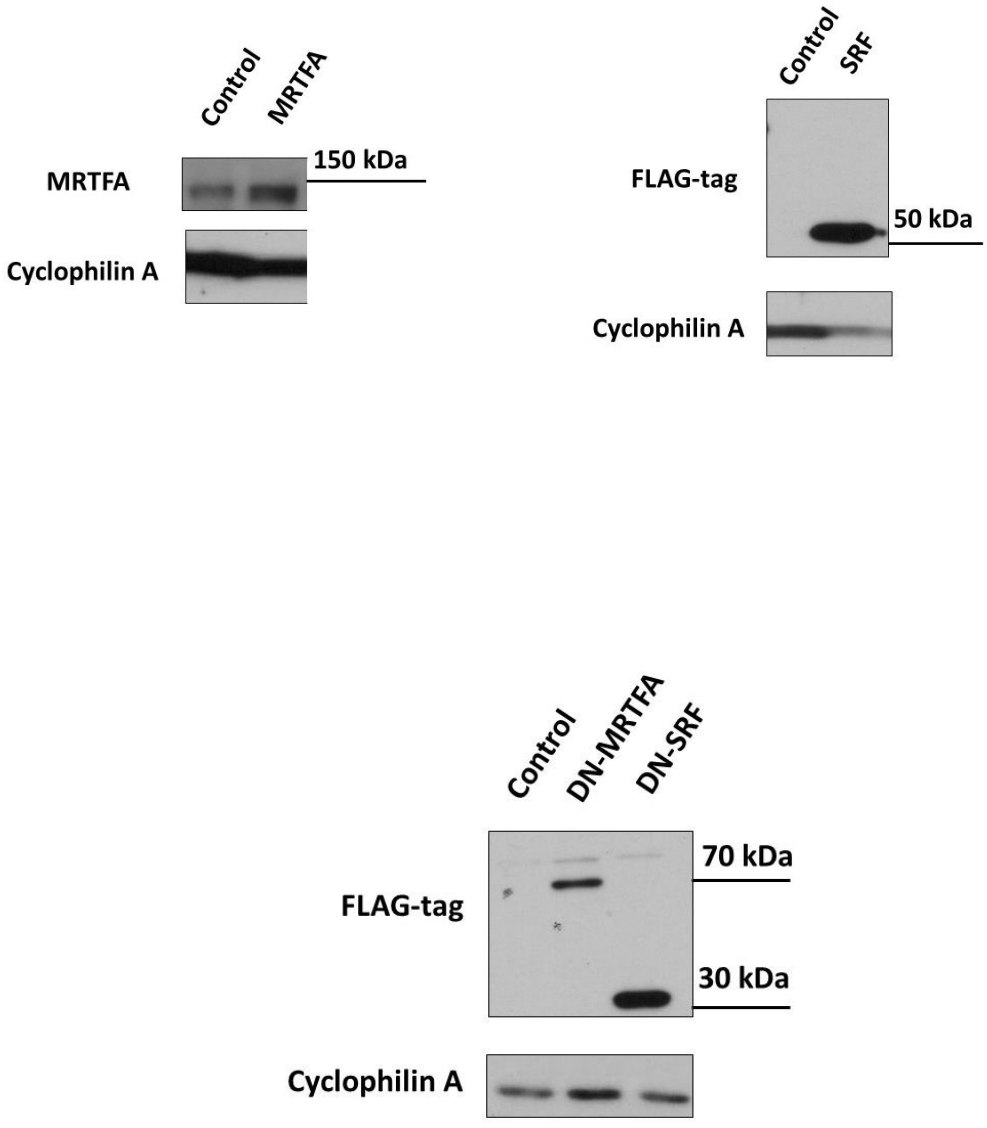
Control
MRTFA
MRTFA
150 kDa
Cyclophilin A
Control
SRF
FLAG-tag
50 kDa
Cyclophilin A
Control
DN-MRTFA
DN-SRF
FLAG-tag
70 kDa
30 kDa
Cyclophilin A

Figure 27. Over-expression of MRTFA and SRF in C3H/10T1/2 cells inhibits adipogenesis, while over-expression of dominant negative variants have the opposite effect.

The C3H/10T1/2 stable cell lines over-expressing MRTFA, SRF, DN-MRTFA and DN-SRF were induced for adipogenic differentiation as described in Figure 25. Except that BMP7 was added to the cells in D for three days prior to adipogenic induction to facilitate the induction of brown fat genes. The phase-contrast microscopic images were captured before harvesting on day 8 of adipogenesis (A). mRNA and proteins samples (n=3) were then extracted from these cells for RT-PCR (B, D) and western blot (C) analysis. The data is presented as in Figure 25. Student's T-test was performed to assess the statistical significance (*$p<0.05$, **$p<0.01$).

Figure 27

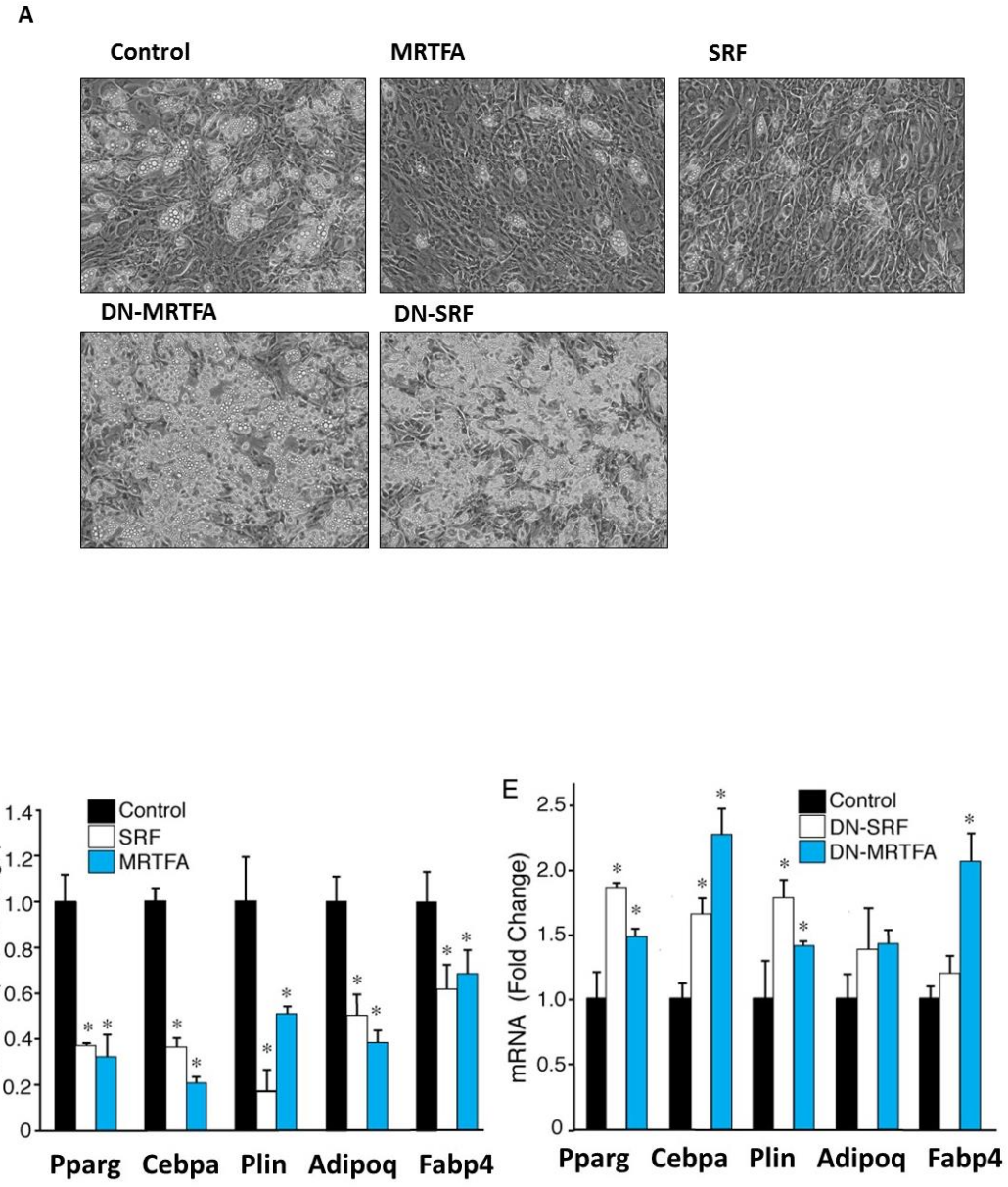
A
Control
MRTFA
SRF
DN-MRTFA
DN-SRF
B
Control
SRF
MRTFA
mRNA (Fold Change)
Pparg
Cebpa
Plin
Adipoq
Fabp4
E
Control
DN-SRF
DN-MRTFA
mRNA (Fold Change)
Pparg
Cebpa
Plin
Adipoq
Fabp4

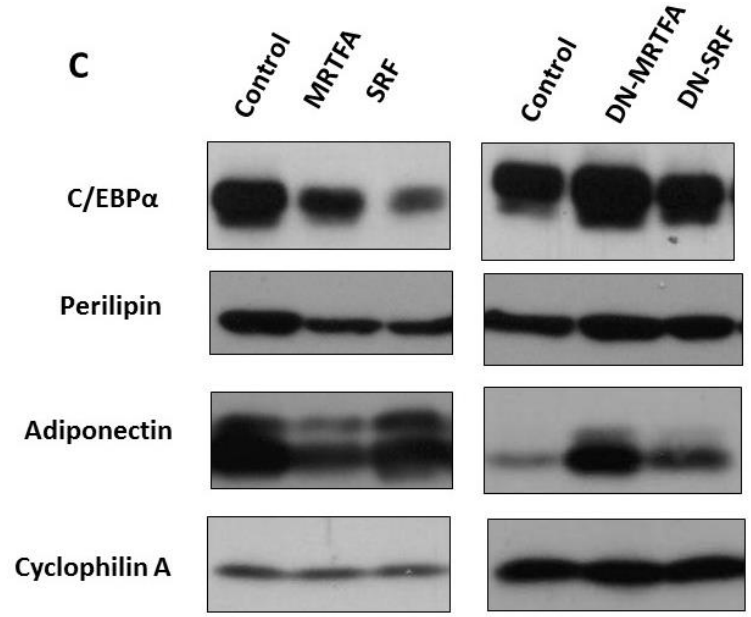
C
Control
MRTFA
SRF
Control
DN-MRTFA
DN-SRF
C/EBPα
Perilipin
Adiponectin
Cyclophilin A

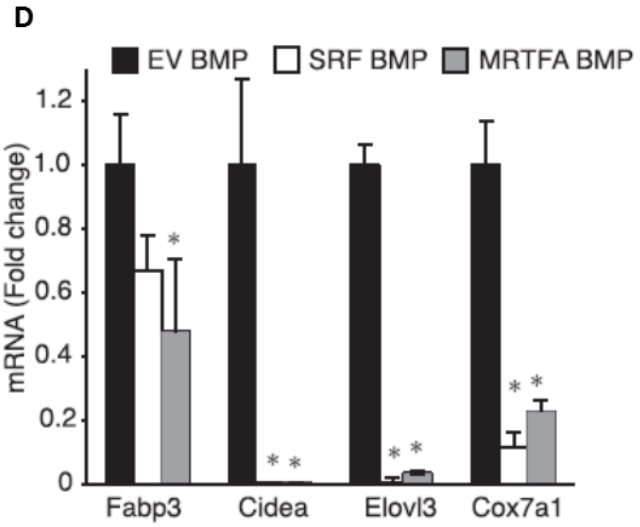
D
EV BMP
SRF BMP
MRTFA BMP
mRNA (Fold change)
1.2
1.0
0.8
0.6
0.4
0.2
0
Fabp3
Cidea
Elovl3
Cox7a1

Figure 28. Over-expression of MRTFA and SRF in C3H/10T1/2 cells enhances osteoblastogenesis, while over-expression of the dominant negative variants have the opposite effect.

The C3H/10T1/2 stable cell lines over-expressing MRTFA, SRF, DN-MRTFA and DN-SRF were induced with osteoblastogenic media containing β-glycerophosphate, ascorbic acid and dexamethasone for 21 days upon reaching confluence. The phase-contrast images were captured at day 7 of differentiation (A). mRNA samples (n=3) were extracted from these cells at day 21 of differentiation for RT-PCR (B, C) analysis. The data is presented according to Figure 25 (*$p<0.05$).

Figure 28

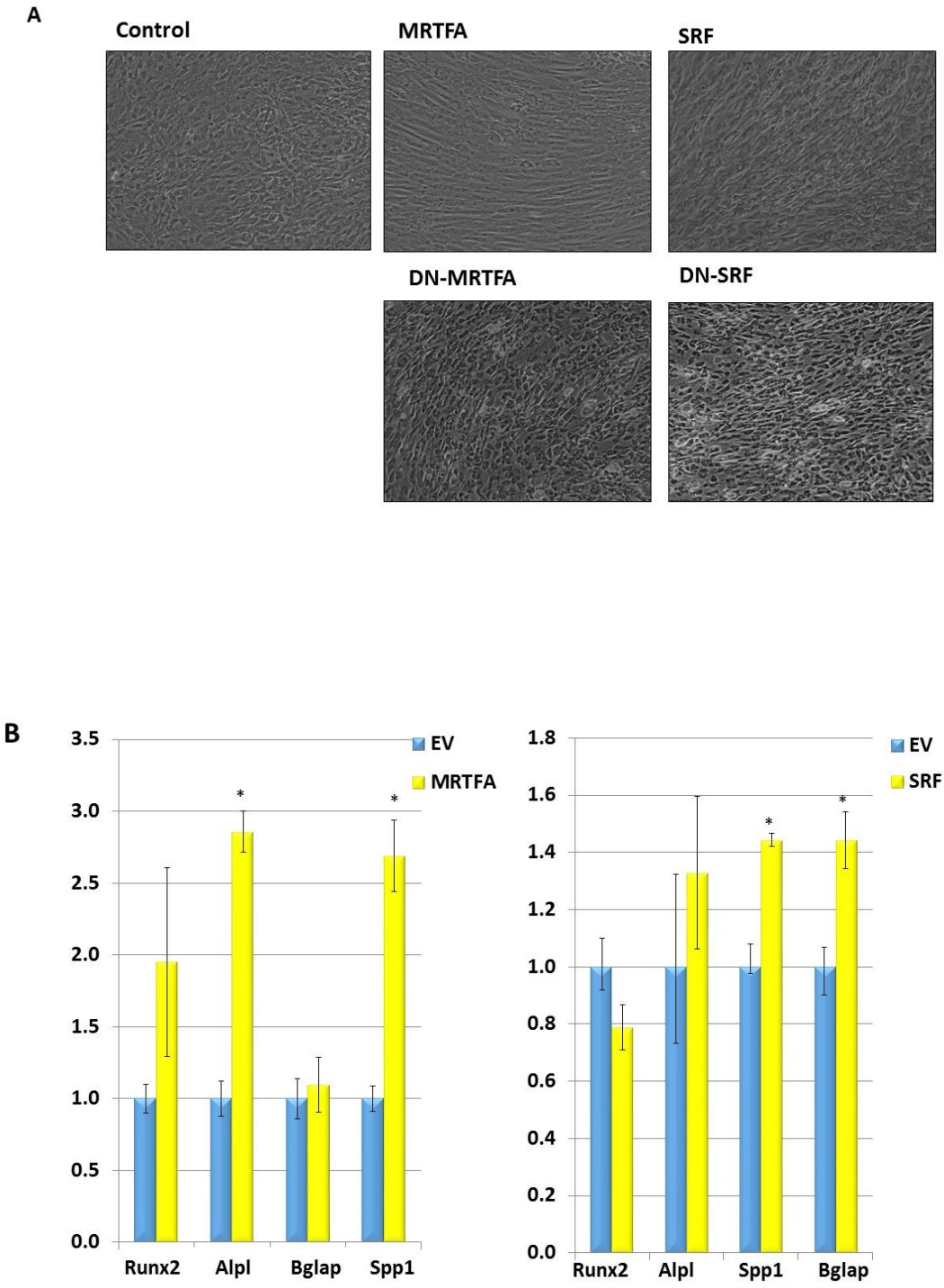
A
Control
MRTFA
SRF
DN-MRTFA
DN-SRF
B
EV
MRTFA
3.5
3.0
2.5
2.0
1.5
1.0
0.5
0.0
*
*
Runx2
Alpl
Bglap
Spp1
EV
SRF
1.8
1.6
1.4
1.2
1.0
0.8
0.6
0.4
0.2
0.0
*
*
Runx2
Alpl
Spp1
Bglap

C

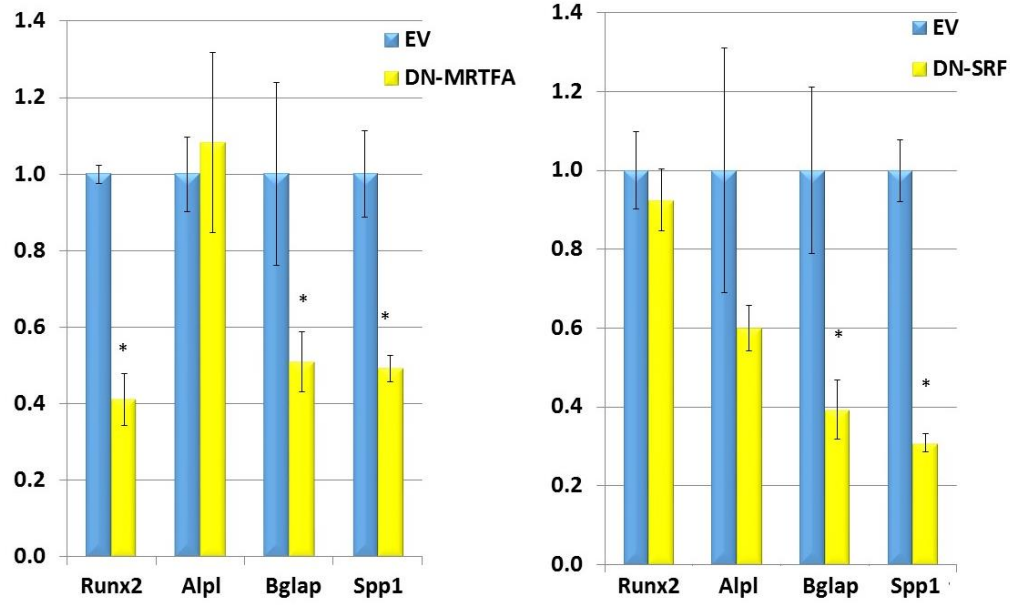
1.4
1.2
1.0
0.8
0.6
0.4
0.2
0.0
EV
DN-MRTFA
*
*
*
Runx2
Alpl
Bglap
Spp1
1.4
1.2
1.0
0.8
0.6
0.4
0.2
0.0
EV
DN-SRF
*
*
Runx2
Alpl
Bglap
Spp1

Discussion

In this chapter, we demonstrated that MRTFA, SRF and their select target genes were down-regulated during adipogenesis at an early stage. Over-expressing MRTFA or SRF inhibited adipogenesis by reducing adipogenic gene expression, including some of the brown fat genes. In contrast, over-expressing DN-MRTFA or DN-SRF promoted adipogenesis by enhancing adipogenic genes. In contrast, MRTFA or SRF over-expression increased osteoblast differentiation while the dominant negative variants had the opposite effects.

The down-regulation of MRTFA, MRTFB, SRF and their targets genes such as SMA, Collagen1α1 and Collagen3α1 occurred mostly from days 0 to 2 of adipogenic differentiation. The degree of reduction of these genes was significant, averaging about 60% to 80% reduction as compared to the baseline levels. The timing of the down-regulation for these genes suggests that inhibition of the MRTFA/SRF pathway is necessary for the proper maturation of pre-adipocytes. The similar patterns of gene expression for MRTFA and MRTFB indicate potentially overlapping functions for these two factors during adipogenesis. Therefore, in the results described in chapters the last 2 sections, MRTFB activity might be functionally compensating for the loss of MRTFA thus minimizing the severity of the observed osteoporotic phenotype.

By establishing C3H/10T1/2 stable over-expression cell lines, we manipulated the transcriptional activity of MRTFA/SRF to study the role of this pathway in MSC commitment. MRTFA and SRF over-expression inhibited adipogenesis in these MSCs

while the dominant negative variants had the opposite effect, which is consistent with published findings (Nobusue, Onishi *et al*. 2014, McDonald, Li *et al*. 2015). MRTFA and SRF appear to be negative regulators for adipogenesis. We maintain that MRTFA and SRF may be involved in the regulation of both the early fate commitment to adipose lineage as well as the morphological differentiation. The exact mechanisms of these effects will be further investigated by other group members in future studies.

MRTFA and SRF over-expression enhanced osteoblastogenesis in MSCs whereas their dominant negative variants had the opposite effects. We speculate that the enhancement of MRTFA/SRF pathway facilitates the necessary cytoskeletal reorganization to accommodate to osteoblast differentiation. Interestingly, there was adipocyte formation in both DN-MRTFA and DN-SRF over-expression cell lines even when they were constantly induced with osteoblastogenic factors. In fact, we were still able to detect certain adipogenic proteins such as adiponectin and FABP4 in these cells. Ablation of the MRTFA/SRF pathway was sufficient to bypass the osteoblastogenic cues in the growth media and drove the MSCs differentiation into adipocytes through alteration of their cytoskeletal signaling.

Summary

We propose that the actin-MRTFA-SRF circuit acts downstream of Rho-ROCK signaling to promote osteoblastogenesis and inhibit adipogenesis in the MSCs. As demonstrated by McBeath (McBeath, Pirone et al. 2004), when activated by mechanical tension, Rho-ROCK signaling activates downstream effectors to promote the

incorporation of G-actin to F-actin. MRTFA bound with G-actin is released for nuclear translocation and subsequent co-activation of SRF target genes. We hypothesize that the activation of these genes promotes a spreading and elongated cell shape, which primes the MSCs for osteoblastogenesis. In contrast, when the activation of these genes is inhibited due to MRTFA ablation, the MSCs adopt a rounded shape which is permissive for adipogenesis (Figure 29).

This study identifies MRTFA as a crucial regulator of skeletal homeostasis *via* regulating the balance between adipogenic and osteoblastogenic differentiation in the MSCs, and thus holds promise as a potential target for therapeutic intervention for osteoporosis.

Figure 29. A model of actin-MRTFA-SRF circuit regulating the MSC fate commitment.

This thesis showed that the actin-MRTFA-SRF circuit is acting downstream of Rho-ROCK signaling to promote osteoblastogenesis and inhibit adipogenesis in the MSCs (described in the summary section).

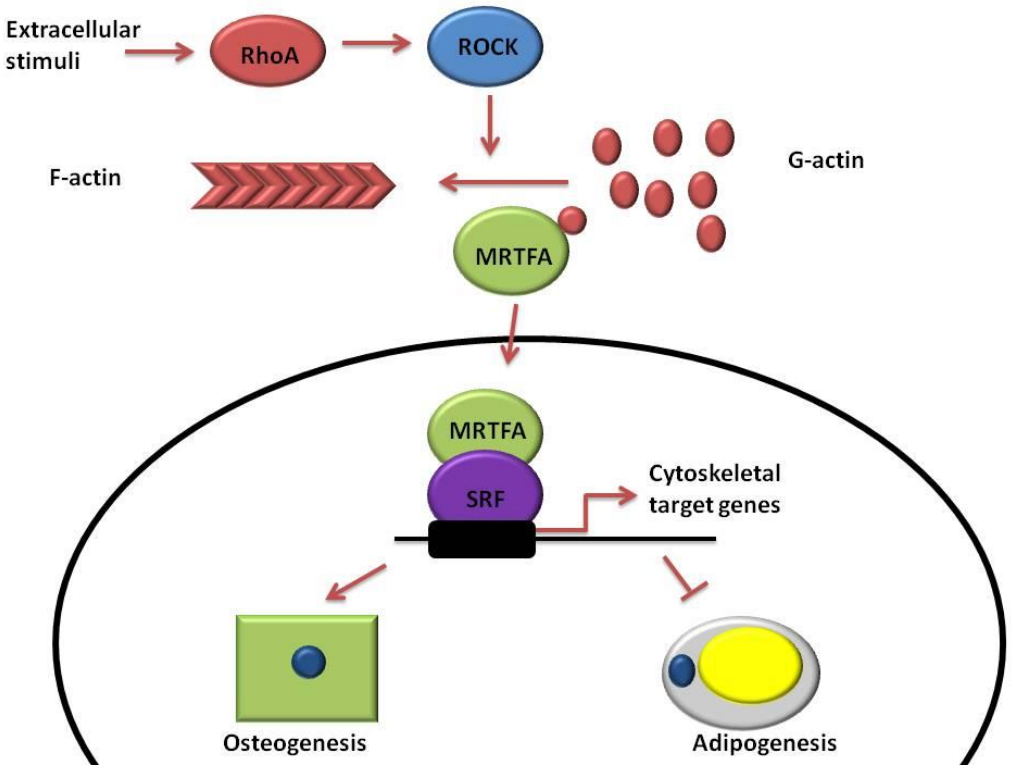

FUTURE DIRECTIONS

The mechanisms behind the fate divergence of MSCs in response to BMP signaling (a pathway that positively regulates both adipogenesis and osteoblastogenesis) is still poorly understood. It appears that the orchestration of various pathways will jointly dictate which transcriptional cascades will be activated by BMPs (Kang *et al*., 2009). Whether cytoskeletal signaling is involved in BMP-mediated MSCs fate divergence is worth further investigation. Using the MRTFA KO mice, MSCs and C3H/10T1/2 over-expression cell lines, whether BMPs will preferably activate adipogenesis *versus* osteoblastogenesis program in the MRTFA KO MSCs will be studied.

Investigation into the role of MRTFA-dependent SRF target genes in the regulation of early MSCs commitment is planned for follow-up studies by others in the Farmer laboratory. The target genes co-activated by MRTFs are mostly cell contractile proteins and regulators for actin related proteins (Olson *et al*., 2010). Genes involved in the regulation of actin dynamics include actin itself, regulators of actin turnover and regulators of actin dynamics. We hypothesize that these target genes downstream of MRTFA play important roles in regulating the MSCs commitment either directly or indirectly and this regulation appears to happen prior to the morphological differentiation.

REFERENCES

List of Journal Abbreviations

Am J Clin Nutr	American Journal of Clinical Research
Am J Hum Genet	The American Journal of Human Genetics
Am J Physiol Cell Physiol	American Journal of Physiology Cell Physiology
Am J Physiol Heart Circ Physiol	American Journal of Physiology Heart and Circulatory Physiology
Am J Physiol Endocrinol Metab	American Journal of Physiology Endocrinology and metabolism
Am J Physiol Gastrointest Liver Physiol	American Journal of Physiology Gastrointestinal and Liver Physiology
Ann NY Acad Sci	Annals of the New York Academy of Sciences
Annu Rev Biophys Biomol Struct	Annual Review of Biophysics and Biomolecular Structure
Annu Rev Cell Dev Biol	Annual Review of Cell and Developmental Biology
Annu Rev Genomics Hum Genet	Annual Review of Genomics and Human Genetics
Arch Biochem Biophys	Archives of Biochemistry and Biophysics
Arch Intern Med	Archives of Internal Medicine
Arq Bras Endocrinol Metabol	Archives of Endocrinology and Metabolism
Biochem J	Biochemical Journal
Biomed Res Int	BioMed Research International

Calcif Tissue Int	Calcified Tissue International
Cancer Res	Cancer Research
Cell Metab	Cell Metabolism
Cell Mol Life Sci	Cellular and Molecular Life Sciences
Cell Tissue Res	Cell and Tissue Research
Circ Res	Circulation Research
Clin Oral Investig	Clinical Oral Investigations
Clin Orthop Relat Res	Clinical Orthopedics and Related Research
Clin Sci (Lond)	Clinical Science (Lond)
Cochrane Database Syst Rev	Cochrane Database Systemic Reviews
Curr Mol Pharmacol	Current Molecular Pharmacology
Curr Opin Cell Biol	Current Opinion in Cell Biology
Curr Opin Genet Dev	Current Opinion in Genetics and Development
Curr Opin Rheumatol	Current Opinion in Rheumatology
Cytokine Growth Factor Rev	Cytokine Growth Factor Reviews
Cytometry A	Cytometry Part A
Dev Cell	Developmental Cell
EMBO J	European Molecular Biology Organization Journal
Endocr Rev	Endocrine Reviews
Eur J Biochem	European Journal of Biochemistry
Eur J Cell Biol	European Journal of Cell Biology

Eur J Heart Fail	European Journal of Heart Failure
FEBS J	Federation of European Biochemical Societies Journal
Genes Dev	Genes and Development
Genome Res	Genome Research
Hum Gene Ther	Human Gene Therepy
Int J Biol Sci	International Journal of Biological Sciences
Int J Biochem Cell Biol	The International Journal of Biochemistry and Cell Biology
Int J Obes	International Journal of Obesity
Int J Obes Relat Metab Disord	International Journal of Obesity and Related Metabolic Disorders
JAMA	The Journal of American Medicine Association
J Am Coll Nutr	Journal of the American College of Nutrition
J Biol Chem	Journal of Biological Chemistry
J Bone Miner Res	Journal of Bone and Mineral Research
J Cell Biochem	Journal of Cellular Biochemistry
J Cell Biochem Suppl	Journal of Cellular Biochemistry, Supplement
J Cell Physiol	Journal of Cell Physiology
J Cell Sci	Journal of Cell Science
J Clin Endocrinol Metab	Journal of Clinical Endocrinology and Metabolism

J Clin Invest	Journal of Clinical Investigation
J Dent Res	Journal of Dental Research
J Endocrinol	Journal of Endocinology
J Endocrinol Invest	Journal of Endocrinological Investigation
J Mol Cell Cardiol	Journal of Molecular and Cellular Cardiology
J Mol Endocrinol	Journal of Molecular Endocrinology
J Orthop Res	Journal of Orthopedic Research
J Orthop Surg Res	Journal of Orthopedic Surgery and Research
J Womens Health (Larchmt)	Journal of Women's Health (Larchmt)
Kidney Int	Kidney International
Lab Invest	Laboratory Investigation
Mol Cancer Ther	Molecular Cancer Therapeutics
Mol Cell	Molecular Cell
Mol Cell Biol	Molecular and Cell Biology
Mol Cell Endocrinol	Molecular and Cellular Endocrinology
Med Clin North Am	Medical Clinics of North America
Mol Endocrinol	Molecular Endocrinology
Mol Pharmacol	Molecular Pharmacology
Nat Clin Pract Rheumatol	Nature Clinical Practice Rheumatology
Nat Commun	Nature Communications
Nat Genet	Nature Genetics
Nat Med	Nature Medicine

Nat Neurosci	Nature Neuroscience
Nat Rev Mol Cell Biol	Nature Reviews Molecular Cell Biology
N Engl J Med	The New England Journal of Medicine
Nutr Rev	Nutrition Reviews
Obes Res	Obesity Research
Osteoporo Int	Osteoporosis International
Pediatr Nephrol	Pediatric Nephrology
Physiol Genomics	Physiological Genomics
Physiol Rev	Physiological Reviews
PLoS One	Public Library of Science One
Prev Med	Preventative Medicine
Proc Natl Acad Sci	Proceedings of the National Academy of Sciences
South Med J	Southern Medical Journal
Stem Cells Dev	Stem Cells and Development
Stem Cell Rev	Stem Cell Reviews
Stem Cells Transl Med	Stem Cells Translational Medicine
Trends Biochem Sci	Trends in Biochemical Sciences
Trends Cell Biol	Trends in Cell Biology
Trends Mol Med	Trends in Molecular Medicine
Trends Genet	Trends in Genetics
Trends Immunol	Trends in Immunology
Trends Mol Med	Trends in Molecular Medicine
Trends Pharmacol Sci	Trends in Pharmacological Science

World Health Organ Tech Rep Ser	World Health Organization Technical Report Series
World J Orthop	World Journal of Orthopedics
Z Rheumatol	Zeitschrift für Rheumatologie

(WHO 2000). "Obesity: preventing and managing the global epidemic. Report of a WHO consultation." World Health Organ Tech Rep Ser **894**: i-xii, 1-253.

(NIH 2001). "NIH Consensus Development Panel on Osteoporosis Prevention, Diagnosis, and Therapy, March 7-29, 2000: highlights of the conference." South Med J **94**(6): 569-573.

Alberti, S., S. M. Krause, O. Kretz, U. Philippar, T. Lemberger, E. Casanova, F. F. Wiebel, H. Schwarz, M. Frotscher, G. Schutz and A. Nordheim (2005). "Neuronal migration in the murine rostral migratory stream requires serum response factor." Proc Natl Acad Sci U S A **102**(17): 6148-6153.

Ali, A. A., R. S. Weinstein, S. A. Stewart, A. M. Parfitt, S. C. Manolagas and R. L. Jilka (2005). "Rosiglitazone causes bone loss in mice by suppressing osteoblast differentiation and bone formation." Endocrinology **146**(3): 1226-1235.

Ali, A. T., W. E. Hochfeld, R. Myburgh and M. S. Pepper (2013). "Adipocyte and adipogenesis." Eur J Cell Biol **92**(6-7): 229-236.

Aravind, L. and E. V. Koonin (2000). "SAP - a putative DNA-binding motif involved in chromosomal organization." Trends Biochem Sci **25**(3): 112-114.

Arsenian, S., B. Weinhold, M. Oelgeschlager, U. Ruther and A. Nordheim (1998). "Serum response factor is essential for mesoderm formation during mouse embryogenesis." EMBO J **17**(21): 6289-6299.

Aubin, J. E. (1998). "Bone stem cells." J Cell Biochem Suppl **30-31**: 73-82.

Baldock, P. A. and J. A. Eisman (2004). "Genetic determinants of bone mass." Curr Opin Rheumatol **16**(4): 450-456.

Baron, R. and E. Hesse (2012). "Update on bone anabolics in osteoporosis treatment: rationale, current status, and perspectives." J Clin Endocrinol Metab **97**(2): 311-325.

Belaguli, N. S., J. L. Sepulveda, V. Nigam, F. Charron, M. Nemer and R. J. Schwartz (2000). "Cardiac tissue enriched factors serum response factor and GATA-4 are mutual coregulators." Mol Cell Biol **20**(20): 7550-7558.

Benson, C. C., Q. Zhou, X. Long and J. M. Miano (2011). "Identifying functional single nucleotide polymorphisms in the human CArGome." Physiol Genomics **43**(18): 1038-1048.

Beresford, J. N., J. H. Bennett, C. Devlin, P. S. Leboy and M. E. Owen (1992). "Evidence for an inverse relationship between the differentiation of adipocytic and osteogenic cells in rat marrow stromal cell cultures." J Cell Sci **102 (Pt 2)**: 341-351.

Bessesen, D. H. (2008). "Update on obesity." J Clin Endocrinol Metab **93**(6): 2027-2034.

Black, D. M., P. D. Delmas, R. Eastell, I. R. Reid, S. Boonen, J. A. Cauley, F. Cosman, P. Lakatos, P. C. Leung, Z. Man, C. Mautalen, P. Mesenbrink, H. Hu, J. Caminis, K. Tong, T. Rosario-Jansen, J. Krasnow, T. F. Hue, D. Sellmeyer, E. F. Eriksen, S. R. Cummings and H. P. F. Trial (2007). "Once-yearly zoledronic acid for treatment of postmenopausal osteoporosis." N Engl J Med **356**(18): 1809-1822.

Black, D. M., S. L. Greenspan, K. E. Ensrud, L. Palermo, J. A. McGowan, T. F. Lang, P. Garnero, M. L. Bouxsein, J. P. Bilezikian, C. J. Rosen and T. H. S. I. Pa (2003). "The effects of parathyroid hormone and alendronate alone or in combination in postmenopausal osteoporosis." N Engl J Med **349**(13): 1207-1215.

Black, D. M., A. V. Schwartz, K. E. Ensrud, J. A. Cauley, S. Levis, S. A. Quandt, S. Satterfield, R. B. Wallace, D. C. Bauer, L. Palermo, L. E. Wehren, A. Lombardi, A. C. Santora, S. R. Cummings and F. R. Group (2006). "Effects of continuing or stopping alendronate after 5 years of treatment: the Fracture Intervention Trial Long-term Extension (FLEX): a randomized trial." JAMA **296**(24): 2927-2938.

Black, D. M., D. E. Thompson, D. C. Bauer, K. Ensrud, T. Musliner, M. C. Hochberg, M. C. Nevitt, S. Suryawanshi, S. R. Cummings and T. Fracture Intervention (2000). "Fracture risk reduction with alendronate in women with osteoporosis: the Fracture Intervention Trial. FIT Research Group." J Clin Endocrinol Metab **85**(11): 4118-4124.

Bouxsein, M. L., S. K. Boyd, B. A. Christiansen, R. E. Guldberg, K. J. Jepsen and R. Muller (2010). "Guidelines for assessment of bone microstructure in rodents using micro-computed tomography." J Bone Miner Res **25**(7): 1468-1486.

Bowers, R. R., J. W. Kim, T. C. Otto and M. D. Lane (2006). "Stable stem cell commitment to the adipocyte lineage by inhibition of DNA methylation: role of the BMP-4 gene." Proc Natl Acad Sci U S A **103**(35): 13022-13027.

Boyden, L. M., J. Mao, J. Belsky, L. Mitzner, A. Farhi, M. A. Mitnick, D. Wu, K. Insogna and R. P. Lifton (2002). "High bone density due to a mutation in LDL-receptor-related protein 5." N Engl J Med **346**(20): 1513-1521.

Brown, S. A. and C. J. Rosen (2003). "Osteoporosis." Med Clin North Am **87**(5): 1039-1063.

Brunetti, G., M. F. Faienza, L. Piacente, A. Ventura, A. Oranger, C. Carbone, A. D. Benedetto, G. Colaianni, M. Gigante, G. Mori, L. Gesualdo, S. Colucci, L. Cavallo and M. Grano (2013). "High dickkopf-1 levels in sera and leukocytes from children with 21-hydroxylase deficiency on chronic glucocorticoid treatment." Am J Physiol Endocrinol Metab **304**(5): E546-554.

Burge, R., B. Dawson-Hughes, D. H. Solomon, J. B. Wong, A. King and A. Tosteson (2007). "Incidence and economic burden of osteoporosis-related fractures in the United States, 2005-2025." J Bone Miner Res **22**(3): 465-475.

Cannon, B. and J. Nedergaard (2004). "Brown adipose tissue: function and physiological significance." Physiol Rev **84**(1): 277-359.

Cao, J. J. (2011). "Effects of obesity on bone metabolism." J Orthop Surg Res **6**: 30.

Cao, J. J., L. Sun and H. Gao (2010). "Diet-induced obesity alters bone remodeling leading to decreased femoral trabecular bone mass in mice." Ann N Y Acad Sci **1192**: 292-297.

Cao, Z., R. M. Umek and S. L. McKnight (1991). "Regulated expression of three C/EBP isoforms during adipose conversion of 3T3-L1 cells." Genes Dev **5**(9): 1538-1552.

Caplan, A. I. and S. P. Bruder (2001). "Mesenchymal stem cells: building blocks for molecular medicine in the 21st century." Trends Mol Med **7**(6): 259-264.

Carroll, S. H., N. A. Wigner, N. Kulkarni, H. Johnston-Cox, L. C. Gerstenfeld and K. Ravid (2012). "A2B adenosine receptor promotes mesenchymal stem cell differentiation to osteoblasts and bone formation in vivo." J Biol Chem **287**(19): 15718-15727.

Carvalho, R. S., J. L. Schaffer and L. C. Gerstenfeld (1998). "Osteoblasts induce osteopontin expression in response to attachment on fibronectin: demonstration of a common role for integrin receptors in the signal transduction processes of cell attachment and mechanical stimulation." J Cell Biochem **70**(3): 376-390.

Chamberlain, G., J. Fox, B. Ashton and J. Middleton (2007). "Concise review: mesenchymal stem cells: their phenotype, differentiation capacity, immunological features, and potential for homing." Stem Cells **25**(11): 2739-2749.

Chang, W., J. Rickers-Haunerland and N. H. Haunerland (2001). "Induction of cardiac FABP gene expression by long chain fatty acids in cultured rat muscle cells." Mol Cell Biochem **221**(1-2): 127-132.

Chang, Y. F., J. Wei, X. Liu, Y. H. Chen, M. D. Layne and S. F. Yet (2003). "Identification of a CArG-independent region of the cysteine-rich protein 2 promoter that

directs expression in the developing vasculature." Am J Physiol Heart Circ Physiol **285**(4): H1675-1683.

Charvet, C., C. Houbron, A. Parlakian, J. Giordani, C. Lahoute, A. Bertrand, A. Sotiropoulos, L. Renou, A. Schmitt, J. Melki, Z. Li, D. Daegelen and D. Tuil (2006). "New role for serum response factor in postnatal skeletal muscle growth and regeneration via the interleukin 4 and insulin-like growth factor 1 pathways." Mol Cell Biol **26**(17): 6664-6674.

Chen, C. Y. and R. J. Schwartz (1996). "Recruitment of the tinman homolog Nkx-2.5 by serum response factor activates cardiac alpha-actin gene transcription." Mol Cell Biol **16**(11): 6372-6384.

Chen, D., X. Ji, M. A. Harris, J. Q. Feng, G. Karsenty, A. J. Celeste, V. Rosen, G. R. Mundy and S. E. Harris (1998). "Differential roles for bone morphogenetic protein (BMP) receptor type IB and IA in differentiation and specification of mesenchymal precursor cells to osteoblast and adipocyte lineages." J Cell Biol **142**(1): 295-305.

Chen, G., C. Deng and Y. P. Li (2012). "TGF-beta and BMP signaling in osteoblast differentiation and bone formation." Int J Biol Sci **8**(2): 272-288.

Chen, J., K. Yuan, X. Mao, J. M. Miano, H. Wu and Y. Chen (2012). "Serum response factor regulates bone formation via IGF-1 and Runx2 signals." J Bone Miner Res **27**(8): 1659-1668.

Colaianni, G., G. Brunetti, M. F. Faienza, S. Colucci and M. Grano (2014). "Osteoporosis and obesity: Role of Wnt pathway in human and murine models." World J Orthop **5**(3): 242-246.

Corselli, M., M. Crisan, I. R. Murray, C. C. West, J. Scholes, F. Codrea, N. Khan and B. Peault (2013). "Identification of perivascular mesenchymal stromal/stem cells by flow cytometry." Cytometry A **83**(8): 714-720.

Creemers, E. E., L. B. Sutherland, J. Oh, A. C. Barbosa and E. N. Olson (2006). "Coactivation of MEF2 by the SAP domain proteins myocardin and MASTR." Mol Cell **23**(1): 83-96.

Crisan, M., S. Yap, L. Casteilla, C. W. Chen, M. Corselli, T. S. Park, G. Andriolo, B. Sun, B. Zheng, L. Zhang, C. Norotte, P. N. Teng, J. Traas, R. Schugar, B. M. Deasy, S. Badylak, H. J. Buhring, J. P. Giacobino, L. Lazzari, J. Huard and B. Peault (2008). "A perivascular origin for mesenchymal stem cells in multiple human organs." Cell Stem Cell **3**(3): 301-313.

Cummings, S. R., D. M. Black, D. E. Thompson, W. B. Applegate, E. Barrett-Connor, T. A. Musliner, L. Palermo, R. Prineas, S. M. Rubin, J. C. Scott, T. Vogt, R. Wallace, A. J. Yates and A. Z. LaCroix (1998). "Effect of alendronate on risk of fracture in women with low bone density but without vertebral fractures: results from the Fracture Intervention Trial." JAMA **280**(24): 2077-2082.

Dalton, S. and R. Treisman (1992). "Characterization of SAP-1, a protein recruited by serum response factor to the c-fos serum response element." Cell **68**(3): 597-612.

David, V., A. Martin, M. H. Lafage-Proust, L. Malaval, S. Peyroche, D. B. Jones, L. Vico and A. Guignandon (2007). "Mechanical loading down-regulates peroxisome proliferator-activated receptor gamma in bone marrow stromal cells and favors osteoblastogenesis at the expense of adipogenesis." Endocrinology **148**(5): 2553-2562.

de Gregorio, L. H., P. G. Lacativa, A. C. Melazzi and L. A. Russo (2006). "Glucocorticoid-induced osteoporosis." Arq Bras Endocrinol Metabol **50**(4): 793-801.

Derynck, R. and Y. E. Zhang (2003). "Smad-dependent and Smad-independent pathways in TGF-beta family signalling." Nature **425**(6958): 577-584.

Du, K. L., M. Chen, J. Li, J. J. Lepore, P. Mericko and M. S. Parmacek (2004). "Megakaryoblastic leukemia factor-1 transduces cytoskeletal signals and induces smooth muscle cell differentiation from undifferentiated embryonic stem cells." J Biol Chem **279**(17): 17578-17586.

Du, K. L., H. S. Ip, J. Li, M. Chen, F. Dandre, W. Yu, M. M. Lu, G. K. Owens and M. S. Parmacek (2003). "Myocardin is a critical serum response factor cofactor in the transcriptional program regulating smooth muscle cell differentiation." Mol Cell Biol **23**(7): 2425-2437.

Ducy, P. and G. Karsenty (2000). "The family of bone morphogenetic proteins." Kidney Int **57**(6): 2207-2214.

Ducy, P., R. Zhang, V. Geoffroy, A. L. Ridall and G. Karsenty (1997). "Osf2/Cbfa1: a transcriptional activator of osteoblast differentiation." Cell **89**(5): 747-754.

Evelyn, C. R., S. M. Wade, Q. Wang, M. Wu, J. A. Iniguez-Lluhi, S. D. Merajver and R. R. Neubig (2007). "CCG-1423: a small-molecule inhibitor of RhoA transcriptional signaling." Mol Cancer Ther **6**(8): 2249-2260.

Faienza, M. F., G. Brunetti, S. Colucci, L. Piacente, M. Ciccarelli, L. Giordani, G. C. Del Vecchio, M. D'Amore, L. Albanese, L. Cavallo and M. Grano (2009). "Osteoclastogenesis in children with 21-hydroxylase deficiency on long-term

glucocorticoid therapy: the role of receptor activator of nuclear factor-kappaB ligand/osteoprotegerin imbalance." J Clin Endocrinol Metab **94**(7): 2269-2276.

Farmer, S. R. (2006). "Transcriptional control of adipocyte formation." Cell Metab **4**(4): 263-273.

Fleige, A., S. Alberti, L. Grobe, U. Frischmann, R. Geffers, W. Muller, A. Nordheim and A. Schippers (2007). "Serum response factor contributes selectively to lymphocyte development." J Biol Chem **282**(33): 24320-24328.

Gary-Bobo, G., A. Parlakian, B. Escoubet, C. A. Franco, S. Clement, P. Bruneval, D. Tuil, D. Daegelen, D. Paulin, Z. Li and M. Mericskay (2008). "Mosaic inactivation of the serum response factor gene in the myocardium induces focal lesions and heart failure." Eur J Heart Fail **10**(7): 635-645.

Gaur, T., C. J. Lengner, H. Hovhannisyan, R. A. Bhat, P. V. Bodine, B. S. Komm, A. Javed, A. J. van Wijnen, J. L. Stein, G. S. Stein and J. B. Lian (2005). "Canonical WNT signaling promotes osteogenesis by directly stimulating Runx2 gene expression." J Biol Chem **280**(39): 33132-33140.

Gimble, J. M., C. E. Robinson, X. Wu, K. A. Kelly, B. R. Rodriguez, S. A. Kliewer, J. M. Lehmann and D. C. Morris (1996). "Peroxisome proliferator-activated receptor-gamma activation by thiazolidinediones induces adipogenesis in bone marrow stromal cells." Mol Pharmacol **50**(5): 1087-1094.

Gineitis, D. and R. Treisman (2001). "Differential usage of signal transduction pathways defines two types of serum response factor target gene." J Biol Chem **276**(27): 24531-24539.

Giustina, A., G. Mazziotti and E. Canalis (2008). "Growth hormone, insulin-like growth factors, and the skeleton." Endocr Rev **29**(5): 535-559.

Glass, D. A., 2nd and G. Karsenty (2007). "In vivo analysis of Wnt signaling in bone." Endocrinology **148**(6): 2630-2634.

Goulding, A., R. W. Taylor, I. E. Jones, K. A. McAuley, P. J. Manning and S. M. Williams (2000). "Overweight and obese children have low bone mass and area for their weight." Int J Obes Relat Metab Disord **24**(5): 627-632.

Govoni, K. E. (2012). "Insulin-like growth factor-I molecular pathways in osteoblasts: potential targets for pharmacological manipulation." Curr Mol Pharmacol **5**(2): 143-152.

Gregoire, F. M., C. M. Smas and H. S. Sul (1998). "Understanding adipocyte differentiation." Physiol Rev **78**(3): 783-809.

Guettler, S., M. K. Vartiainen, F. Miralles, B. Larijani and R. Treisman (2008). "RPEL motifs link the serum response factor cofactor MAL but not myocardin to Rho signaling via actin binding." Mol Cell Biol **28**(2): 732-742.

Gumbiner, B. M. (1996). "Cell adhesion: the molecular basis of tissue architecture and morphogenesis." Cell **84**(3): 345-357.

Guo, J. and G. Wu (2012). "The signaling and functions of heterodimeric bone morphogenetic proteins." Cytokine Growth Factor Rev **23**(1-2): 61-67.

Hadjidakis, D. J. and Androulakis, II (2006). "Bone remodeling." Ann N Y Acad Sci **1092**: 385-396.

Halene, S., Y. Gao, K. Hahn, S. Massaro, J. E. Italiano, Jr., V. Schulz, S. Lin, G. M. Kupfer and D. S. Krause (2010). "Serum response factor is an essential transcription factor in megakaryocytic maturation." Blood **116**(11): 1942-1950.

Hamrick, M. W., C. Pennington, D. Newton, D. Xie and C. Isales (2004). "Leptin deficiency produces contrasting phenotypes in bones of the limb and spine." Bone **34**(3): 376-383.

Harris, S. T., N. B. Watts, H. K. Genant, C. D. McKeever, T. Hangartner, M. Keller, C. H. Chesnut, 3rd, J. Brown, E. F. Eriksen, M. S. Hoseyni, D. W. Axelrod and P. D. Miller (1999). "Effects of risedronate treatment on vertebral and nonvertebral fractures in women with postmenopausal osteoporosis: a randomized controlled trial. Vertebral Efficacy With Risedronate Therapy (VERT) Study Group." JAMA **282**(14): 1344-1352.

Hipskind, R. A., V. N. Rao, C. G. Mueller, E. S. Reddy and A. Nordheim (1991). "Ets-related protein Elk-1 is homologous to the c-fos regulatory factor p62TCF." Nature **354**(6354): 531-534.

Ho, H. Y., R. Rohatgi, A. M. Lebensohn, M. Le, J. Li, S. P. Gygi and M. W. Kirschner (2004). "Toca-1 mediates Cdc42-dependent actin nucleation by activating the N-WASP-WIP complex." Cell **118**(2): 203-216.

Hogan, B. L. (1996). "Bone morphogenetic proteins in development." Curr Opin Genet Dev **6**(4): 432-438.

Hong, J. H., E. S. Hwang, M. T. McManus, A. Amsterdam, Y. Tian, R. Kalmukova, E. Mueller, T. Benjamin, B. M. Spiegelman, P. A. Sharp, N. Hopkins and M. B. Yaffe (2005). "TAZ, a transcriptional modulator of mesenchymal stem cell differentiation." Science **309**(5737): 1074-1078.

Horwitz, M. J., M. B. Tedesco, A. Garcia-Ocana, S. M. Sereika, L. Prebehala, A. Bisello, B. W. Hollis, C. M. Gundberg and A. F. Stewart (2010). "Parathyroid hormone-related protein for the treatment of postmenopausal osteoporosis: defining the maximal tolerable dose." J Clin Endocrinol Metab **95**(3): 1279-1287.

Howe, T. E., B. Shea, L. J. Dawson, F. Downie, A. Murray, C. Ross, R. T. Harbour, L. M. Caldwell and G. Creed (2011). "Exercise for preventing and treating osteoporosis in postmenopausal women." Cochrane Database Syst Rev(7): CD000333.

Huang, J., L. Cheng, J. Li, M. Chen, D. Zhou, M. M. Lu, A. Proweller, J. A. Epstein and M. S. Parmacek (2008). "Myocardin regulates expression of contractile genes in smooth muscle cells and is required for closure of the ductus arteriosus in mice." J Clin Invest **118**(2): 515-525.

Huang, J., M. Min Lu, L. Cheng, L. J. Yuan, X. Zhu, A. L. Stout, M. Chen, J. Li and M. S. Parmacek (2009). "Myocardin is required for cardiomyocyte survival and maintenance of heart function." Proc Natl Acad Sci U S A **106**(44): 18734-18739.

Jackson, W. M., L. J. Nesti and R. S. Tuan (2012). "Concise review: clinical translation of wound healing therapies based on mesenchymal stem cells." Stem Cells Transl Med **1**(1): 44-50.

Jaffe, A. B. and A. Hall (2005). "Rho GTPases: biochemistry and biology." Annu Rev Cell Dev Biol **21**: 247-269.

James, A. W. (2013). "Review of Signaling Pathways Governing MSC Osteogenic and Adipogenic Differentiation." Scientifica (Cairo) **2013**: 684736.

James, A. W., J. N. Zara, M. Corselli, A. Askarinam, A. M. Zhou, A. Hourfar, A. Nguyen, S. Megerdichian, G. Asatrian, S. Pang, D. Stoker, X. Zhang, B. Wu, K. Ting, B. Peault and C. Soo (2012). "An abundant perivascular source of stem cells for bone tissue engineering." Stem Cells Transl Med **1**(9): 673-684.

James, A. W., J. N. Zara, X. Zhang, A. Askarinam, R. Goyal, M. Chiang, W. Yuan, L. Chang, M. Corselli, J. Shen, S. Pang, D. Stoker, B. Wu, K. Ting, B. Peault and C. Soo (2012). "Perivascular stem cells: a prospectively purified mesenchymal stem cell population for bone tissue engineering." Stem Cells Transl Med **1**(6): 510-519.

Janknecht, R., W. H. Ernst, V. Pingoud and A. Nordheim (1993). "Activation of ternary complex factor Elk-1 by MAP kinases." EMBO J **12**(13): 5097-5104.

Justesen, J., K. Stenderup, E. N. Ebbesen, L. Mosekilde, T. Steiniche and M. Kassem (2001). "Adipocyte tissue volume in bone marrow is increased with aging and in patients with osteoporosis." Biogerontology **2**(3): 165-171.

Kanai, F., P. A. Marignani, D. Sarbassova, R. Yagi, R. A. Hall, M. Donowitz, A. Hisaminato, T. Fujiwara, Y. Ito, L. C. Cantley and M. B. Yaffe (2000). "TAZ: a novel transcriptional co-activator regulated by interactions with 14-3-3 and PDZ domain proteins." EMBO J **19**(24): 6778-6791.

Kang, Q., W. X. Song, Q. Luo, N. Tang, J. Luo, X. Luo, J. Chen, Y. Bi, B. C. He, J. K. Park, W. Jiang, Y. Tang, J. Huang, Y. Su, G. H. Zhu, Y. He, H. Yin, Z. Hu, Y. Wang, L. Chen, G. W. Zuo, X. Pan, J. Shen, T. Vokes, R. R. Reid, R. C. Haydon, H. H. Luu and T. C. He (2009). "A comprehensive analysis of the dual roles of BMPs in regulating adipogenic and osteogenic differentiation of mesenchymal progenitor cells." Stem Cells Dev **18**(4): 545-559.

Katagiri, T., M. Imada, T. Yanai, T. Suda, N. Takahashi and R. Kamijo (2002). "Identification of a BMP-responsive element in Id1, the gene for inhibition of myogenesis." Genes Cells **7**(9): 949-960.

Kawai, M. and C. J. Rosen (2009). "Insulin-like growth factor-I and bone: lessons from mice and men." Pediatr Nephrol **24**(7): 1277-1285.

Kling, J. M., B. L. Clarke and N. P. Sandhu (2014). "Osteoporosis prevention, screening, and treatment: a review." J Womens Health (Larchmt) **23**(7): 563-572.

Knoll, B., O. Kretz, C. Fiedler, S. Alberti, G. Schutz, M. Frotscher and A. Nordheim (2006). "Serum response factor controls neuronal circuit assembly in the hippocampus." Nat Neurosci **9**(2): 195-204.

Komori, T., H. Yagi, S. Nomura, A. Yamaguchi, K. Sasaki, K. Deguchi, Y. Shimizu, R. T. Bronson, Y. H. Gao, M. Inada, M. Sato, R. Okamoto, Y. Kitamura, S. Yoshiki and T. Kishimoto (1997). "Targeted disruption of Cbfa1 results in a complete lack of bone formation owing to maturational arrest of osteoblasts." Cell **89**(5): 755-764.

Koutnikova, H., T. A. Cock, M. Watanabe, S. M. Houten, M. F. Champy, A. Dierich and J. Auwerx (2003). "Compensation by the muscle limits the metabolic consequences of lipodystrophy in PPAR gamma hypomorphic mice." Proc Natl Acad Sci U S A **100**(24): 14457-14462.

Kretzschmar, M., F. Liu, A. Hata, J. Doody and J. Massague (1997). "The TGF-beta family mediator Smad1 is phosphorylated directly and activated functionally by the BMP receptor kinase." Genes Dev **11**(8): 984-995.

Krings, A., S. Rahman, S. Huang, Y. Lu, P. J. Czernik and B. Lecka-Czernik (2012). "Bone marrow fat has brown adipose tissue characteristics, which are attenuated with aging and diabetes." Bone **50**(2): 546-552.

Lane, N. E. and W. Yao (2010). "Glucocorticoid-induced bone fragility." Ann N Y Acad Sci **1192**: 81-83.

Latasa, M. U., D. Couton, C. Charvet, A. Lafanechere, J. E. Guidotti, Z. Li, D. Tuil, D. Daegelen, C. Mitchell and H. Gilgenkrantz (2007). "Delayed liver regeneration in mice lacking liver serum response factor." Am J Physiol Gastrointest Liver Physiol **292**(4): G996-G1001.

Lazarenko, O. P., S. O. Rzonca, L. J. Suva and B. Lecka-Czernik (2006). "Netoglitazone is a PPAR-gamma ligand with selective effects on bone and fat." Bone **38**(1): 74-84.

Le Clainche, C. and M. F. Carlier (2008). "Regulation of actin assembly associated with protrusion and adhesion in cell migration." Physiol Rev **88**(2): 489-513.

Lecka-Czernik, B., E. J. Moerman, D. F. Grant, J. M. Lehmann, S. C. Manolagas and R. L. Jilka (2002). "Divergent effects of selective peroxisome proliferator-activated receptor-gamma 2 ligands on adipocyte versus osteoblast differentiation." Endocrinology **143**(6): 2376-2384.

Lerner, U. H. (2006). "Bone remodeling in post-menopausal osteoporosis." J Dent Res **85**(7): 584-595.

Levi, B. and M. T. Longaker (2011). "Concise review: adipose-derived stromal cells for skeletal regenerative medicine." Stem Cells **29**(4): 576-582.

Li, S., S. Chang, X. Qi, J. A. Richardson and E. N. Olson (2006). "Requirement of a myocardin-related transcription factor for development of mammary myoepithelial cells." Mol Cell Biol **26**(15): 5797-5808.

Li, S., D. Z. Wang, Z. Wang, J. A. Richardson and E. N. Olson (2003). "The serum response factor coactivator myocardin is required for vascular smooth muscle development." Proc Natl Acad Sci U S A **100**(16): 9366-9370.

Little, R. D., J. P. Carulli, R. G. Del Mastro, J. Dupuis, M. Osborne, C. Folz, S. P. Manning, P. M. Swain, S. C. Zhao, B. Eustace, M. M. Lappe, L. Spitzer, S. Zweier, K. Braunschweiger, Y. Benchekroun, X. Hu, R. Adair, L. Chee, M. G. FitzGerald, C. Tulig, A. Caruso, N. Tzellas, A. Bawa, B. Franklin, S. McGuire, X. Nogues, G. Gong, K. M. Allen, A. Anisowicz, A. J. Morales, P. T. Lomedico, S. M. Recker, P. Van Eerdewegh, R. R. Recker and M. L. Johnson (2002). "A mutation in the LDL receptor-related protein 5 gene results in the autosomal dominant high-bone-mass trait." Am J Hum Genet **70**(1): 11-19.

Liu, Y. Z., Y. J. Liu, R. R. Recker and H. W. Deng (2003). "Molecular studies of identification of genes for osteoporosis: the 2002 update." J Endocrinol **177**(2): 147-196.

Livingstone, C. (2013). "Insulin-like growth factor-I (IGF-I) and clinical nutrition." Clin Sci (Lond) **125**(6): 265-280.

Luchsinger, L. L., C. A. Patenaude, B. D. Smith and M. D. Layne (2011). "Myocardin-related transcription factor-A complexes activate type I collagen expression in lung fibroblasts." J Biol Chem **286**(51): 44116-44125.

Luu, H. H., W. X. Song, X. Luo, D. Manning, J. Luo, Z. L. Deng, K. A. Sharff, A. G. Montag, R. C. Haydon and T. C. He (2007). "Distinct roles of bone morphogenetic proteins in osteogenic differentiation of mesenchymal stem cells." J Orthop Res **25**(5): 665-677.

Ma, Z., S. W. Morris, V. Valentine, M. Li, J. A. Herbrick, X. Cui, D. Bouman, Y. Li, P. K. Mehta, D. Nizetic, Y. Kaneko, G. C. Chan, L. C. Chan, J. Squire, S. W. Scherer and J. K. Hitzler (2001). "Fusion of two novel genes, RBM15 and MKL1, in the t(1;22)(p13;q13) of acute megakaryoblastic leukemia." Nat Genet **28**(3): 220-221.

Manson, J. E. and K. A. Martin (2001). "Clinical practice. Postmenopausal hormone-replacement therapy." N Engl J Med **345**(1): 34-40.

Matsuo, K. and N. Irie (2008). "Osteoclast-osteoblast communication." Arch Biochem Biophys **473**(2): 201-209.

McBeath, R., D. M. Pirone, C. M. Nelson, K. Bhadriraju and C. S. Chen (2004). "Cell shape, cytoskeletal tension, and RhoA regulate stem cell lineage commitment." Dev Cell **6**(4): 483-495.

McClung, M. R., P. Geusens, P. D. Miller, H. Zippel, W. G. Bensen, C. Roux, S. Adami, I. Fogelman, T. Diamond, R. Eastell, P. J. Meunier, J. Y. Reginster and G. Hip Intervention Program Study (2001). "Effect of risedronate on the risk of hip fracture in elderly women. Hip Intervention Program Study Group." N Engl J Med **344**(5): 333-340.

McDonald, M. E., C. Li, H. Bian, B. D. Smith, M. D. Layne and S. R. Farmer (2015). "Myocardin-related transcription factor a regulates conversion of progenitors to beige adipocytes." Cell **160**(1-2): 105-118.

Melton, L. J., 3rd (2001). "The prevalence of osteoporosis: gender and racial comparison." Calcif Tissue Int **69**(4): 179-181.

Mendez, M. G. and P. A. Janmey (2012). "Transcription factor regulation by mechanical stress." Int J Biochem Cell Biol **44**(5): 728-732.

Messerli, F. H., B. Christie, J. G. DeCarvalho, G. G. Aristimuno, D. H. Suarez, G. R. Dreslinski and E. D. Frohlich (1981). "Obesity and essential hypertension.

Hemodynamics, intravascular volume, sodium excretion, and plasma renin activity." Arch Intern Med **141**(1): 81-85.

Meunier, P., J. Aaron, C. Edouard and G. Vignon (1971). "Osteoporosis and the replacement of cell populations of the marrow by adipose tissue. A quantitative study of 84 iliac bone biopsies." Clin Orthop Relat Res **80**: 147-154.

Miano, J. M. (2003). "Serum response factor: toggling between disparate programs of gene expression." J Mol Cell Cardiol **35**(6): 577-593.

Miano, J. M. (2010). "Role of serum response factor in the pathogenesis of disease." Lab Invest **90**(9): 1274-1284.

Miano, J. M., X. Long and K. Fujiwara (2007). "Serum response factor: master regulator of the actin cytoskeleton and contractile apparatus." Am J Physiol Cell Physiol **292**(1): C70-81.

Mikkelsen, T. S., Z. Xu, X. Zhang, L. Wang, J. M. Gimble, E. S. Lander and E. D. Rosen (2010). "Comparative epigenomic analysis of murine and human adipogenesis." Cell **143**(1): 156-169.

Millard, T. H., S. J. Sharp and L. M. Machesky (2004). "Signalling to actin assembly via the WASP (Wiskott-Aldrich syndrome protein)-family proteins and the Arp2/3 complex." Biochem J **380**(Pt 1): 1-17.

Miralles, F., G. Posern, A. I. Zaromytidou and R. Treisman (2003). "Actin dynamics control SRF activity by regulation of its coactivator MAL." Cell **113**(3): 329-342.

Mizuno, H., M. Tobita and A. C. Uysal (2012). "Concise review: Adipose-derived stem cells as a novel tool for future regenerative medicine." Stem Cells **30**(5): 804-810.

Montagnani, A. (2014). "Bone anabolics in osteoporosis: Actuality and perspectives." World J Orthop **5**(3): 247-254.

Mouilleron, S., S. Guettler, C. A. Langer, R. Treisman and N. Q. McDonald (2008). "Molecular basis for G-actin binding to RPEL motifs from the serum response factor coactivator MAL." EMBO J **27**(23): 3198-3208.

Mundy, G. R. (2007). "Osteoporosis and inflammation." Nutr Rev **65**(12 Pt 2): S147-151.

Muruganandan, S., A. A. Roman and C. J. Sinal (2009). "Adipocyte differentiation of bone marrow-derived mesenchymal stem cells: cross talk with the osteoblastogenic program." Cell Mol Life Sci **66**(2): 236-253.

Nakashima, K. and B. de Crombrugghe (2003). "Transcriptional mechanisms in osteoblast differentiation and bone formation." Trends Genet **19**(8): 458-466.

Nakashima, K., X. Zhou, G. Kunkel, Z. Zhang, J. M. Deng, R. R. Behringer and B. de Crombrugghe (2002). "The novel zinc finger-containing transcription factor osterix is required for osteoblast differentiation and bone formation." Cell **108**(1): 17-29.

Neumann, E. and G. Schett (2007). "[Bone metabolism: molecular mechanisms]." Z Rheumatol **66**(4): 286-289.

Neve, A., A. Corrado and F. P. Cantatore (2011). "Osteoblast physiology in normal and pathological conditions." Cell Tissue Res **343**(2): 289-302.

Niu, Z., W. Yu, S. X. Zhang, M. Barron, N. S. Belaguli, M. D. Schneider, M. Parmacek, A. Nordheim and R. J. Schwartz (2005). "Conditional mutagenesis of the murine serum response factor gene blocks cardiogenesis and the transcription of downstream gene targets." J Biol Chem **280**(37): 32531-32538.

Nobusue, H., N. Onishi, T. Shimizu, E. Sugihara, Y. Oki, Y. Sumikawa, T. Chiyoda, K. Akashi, H. Saya and K. Kano (2014). "Regulation of MKL1 via actin cytoskeleton dynamics drives adipocyte differentiation." Nat Commun **5**: 3368.

Norman, C., M. Runswick, R. Pollock and R. Treisman (1988). "Isolation and properties of cDNA clones encoding SRF, a transcription factor that binds to the c-fos serum response element." Cell **55**(6): 989-1003.

Ogden, C. L., M. D. Carroll, L. R. Curtin, M. A. McDowell, C. J. Tabak and K. M. Flegal (2006). "Prevalence of overweight and obesity in the United States, 1999-2004." JAMA **295**(13): 1549-1555.

Oh, J., J. A. Richardson and E. N. Olson (2005). "Requirement of myocardin-related transcription factor-B for remodeling of branchial arch arteries and smooth muscle differentiation." Proc Natl Acad Sci U S A **102**(42): 15122-15127.

Olson, E. N. and A. Nordheim (2010). "Linking actin dynamics and gene transcription to drive cellular motile functions." Nat Rev Mol Cell Biol **11**(5): 353-365.

Parlakian, A., C. Charvet, B. Escoubet, M. Mericskay, J. D. Molkentin, G. Gary-Bobo, L. J. De Windt, M. A. Ludosky, D. Paulin, D. Daegelen, D. Tuil and Z. Li (2005). "Temporally controlled onset of dilated cardiomyopathy through disruption of the SRF gene in adult heart." Circulation **112**(19): 2930-2939.

Parmacek, M. S. (2007). "Myocardin-related transcription factors: critical coactivators regulating cardiovascular development and adaptation." Circ Res **100**(5): 633-644.

Peng, X. D., P. Z. Xu, M. L. Chen, A. Hahn-Windgassen, J. Skeen, J. Jacobs, D. Sundararajan, W. S. Chen, S. E. Crawford, K. G. Coleman and N. Hay (2003). "Dwarfism, impaired skin development, skeletal muscle atrophy, delayed bone development, and impeded adipogenesis in mice lacking Akt1 and Akt2." Genes Dev **17**(11): 1352-1365.

Phimphilai, M., Z. Zhao, H. Boules, H. Roca and R. T. Franceschi (2006). "BMP signaling is required for RUNX2-dependent induction of the osteoblast phenotype." J Bone Miner Res **21**(4): 637-646.

Pipes, G. C., E. E. Creemers and E. N. Olson (2006). "The myocardin family of transcriptional coactivators: versatile regulators of cell growth, migration, and myogenesis." Genes Dev **20**(12): 1545-1556.

Pittenger, M. F., A. M. Mackay, S. C. Beck, R. K. Jaiswal, R. Douglas, J. D. Mosca, M. A. Moorman, D. W. Simonetti, S. Craig and D. R. Marshak (1999). "Multilineage potential of adult human mesenchymal stem cells." Science **284**(5411): 143-147.

Pollard, T. D. (2007). "Regulation of actin filament assembly by Arp2/3 complex and formins." Annu Rev Biophys Biomol Struct **36**: 451-477.

Posern, G., F. Miralles, S. Guettler and R. Treisman (2004). "Mutant actins that stabilise F-actin use distinct mechanisms to activate the SRF coactivator MAL." EMBO J **23**(20): 3973-3983.

Posern, G. and R. Treisman (2006). "Actin' together: serum response factor, its cofactors and the link to signal transduction." Trends Cell Biol **16**(11): 588-596.

Proff, P. and P. Romer (2009). "The molecular mechanism behind bone remodelling: a review." Clin Oral Investig **13**(4): 355-362.

Qiu, W., T. E. Andersen, J. Bollerslev, S. Mandrup, B. M. Abdallah and M. Kassem (2007). "Patients with high bone mass phenotype exhibit enhanced osteoblast differentiation and inhibition of adipogenesis of human mesenchymal stem cells." J Bone Miner Res **22**(11): 1720-1731.

Raisz, L. G. (2005). "Pathogenesis of osteoporosis: concepts, conflicts, and prospects." J Clin Invest **115**(12): 3318-3325.

Recker, R. R. and R. P. Heaney (1993). "Peak bone mineral density in young women." JAMA **270**(24): 2926-2927.

Reddi, A. H. (2005). "BMPs: from bone morphogenetic proteins to body morphogenetic proteins." Cytokine Growth Factor Rev **16**(3): 249-250.

Reznikoff, C. A., J. S. Bertram, D. W. Brankow and C. Heidelberger (1973). "Quantitative and qualitative studies of chemical transformation of cloned C3H mouse embryo cells sensitive to postconfluence inhibition of cell division." Cancer Res **33**(12): 3239-3249.

Rizzoli, R., K. Akesson, M. Bouxsein, J. A. Kanis, N. Napoli, S. Papapoulos, J. Y. Reginster and C. Cooper (2011). "Subtrochanteric fractures after long-term treatment with bisphosphonates: a European Society on Clinical and Economic Aspects of Osteoporosis and Osteoarthritis, and International Osteoporosis Foundation Working Group Report." Osteoporos Int **22**(2): 373-390.

Rosen, C. J. and M. L. Bouxsein (2006). "Mechanisms of disease: is osteoporosis the obesity of bone?" Nat Clin Pract Rheumatol **2**(1): 35-43.

Rosen, E. D. and O. A. MacDougald (2006). "Adipocyte differentiation from the inside out." Nat Rev Mol Cell Biol **7**(12): 885-896.

Rosen, E. D., C. J. Walkey, P. Puigserver and B. M. Spiegelman (2000). "Transcriptional regulation of adipogenesis." Genes Dev **14**(11): 1293-1307.

Rzonca, S. O., L. J. Suva, D. Gaddy, D. C. Montague and B. Lecka-Czernik (2004). "Bone is a target for the antidiabetic compound rosiglitazone." Endocrinology **145**(1): 401-406.

Schmidt, A. and A. Hall (2002). "Guanine nucleotide exchange factors for Rho GTPases: turning on the switch." Genes Dev **16**(13): 1587-1609.

Schratt, G., U. Philippar, J. Berger, H. Schwarz, O. Heidenreich and A. Nordheim (2002). "Serum response factor is crucial for actin cytoskeletal organization and focal adhesion assembly in embryonic stem cells." J Cell Biol **156**(4): 737-750.

Sen, B., Z. Xie, N. Case, M. Ma, C. Rubin and J. Rubin (2008). "Mechanical strain inhibits adipogenesis in mesenchymal stem cells by stimulating a durable beta-catenin signal." Endocrinology **149**(12): 6065-6075.

Sepulveda, J. L., S. Vlahopoulos, D. Iyer, N. Belaguli and R. J. Schwartz (2002). "Combinatorial expression of GATA4, Nkx2-5, and serum response factor directs early cardiac gene activity." J Biol Chem **277**(28): 25775-25782.

Shaw, P. E., H. Schroter and A. Nordheim (1989). "The ability of a ternary complex to form over the serum response element correlates with serum inducibility of the human c-fos promoter." Cell **56**(4): 563-572.

Shi, Y. and J. Massague (2003). "Mechanisms of TGF-beta signaling from cell membrane to the nucleus." Cell **113**(6): 685-700.

Shore, P. and A. D. Sharrocks (1995). "The MADS-box family of transcription factors." Eur J Biochem **229**(1): 1-13.

Sikavitsas, V. I., J. S. Temenoff and A. G. Mikos (2001). "Biomaterials and bone mechanotransduction." Biomaterials **22**(19): 2581-2593.

Small, E. M., A. S. Warkman, D. Z. Wang, L. B. Sutherland, E. N. Olson and P. A. Krieg (2005). "Myocardin is sufficient and necessary for cardiac gene expression in Xenopus." Development **132**(5): 987-997.

Sorensen, M. B., A. M. Rosenfalck, L. Hojgaard and B. Ottesen (2001). "Obesity and sarcopenia after menopause are reversed by sex hormone replacement therapy." Obes Res **9**(10): 622-626.

Sotiropoulos, A., D. Gineitis, J. Copeland and R. Treisman (1999). "Signal-regulated activation of serum response factor is mediated by changes in actin dynamics." Cell **98**(2): 159-169.

Spiegelman, B. M. and S. R. Farmer (1982). "Decreases in tubulin and actin gene expression prior to morphological differentiation of 3T3 adipocytes." Cell **29**(1): 53-60.

Spiegelman, B. M. and C. A. Ginty (1983). "Fibronectin modulation of cell shape and lipogenic gene expression in 3T3-adipocytes." Cell **35**(3 Pt 2): 657-666.

Sun, K., M. A. Battle, R. P. Misra and S. A. Duncan (2009). "Hepatocyte expression of serum response factor is essential for liver function, hepatocyte proliferation and survival, and postnatal body growth in mice." Hepatology **49**(5): 1645-1654.

Sun, Q., G. Chen, J. W. Streb, X. Long, Y. Yang, C. J. Stoeckert, Jr. and J. M. Miano (2006). "Defining the mammalian CArGome." Genome Res **16**(2): 197-207.

Sun, Y., K. Boyd, W. Xu, J. Ma, C. W. Jackson, A. Fu, J. M. Shillingford, G. W. Robinson, L. Hennighausen, J. K. Hitzler, Z. Ma and S. W. Morris (2006). "Acute myeloid leukemia-associated Mkl1 (Mrtf-a) is a key regulator of mammary gland function." Mol Cell Biol **26**(15): 5809-5826.

Thomas, C. H., J. H. Collier, C. S. Sfeir and K. E. Healy (2002). "Engineering gene expression and protein synthesis by modulation of nuclear shape." Proc Natl Acad Sci U S A **99**(4): 1972-1977.

Treisman, R. (1986). "Identification of a protein-binding site that mediates transcriptional response of the c-fos gene to serum factors." Cell **46**(4): 567-574.

Tseng, Y. H., E. Kokkotou, T. J. Schulz, T. L. Huang, J. N. Winnay, C. M. Taniguchi, T. T. Tran, R. Suzuki, D. O. Espinoza, Y. Yamamoto, M. J. Ahrens, A. T. Dudley, A. W. Norris, R. N. Kulkarni and C. R. Kahn (2008). "New role of bone morphogenetic protein 7 in brown adipogenesis and energy expenditure." Nature **454**(7207): 1000-1004.

Van Wesenbeeck, L., E. Cleiren, J. Gram, R. K. Beals, O. Benichou, D. Scopelliti, L. Key, T. Renton, C. Bartels, Y. Gong, M. L. Warman, M. C. De Vernejoul, J. Bollerslev and W. Van Hul (2003). "Six novel missense mutations in the LDL receptor-related protein 5 (LRP5) gene in different conditions with an increased bone density." Am J Hum Genet **72**(3): 763-771.

Vartiainen, M. K., S. Guettler, B. Larijani and R. Treisman (2007). "Nuclear actin regulates dynamic subcellular localization and activity of the SRF cofactor MAL." Science **316**(5832): 1749-1752.

Ventura, A., G. Brunetti, S. Colucci, A. Oranger, F. Ladisa, L. Cavallo, M. Grano and M. F. Faienza (2013). "Glucocorticoid-induced osteoporosis in children with 21-hydroxylase deficiency." Biomed Res Int **2013**: 250462.

Vernochet, C., K. E. Davis, P. E. Scherer and S. R. Farmer (2010). "Mechanisms regulating repression of haptoglobin production by peroxisome proliferator-activated receptor-gamma ligands in adipocytes." Endocrinology **151**(2): 586-594.

Vernochet, C., S. B. Peres and S. R. Farmer (2009). "Mechanisms of obesity and related pathologies: transcriptional control of adipose tissue development." FEBS J **276**(20): 5729-5737.

Wabitsch, M., H. Hauner, E. Heinze and W. M. Teller (1995). "The role of growth hormone/insulin-like growth factors in adipocyte differentiation." Metabolism **44**(10 Suppl 4): 45-49.

Wada, T., T. Nakashima, N. Hiroshi and J. M. Penninger (2006). "RANKL-RANK signaling in osteoclastogenesis and bone disease." Trends Mol Med **12**(1): 17-25.

Wang, D., P. S. Chang, Z. Wang, L. Sutherland, J. A. Richardson, E. Small, P. A. Krieg and E. N. Olson (2001). "Activation of cardiac gene expression by myocardin, a transcriptional cofactor for serum response factor." Cell **105**(7): 851-862.

Wang, D., J. Prakash, P. Nguyen, B. N. Davis-Dusenbery, N. S. Hill, M. D. Layne, A. Hata and G. Lagna (2012). "Bone morphogenetic protein signaling in vascular disease: anti-inflammatory action through myocardin-related transcription factor A." J Biol Chem **287**(33): 28067-28077.

Wang, D. Z., S. Li, D. Hockemeyer, L. Sutherland, Z. Wang, G. Schratt, J. A. Richardson, A. Nordheim and E. N. Olson (2002). "Potentiation of serum response factor activity by a family of myocardin-related transcription factors." Proc Natl Acad Sci U S A **99**(23): 14855-14860.

Wang, E. A., D. I. Israel, S. Kelly and D. P. Luxenberg (1993). "Bone morphogenetic protein-2 causes commitment and differentiation in C3H10T1/2 and 3T3 cells." Growth Factors **9**(1): 57-71.

Wang, Z., D. Z. Wang, G. C. Pipes and E. N. Olson (2003). "Myocardin is a master regulator of smooth muscle gene expression." Proc Natl Acad Sci U S A **100**(12): 7129-7134.

Wellen, K. E. and G. S. Hotamisligil (2003). "Obesity-induced inflammatory changes in adipose tissue." J Clin Invest **112**(12): 1785-1788.

Wolf, A. M. and G. A. Colditz (1998). "Current estimates of the economic cost of obesity in the United States." Obes Res **6**(2): 97-106.

Wozney, J. M., V. Rosen, A. J. Celeste, L. M. Mitsock, M. J. Whitters, R. W. Kriz, R. M. Hewick and E. A. Wang (1988). "Novel regulators of bone formation: molecular clones and activities." Science **242**(4885): 1528-1534.

Xian, L., X. Wu, L. Pang, M. Lou, C. J. Rosen, T. Qiu, J. Crane, F. Frassica, L. Zhang, J. P. Rodriguez, J. Xiaofeng, Y. Shoshana, X. Shouhong, E. Argiris, W. Mei and C. Xu (2012). "Matrix IGF-1 maintains bone mass by activation of mTOR in mesenchymal stem cells." Nat Med **18**(7): 1095-1101.

Xiao, G., R. Gopalakrishnan, D. Jiang, E. Reith, M. D. Benson and R. T. Franceschi (2002). "Bone morphogenetic proteins, extracellular matrix, and mitogen-activated protein kinase signaling pathways are required for osteoblast-specific gene expression and differentiation in MC3T3-E1 cells." J Bone Miner Res **17**(1): 101-110.

Yakar, S., H. Kim, H. Zhao, Y. Toyoshima, P. Pennisi, O. Gavrilova and D. Leroith (2005). "The growth hormone-insulin like growth factor axis revisited: lessons from IGF-1 and IGF-1 receptor gene targeting." Pediatr Nephrol **20**(3): 251-254.

Yang, S. J., C. Y. Chen, G. D. Chang, H. C. Wen, C. Y. Chen, S. C. Chang, J. F. Liao and C. H. Chang (2013). "Activation of Akt by advanced glycation end products (AGEs): involvement of IGF-1 receptor and caveolin-1." PLoS One **8**(3): e58100.

Yeh, W. C., Z. Cao, M. Classon and S. L. McKnight (1995). "Cascade regulation of terminal adipocyte differentiation by three members of the C/EBP family of leucine zipper proteins." Genes Dev **9**(2): 168-181.

Yoshida, C. A., H. Yamamoto, T. Fujita, T. Furuichi, K. Ito, K. Inoue, K. Yamana, A. Zanma, K. Takada, Y. Ito and T. Komori (2004). "Runx2 and Runx3 are essential for chondrocyte maturation, and Runx2 regulates limb growth through induction of Indian hedgehog." Genes Dev **18**(8): 952-963.

Zhao, B., T. Katagiri, H. Toyoda, T. Takada, T. Yanai, T. Fukuda, U. I. Chung, T. Koike, K. Takaoka and R. Kamijo (2006). "Heparin potentiates the in vivo ectopic bone formation induced by bone morphogenetic protein-2." J Biol Chem **281**(32): 23246-23253.

Zhao, G. Q. (2003). "Consequences of knocking out BMP signaling in the mouse." Genesis **35**(1): 43-56.

Zigmond, S. H. (2004). "Formin-induced nucleation of actin filaments." Curr Opin Cell Biol **16**(1): 99-105.

CURRICULUM VITAE